CEBAF PROPOSAL COVER SHEET

This Proposal must be mailed to:

CEBAF
Scientific Director's Office
12000 Jefferson Avenue
Newport News, VA 23606

and received on or before 1 October 1991.

A. TITLE: AN INVESTIGATION OF MULTI-NUCLEON PROCESSES AT HIGH Q

B. CONTACT PERSON: W. BERTOZZI

ADDRESS, PHONE, AND ELECTRONIC MAIL ADDRESS:

C. IS THIS PROPOSAL BASED ON A PREVIOUSLY SUBMITTED PROPOSAL OR LETTER OF INTENT?

☐ YES ☐ NO

IF YES, TITLE OF PREVIOUSLY SUBMITTED PROPOSAL OR LETTER OF INTENT:

****

(CEBAF USE ONLY)

Receipt Date 10-1-91

Log Number Assigned PR 91-025

By [redacted]

An Investigation of Multi-Nucleon Processes at High Q

MIT

W. Bertozzi (co-spokesman), D. S. Dale (co-spokesman),

S. Gilad (co-spokesman), L. B. Weinstein (co-spokesman)

University of Virginia

R. W. Lourie, *et al.*

CEBAF

P. E. Ulmer, J. Mougey

William and Mary

J. M. Finn, *et al.*

Members of the Hall A Collaboration are invited to participate.

Abstract

We propose to survey the cross section for coincident cluster knockout, (e,e′X), where X denotes a deuteron, triton, ^{3}He, and ^{4}He. We hope to establish the systematic nature of these reactions, in particular their relative probabilities, their variation with momentum transfer and nuclear size, and their distribution in missing energy. We plan to concentrate on ^{12}C(e,e′X) with some study of Fe(e,e′X). We also propose to study the ^{12}C(e,e′d) reaction in greater detail by performing a Longitudinal/Transverse separation at $Q^2 = 1$ (GeV/c)^2 to examine the underlying reaction mechanism for the two body knockout process. We will simultaneously obtain data on ^{12}C(e,e′p) at large initial momenta ($p_i \approx q/2$).

I. INTRODUCTION

We propose to survey the cross-section for coincident cluster knockout, (e,e'X), where X denotes a deuteron, triton, ^{3}He, and ^{4}He. We hope to establish the systematic nature of these reactions, in particular their relative probabilities, their variation with momentum transfer and nuclear size, and their distribution in missing energy. We plan to concentrate on ^{12}C(e,e'X) with some study of Fe(e,e'X).

We also propose to study the ^{12}C(e,e'd) reaction in greater detail by performing a Longitudinal/Transverse separation at $Q^2 = 1$ (GeV/c)^2. This will extend the recent NIKHEF ^{12}C(e,e'd) studies at $Q^2 < 0.25$ (GeV/c)^2. We will simultaneously obtain data on ^{12}C(e,e'p) at large initial momentum ($p_i \approx q/2$).

The NIKHEF ^{12}C(e,e'd) studies[1] were mostly limited to low values of missing energy (E_{miss} < 10 MeV) at low momentum transfer. They observed two types of processes. One process scales a little slower than the elastic deuteron cross-section and involves T=0 states and the other (wholly transverse) process scales as the deuteron electro-disintegration cross-section and involves the T=1 state. The Saclay collaboration recently measured the ^{6}Li(e,e'd) cross-section for $q < 500$ MeV/c.[2] They find that the strength at deep missing energies (2 holes in the s-shell) exhibits a combination of these two types of scaling, apparently in contradiction with the combination of α-particle models of ^{6}Li and the NIKHEF results on ^{4}He.[3] The ^{6}Li(e,e'd)^{4}He$_{gs}$ cross-section does scale as the elastic deuteron cross-section.[2][4] Recent studies at MIT on the ^{12}C(e,e'd) reaction at $q = 900$ MeV/c and $\omega = 225$ MeV/c (quasi-free deuteron knockout kinematics) show that the reactions involving p-shell nucleons fall less rapidly than the elastic deuteron cross-section. There is also strength at missing energies up to 100 MeV, corresponding to knockout of deuterons composed of two s-shell nucleons and also of an s- and a p- shell nucleon. See figure 1. Protons are also observed at momenta that are about one half of the momentum transfer. In these studies it appears that a correlated

nucleon pair is involved in the reaction and that the electromagnetic interaction connects to a deuteron or an unbound n–p pair in the final state.

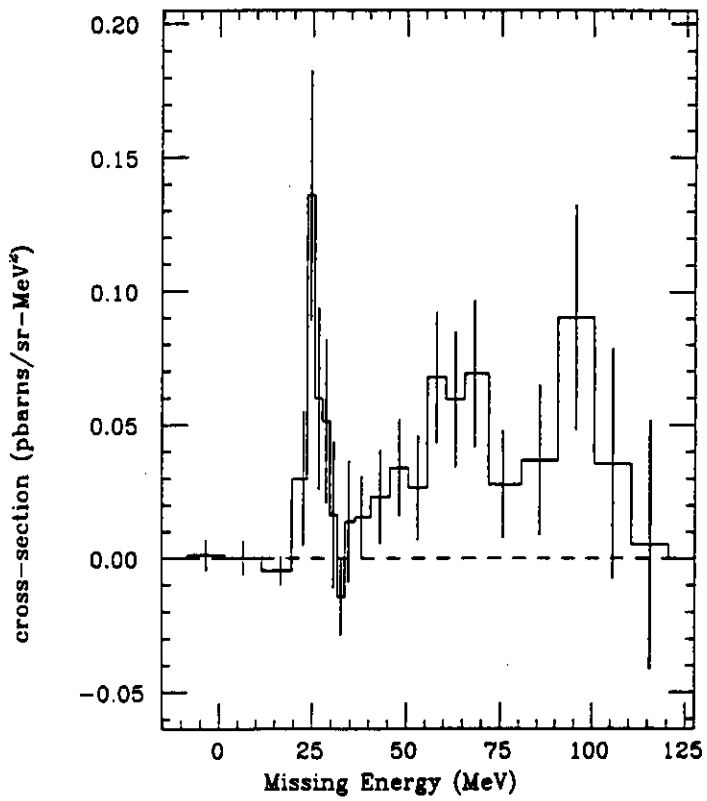

Figure 1: PRELIMINARY ^{12}C(e,e′d) cross-section for missing energy at $q = 900$ MeV/c and $\omega = 225$ MeV.

From recent (e,e′) and (e,e′p) studies of the quasielastic peak, it is clear that the naive description of quasifree scattering from bound neutrons and protons is only part of the story.[5] The large (e,e′) Transverse/Longitudinal ratio is one indication of non-single-nucleonic currents. The large (e,e′p) cross-sections at higher missing energies also indicate the involvement of two- and three-nucleon currents. In addition, the existence of transverse strength in ^{12}C(e,e′p) at $E_{miss} > 50$ MeV (where the longitudinal response function is consistent with zero) informs us that many-body currents are involved and that the many-body currents are predominantly transverse. One fascinating piece of evidence is the A-dependence of the (e,e′) R_L/R_T ratio: R_L/R_T is approximately one for $A < 4$ but is significantly less than one

for $A \geq 4$. This indicates that the transverse multi-nucleon processes require higher nuclear densities.

According to our present understanding of nuclei, we can describe the (e,e′) reaction as proceeding roughly 50% via the interaction of the electron with a mean field assemblage of neutrons and protons. For the remainder of the cross-section, the electron interacts with some other entities. A large part of these other processes involves interaction with two- and three- body systems where the energy and momentum transfer is shared by the nucleons involved. Because the many-body currents appear to be transverse, pion currents may be involved. However, the quasielastic (e,e′p) missing energy spectra provide no evidence of pion involvement because, despite the strong multi-nucleon knockout cross-section, no increase in cross-section is seen at the pion mass ($E_{miss} \approx m_\pi$). Hence, the mechanism behind these many-body currents remains a mystery. Indeed, our phenomenology is not well established. Clarifying this is one of the goals of this proposed study.

That the (e,e′d) process scales roughly as the elementary elastic d(e,e′) and d(e,e′p) processes is a strong hint of two-body correlated structures in the initial states. That it is a quantitative indicator remains to be established. The nature of the currents in many-body processes is presently unknown and mesonic currents or quark degrees of freedom may be involved.

Nevertheless, it is instructive to discuss the (e,e′d) and (e,e′p) processes at our kinematics with the assumption that the electromagnetic coupling is via the charge and magnetic form-factors of the neutron and the proton. At quasifree two-body kinematics, this reaction corresponds to interaction with a nucleon with initial three-momentum $-q/2$. For the work at NIKHEF and Saclay these initial momenta are below 250 MeV/c. These are well within the range of momenta associated with our mean field ideas. For the program that we propose, initial momenta of 500 to 1000 MeV/c are involved. In this region, very little cross-section should be due to mean field phenomena (nucleon-potential interactions). Rather, one expects

that the momentum is established via an elementary nucleon-nucleon interaction. In the reaction, the electron-nucleon collision changes the nucleon initial momentum from $-q/2$ to $+q/2$. The nucleon then emerges with its companion which also has $p = q/2$. Some of the time these two nucleons are combined into a deuteron and some of the time they emerge as np, pp, or nn pairs. Thus it is important to observe deuterons in coincidence with electrons and it is also important to observe protons that have one half of the deuteron energy (ω). The MIT work at $q = 900$ MeV/c establishes that substantial cross-section for (e,e'd) exists. Measuring the (e,e'd) and (e,e'p) reactions at the proposed large momenta should be very helpful in delineating the underlying reaction mechanisms and applicable models. As one component of the study, the transverse and longitudinal structure of the (e,e'd) reaction to well defined states and to deep missing energies will be pursued. We anticipate proposing L/T separations for three- and four- nucleon knockout reactions after we have established the systematic character of these reactions in this experiment.

II. EXPERIMENTAL TECHNIQUES

We will use the Hall A spectrometers in their standard configurations at their standard drift distances. We will use the electron spectrometer with the standard detectors (Čerenkov counters and shower counter) and the hadron spectrometer with the standard focal plane instrumentation, choosing the backup counters to optimize pion rejection and proton-deuteron-triton-^{3}He-^{4}He identification.

Since this is primarily a survey experiment, for most of the measurements we do not need the highest possible energy and angular resolution from the spectrometers and the beam. These measurements can be performed as commissioning experiments. However, we will need both energy and angular resolution for the L/T separation. Good energy resolution ($\approx 10^{-4}$) is desirable for the low Q^2 ^{12}C(e,e'd) measurements to distinguish the low lying states in ^{10}B.

We plan to use a range of carbon and iron targets from 25 to 200 mg/cm^2. The thicker targets will probably be segmented to reduce the range of energy loss of the hadrons exiting the targets.

We plan to use a 100 μamp beam at energies from 0.8 to 4.0 GeV. There is some flexibility in the actual energies we use, although large changes would increase the required beam time. If the signal-to-noise ratio is good enough, we can increase the beam current to reduce beam time.

III. KINEMATICS AND COUNT RATE ESTIMATES

A. Kinematics

We will measure (e,e'X) for Q^2 = 1, 2, and 3 (GeV/c)^2. At each Q^2 point we will choose one beam energy and electron scattering angle. We will measure (e,e'd) and (e,e'p) at quasideuteron kinematics, scanning the missing energy spectrum over at least 200 MeV. We will do this for both carbon and iron. We will then change the electron energy loss (slightly) and the hadron spectrometer angle in order to measure mass-3 and mass-4 knockout at quasifree kinematics. We will measure as much of the missing energy spectrum as the count rates allow.

At Q^2 = 1 (GeV/c)^2 we will also measure the ^{12}C(e,e'd) and ^{12}C(e,e'p) spectra at a back angle in order to perform a Longitudinal/Transverse separation.

Table 1 shows the kinematics for the different measurements and the beam time requested for each point.

B. Count Rate Estimates

Q^2 $(GeV/c)^2$	q (GeV/c)	ω (GeV)	E_o (GeV)	θ_e (°)	θ_{hadron} (°)	Reaction	^{12}C Run Time (days)	Fe Run Time (days)
1.0	1.0	0.30	2.9 0.84	20 90	58.8 31.5	$(e, e'p/d)$ L/T separation	1 4	1 0
1.0	1.0	0.18	2.9	20	71.0	$(e, e'\ ^3H)$ $(e, e'\ ^3He)$ $(e, e'\ ^4He)$	2	2
2.0	1.5	0.56	4.0	20	51.2	$(e, e'p)$ $(e, e'd)$	1	1
2.0	1.5	0.31	4.0	20	42.0	$(e, e'\ ^3H)$ $(e, e'\ ^3He)$ $(e, e'\ ^4He)$	2	2
3.0	1.9	0.83	4.0	25	43.5	$(e, e'p)$ $(e, e'd)$	3	3
3.0	1.9	0.43	4.0	25	32.1	$(e, e'\ ^3H)$ $(e, e'\ ^3He)$ $(e, e'\ ^4He)$	1	0

Table 1: Kinematics and requested run time.

In order to calculate count rate estimates for these experiments we assumed that the ^{12}C(e,e'd) cross-section can be described by the Plane Wave Impulse Approximation (PWIA):

$$\frac{d^6\sigma}{d\Omega_d d\Omega_e d\omega dE_{miss}} = K\sigma_{ed}S(p_i, E_{miss})$$

where K is a kinematic factor, σ_{ed} is the elementary electron-deuteron cross-section ($\sigma_{ed} = \sigma_M(A(Q) + B(Q)\tan^2(\theta_e/2))$ and $S(p_i, E_{miss})$ is the spectral function, the probability of finding a 'deuteron' in the target nucleus with missing energy E_{miss} and initial momentum p_i. Since we are performing all the (e,e'd) measurements at the same kinematical condition, $\omega = Q^2/2m_d$, we are sampling the same range of E_{miss} and p_i for all of the Q^2 points. Thus, in this approximation, the spectral function is independent of Q.

This approximation should underestimate the cross-section for two reasons. 1) Experiments at $Q^2 < 1$ $(GeV/c)^2$ show that the ^{12}C(e,e'd) cross-section decreases slower than the d(e,e') cross-section. 2) Final state interactions should decrease at higher outgoing deuteron energy.

Q^2 $(GeV/c)^2$	E_e (GeV)	θ_e (°)	θ_d (°)	$\sigma_{ee'd}$ (pb/(MeV sr^2))	counts/hour
1.0	2.9	20	58.8	790	17000
1.0	~~2.9~~ 0.8	90	31.5	0.61	13
2.0	4.0	20	51.2	35	1400
3.0	4.0	25	43.5	1.1	68

Table 2: Estimated count rates for ^{12}C(e,e′d).

We have estimated the ^{12}C(e,e′d) cross-sections by extrapolating from the cross-section measured at $q = 900$ MeV/c and $\omega = 225$ MeV at a scattering angle of 85°. We will assume that the Fe(e,e′d) cross-section per unit mass is the same as ^{12}C(e,e′d). This is probably also an underestimate.

We have calculated count rates from these cross-section assuming a 8 msr angular acceptance and a 10% momentum acceptance in both spectrometers. We further assume a 100 μA beam and a 100 mg/cm^2 target. The count rate estimates use an electron final energy acceptance of 10% of ω, the electron energy loss. This will keep the range of p_i and E_{miss} (and hence the spectral function) constant across the experiment. We will, of course, measure the cross-section over the entire range of ω and investigate the ω dependence of the cross-section. The expected cross-sections and count rates are shown in Table 2.

We assume that the cross-section for (e,e′t), (e,e′^{3}He), and (e,e′^{4}He) is five or ten times lower than the (e,e′d) cross-section.

C. Signal-to-Noise Ratios

Q^2 $(GeV/c)^2$	E_e (GeV)	θ_e (°)	θ_d (°)	$\sigma_{ee'}/\sigma_{ee'}\|^{Q^2=1}_{\theta=90°}$	$\sigma_{ed}/\sigma_{ed}\|^{Q^2=1}_{\theta=90°}$	$\sigma_{ee'd}/\sigma_{ee'd}\|^{Q^2=1}_{\theta=90°}$	SNR
1.0	2.9	20	58.8	13	0.8	1300	10^4
1.0	~~2.9~~ 0.8	90	31.5	1	1	1	100
2.0	4.0	20	51.2	1	130	60	50
3.0	4.0	25	43.5	0.1	70	2	30

Table 3: Details of signal-to-noise ratio estimates.

We can extrapolate the expected signal-to-noise ratio (SNR) from ^{12}C(e,e'd) measurements at Bates. At $q = 900$ MeV/c, $\omega = 225$ MeV/c, and $\theta_e = 85°$, the SNR was approximately 1:1 with a peak current of 1.5 mA (average current = 12 μA), a target thickness of 200 mg/cm^2 and a coincidence resolving time of 3.5 ns FWHM. That point is very similar to the $Q^2 = 1$ and $\theta_e = 90°$ point of this measurement. At CEBAF, with a 100 μA beam, a 100 mg/cm^2 target, and a 1 ns coincidence resolving time, the SNR would be 100 with a four times faster count rate.

Extrapolating this result to the other kinematics is more difficult. The SNR is proportional to $\frac{\sigma_{(e,e'd)}}{\sigma_{(e,e')}\sigma_{(e,d)}}$. Thus:

$$\text{SNR} = \frac{\sigma_{(e,e'd)}}{\sigma_{(e,e')}\sigma_{(e,d)}} \cdot \frac{SNR_{Q^2=1,\theta_e=90}}{\frac{\sigma_{(e,e'd)}}{\sigma_{(e,e')}\sigma_{(e,d)}}|_{Q^2=1,\theta_e=90}}$$

We have estimated $\sigma_{(e,e'd)}$ as described above. We can estimate $\sigma_{(e,e')}$ using the code QFS by Lightbody and O'Connell. There is less guidance for estimating $\sigma_{(e,d)}$. We expect that $\sigma_{(e,d)}$ will decrease with increased deuteron angle and increase with increased beam energy. For the purpose of estimating the SNR, we will assume that $\sigma_{(e,d)}$ is proportional to $\sigma_{(e,p)}$ and we will calculate $\sigma_{(e,p)}$ using the code EPC by Lightbody and O'Connell. Table 3 shows the details of the SNR calculation. Using these assumptions, the SNR for ^{12}C(e,e'd) ranges from 30 to 10^4 at $Q^2 = 1$, 2, and 3 $(GeV/c)^2$.

We expect that the SNR for (e,e′X) will be similar to that of (e,e′d)since both the exclusive (e,e′X) cross-sections and the inclusive (e,X) cross-sections will be much lower than the corresponding (e,e′d) and (e,d) values.

IV. BEAM TIME REQUEST

The ^{12}C(e,e′X) survey will require 9 days of beam time. To perform ^{12}C(e,e′d) $Q^2 = 1$ (GeV/c)^2 L/T separation will require 4 more days of beam time. The Fe(e,e′X) survey will require 9 days of beam time. See table 1 for details. If the cross-sections are much higher than estimated, we will also measure the ^{12}C(e,e′t), ^{12}C(e,e′^{3}He), and ^{12}C(e,e′^{4}He) reactions at $Q^2 = 3$ (GeV/c)^2.

The experiment will also need approximately 2 days for normalization and tune-up. There will also be three separate beam energies, four electron spectrometer angles, and six hadron spectrometer angles. At four hours for each energy change and one hour for each spectrometer angle change, this will take one more day.

The total beam time request is 25 days.

References

[1] R. Ent *et al.*, *Phys Rev Lett*, **62** (1989) 24.

[2] J. Mougey, private communication.

[3] E. Jans, *Nuclear Physics*, **A508** (1990) 433c.

[4] R. Ent *et al.*, *Phys Rev Lett*, **57** (1986) 2367.

[5] W. Bertozzi, R.W. Lourie, E.J. Moniz, "Nuclear Response Functions at Large Energy and Momentum Transfer", to appear in **Modern Topics in Electron Scattering**, ed B. Frois and I. Sick.

Deuteron Formation in the Reaction $^{12}C(e,e'd)^{10}B_{T=1}$

R. Ent,[1,2] B. L. Berman,[3] H. P. Blok,[1,2] J. F. J. van den Brand,[2] W. J. Briscoe,[3] E. Jans,[2] G. J. Kramer,[2] J. B. J. M. Lanen,[4] L. Lapikás,[2] B. E. Norum,[5] E. N. M. Quint,[2] A. Saha,[6] G. van der Steenhoven,[1,2] and P. K. A. de Witt Huberts[2]

[1]*Natuurkundig Laboratorium, Vrije Universiteit, 1007 MC Amsterdam, The Netherlands*
[2]*Nationaal Instituut voor Kernfysica en Hoge Energiefysica, Sectie K, 1009 AJ Amsterdam, The Netherlands*
[3]*Department of Physics, The George Washington University, Washington, D.C. 20052*
[4]*Fysisch Laboratorium, Rijksuniversiteit Utrecht, 3508 TA Utrecht, The Netherlands*
[5]*Department of Physics, University of Virginia, Charlottesville, Virginia 22901*
[6]*Physics Division, Continuous Electron Beam Accelerator Facility, Newport News, Virginia 23606*
(Received 19 September 1988)

In the reaction $^{12}C(e,e'd)^{10}B$ the lowest-lying $T=1$ state in ^{10}B is found to be as strongly excited as the $T=0$ ground state of ^{10}B, although the transition to the $T=1$ state is isospin forbidden for direct deuteron knockout. A mechanism integration of a p-n pair in a relative $T=1$ state into a deuteron is proposed to explain this result. This new proposed mechanism is consistent with both the observed purely transverse character of the transition and the momentum-transfer dependence of the cross section.

PACS numbers: 25.30.Fj, 27.20.+n

In this Letter we report on a measurement of the reaction $^{12}C(e,e'd)$ leading to the residual ^{10}B nucleus in its ground and low-lying excited states, with a surprising result. The results of the previous measurements on the $^3He(e,e'd)^1H$ and the $^6Li(e,e'd)^4He$(g.s.) reactions[1,2] could be described well by assuming that the reaction proceeds via direct, quasielastic knockout of a deuteron. The momentum-transfer (q) dependence of the process is the same as that for the elementary electron-deuteron cross section σ_{ed}. Therefore it is surprising that we found the 0^+, $T=1$ state at an excitation energy of 1.74 MeV in ^{10}B to be strongly excited in the $^{12}C(e,e'd)$ experiment, since the transition to this state is isospin forbidden for a direct knockout process. Because the strength of this transition is of similar magnitude as that for the transitions to the ground and first excited states in ^{10}B, which are the strongest isospin-allowed transitions, it seems unlikely that the two-step process $^{12}C(e,e'p)(p,d)^{10}B$ is the dominant process. Hence another reaction mechanism is needed to explain this result.

This mechanism could be the integration of a p-n pair into a deuteron. If an electron is scattered from a deuteron, there is a possibility that the deuteron breaks apart and that the p-n system ends up in a relative ^1S state, which is only slightly unbound. The strength of this breakup channel may even be comparable to that of the elastic channel.[3] Reversing this process, it is possible, if an electron is scattered from a p-n pair in a relative ^1S state *inside* a nucleus, that this p-n pair is emitted as a real deuteron. This "deuteron-integration" mechanism, which involves both spin and isospin flip of the p-n pair, might be responsible for the strong excitation of the $T=1$ state in the reaction $^{12}C(e,e'd)^{10}B$. The occurrence of such a deuteron electrointegration process is very interesting, as this would mean that one could obtain information on correlated p-n pairs in a relative ^1S state inside a nucleus. In this Letter an investigation of the mechanism of the reaction $^{12}C(e,e'd)^{10}B_{1.74\,MeV}$ is described.

Within the one-photon-exchange approximation and with the restriction to the case where the momentum $\mathbf{p}$ of the outgoing deuteron is parallel to the momentum transfer $\mathbf{q}$ (parallel kinematics), the $(e,e'd)$ coincidence cross section can be expressed[4] in terms of two structure functions W_L and W_T:

$$\frac{d^6\sigma}{de'd\mathbf{p}} = K\sigma_{\rm Mott}\frac{q^2}{\mathbf{q}^2}[W_L(\omega,q^2,\mathbf{p}) + \epsilon^{-1}W_T(\omega,q^2,\mathbf{p})], \quad (1)$$

where $\mathbf{e}'$ is the momentum of the outgoing electron, K is a kinematical factor, $\sigma_{\rm Mott}$ is the Mott cross section, q^2 is the squared four-momentum transfer, and ω is the electron energy loss, while the virtual-photon polarization parameter ϵ is given by

$$\epsilon = \left[1+\frac{2\mathbf{q}^2}{q^2}\tan^2\left(\frac{\theta_{e'}}{2}\right)\right]^{-1} \quad (2)$$

with $\theta_{e'}$ the electron-scattering angle.

With only an S-wave component in the $A\to(A-2)+d$ vertex,[5,6] the quasielastic $A(e,e'd)A-2$ coincidence cross section can be factorized in the plane-wave impulse approximation[7] as

$$\frac{d^6\sigma}{de'd\mathbf{p}} = K\sigma_{ed}S(E_m,\mathbf{p}_m), \quad (3)$$

where the spectral function $S(E_m,\mathbf{p}_m)$ is the nuclear structure part, i.e., the probability of finding a deuteron with binding energy E_m and momentum $\mathbf{p}_m$ in the target

 © 1988 The American Physical Society

nucleus, and $K\sigma_{ed}$ is the reaction mechanism part, with σ_{ed} describing the electron-deuteron scattering cross section. Final-state-interaction effects between the outgoing deuteron and the residual nucleus can be approximated by replacing $S(E_m,\mathbf{p}_m)$ with the distorted spectral function $S^D(E_m,\mathbf{p}_m,\mathbf{p})$. The electron-deuteron scattering cross section can be written generally as

$$\sigma_{ed}(q)=\sigma_{\mathrm{Mott}}\frac{q^2}{\mathbf{q}^2}[|F_L(q^2)|^2+\epsilon^{-1}|F_T(q^2)|^2]. \quad (4)$$

For quasielastic deuteron knockout F_L and F_T are the known longitudinal and transverse form factors of the deuteron. For the case of the deuteron-integration process we assume a description similar to Eq. (3), now taking for σ_{ed} the electron-deuteron *integration* cross section, which, assuming validity of time invariance, is the same, apart from spin factors, as the electron-deuteron *disintegration* cross section.[8] By describing the reaction in this way we have implicitly treated the p-n pair as a quasibound singlet deuteron.

We have studied the mechanism of the $^{12}C(e,e'd)$ coincidence reaction in two ways: (I) The longitudinal-transverse character has been investigated by performing measurements at constant $(\omega,\mathbf{q})$ but different incoming electron energy E_0 and electron-scattering angle $\theta_{e'}$. (II) The behavior of the coincidence cross section as a function of q has been investigated by changing the value of q.

The $^{12}C(e,e'd)$ experiment was performed at the NIKHEF-K electron scattering facility.[9] With use of a 15.9-mg/cm^2 carbon target a (typical) missing-energy resolution of 200 keV (FWHM) was achieved. All measurements were performed in parallel kinematics ($\mathbf{p}\|\mathbf{q}$), which means that in the q check the distortions change as the ^{10}B-d center-of-mass energy $E_{\mathrm{c.m.}}$ changes. In the LT check $E_{\mathrm{c.m.}}$ was kept fixed at 52 MeV. For kinematical reasons the missing-momentum region was different in the two cases, i.e., $35<p_m<85$ MeV/c ($p_{m,\mathrm{central}}=60$ MeV/c) and $70<p_m<130$ MeV/c ($p_{m,\mathrm{central}}=100$ MeV/c), respectively. Further kinematical information is given in Table I. The data were analyzed as described in Refs. 2 and 10. An excitation-energy spectrum is shown in Fig. 1. The 3^+ ground state of ^{10}B, the first-excited 1^+ state at $E_x=0.72$ MeV, and the 0^+, $T=1$ state at 1.74 MeV can be seen clearly.

TABLE I. $^{12}C(e,e'd)$ kinematics.

p_m (MeV/c)	E_0 (MeV)	ϵ^{-1}	q^2 (fm^{-2})	$E_{\mathrm{c.m.}}$ (MeV)
60	313	3.93	4.45	52
60	337	3.02	4.45	52
60	406	2.00	4.45	52
60	466	1.64	4.45	52
100	481	1.27	2.29	40
100	481	1.43	3.30	52
100	481	1.57	4.07	61

To check the L/T behavior of the reaction $^{12}C(e,e'd)^{10}B_{1.74\,\mathrm{MeV}}$, a Rosenbluth separation has been performed: the measured cross sections at $p_m=60$ MeV/c (see Table I) were divided by $K\sigma_{\mathrm{Mott}}q^2/\mathbf{q}^2$, which, according to Eq. (1), yields the sum $W_L+\epsilon^{-1}W_T$. This sum is plotted as a function of ϵ^{-1} in Fig. 2. A linear least-squares fit to the data gives $W_L=(-0.2\pm0.4)\times10^{-10}$ (MeV/c)$^{-3}$ and $W_T=(1.2\pm0.2)\times10^{-10}$ (MeV/c)$^{-3}$. Thus the data indicate within the uncertainties a purely transverse process. Since the center-of-mass energy $E_{\mathrm{c.m.}}$ was kept fixed in our kinematics, and the distortions are not expected to be very different[11] for W_L and W_T, this conclusion is not influenced by distortion effects. The purely transverse character of the reaction is consistent with an explanation in terms of the deuteron-integration mechanism. The results of the LT check speak against a two-step reaction mechanism because the process $(e,e'p)(p,d)$ is not expected to be a purely transverse process, since the reaction $(e,e'p)$ has a predominantly longitudinal character, and we do not see how the (p,d) part can change this character significantly. The $(e,e'n)(n,d)$ process would be purely transverse, but in our kinematics the $(e,e'n)$ cross section is much smaller than that for $(e,e'p)$. It should be mentioned that for the first two isospin-allowed transitions we found W_L values significantly different from zero, indicating the expected difference in reaction mechanism.

The second check is to investigate whether the q dependence of the cross section follows that of the deuteron electrodisintegration cross section. This was done by taking data for three values of q^2, and by keeping p_m constant at 100 MeV/c. The q behavior of the measured $^{12}C(e,e'd)^{10}B_{1.74\,\mathrm{MeV}}$ cross section and that of the deu-

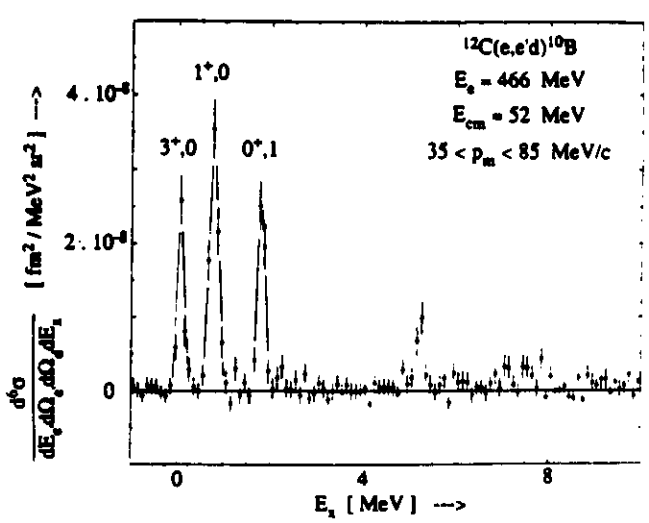

FIG. 1. Excitation-energy spectrum of the reaction $^{12}C(e,e'd)^{10}B$. Labels indicate J^π, T.

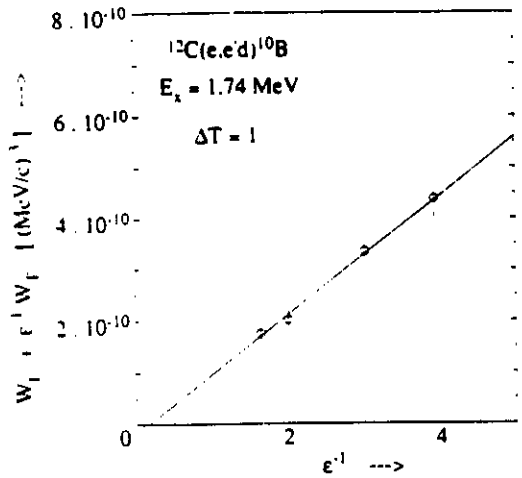

FIG. 2. Rosenbluth plot for the reaction $^{12}C(e, e'd)^{10}B_{1.74\,MeV}$. The solid line represents the best straight-line fit to the data.

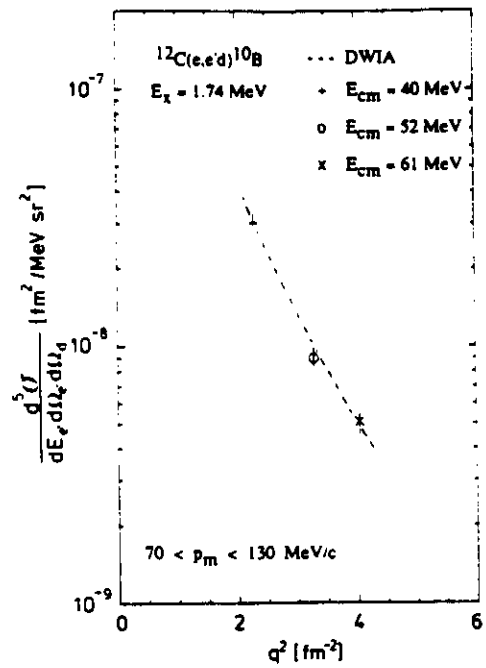

FIG. 3. Measured cross section for the reaction $^{12}C(e, e'd)^{10}B_{1.74\,MeV}$ as a function of the momentum transfer squared. The dashed curve indicates the behavior (normalized at the lowest q^2) of the calculated deuteron disintegration cross section.

teron disintegration cross section are compared in Fig. 3. We used calculations by Fabian and Arenhövel,[12] which include meson-exchange currents and ground-state isobar components for the deuteron disintegration process. These calculations give a good description of the measured deuteron disintegration cross sections in the q range of the present experiment.[4] The calculated cross sections have been integrated over the energy region 0–3 MeV above threshold, because the major contribution of the ^1S p-n state is expected to be concentrated below 3 MeV above threshold. We explicitly calculated the effect of the changing final-state interaction, due to different values of $E_{c.m.}$, by using the factorized distorted-wave impulse approximation (DWIA) code PEEP.[13] The global optical-model parameter set of Hinterberger *et al.*[14] and an $l=0$ bound-state wave function of the Woods-Saxon type were used to estimate these distortion effects for $p_m \cong 100$ MeV/c. The differences in final-state interaction are taken into account in the calculated disintegration cross section. As can be seen in Fig. 3 the variation in measured coincidence cross sections is a factor of 5.9 ± 1.2, which agrees well with the variation in the calculated deuteron disintegration cross section of 6.2 ± 0.3, where the uncertainty is due to distortion effects. The choice of the integration interval of 0–3 MeV above threshold has little influence ($<1\%$) on this factor.

In hadron-induced deuteron-knockout experiments a mechanism where the hadronic particle changes a p-n ($S=0$, $T=1$) pair into a deuteron can also take place. In the reaction $^{12}C(p,pd)^{10}B$, the excitation of the $^{10}B_{1.74\,MeV}$ state indeed can be described reasonably well by such a mechanism.[15] However, these data do not exclude other mechanisms, since the general trend of the experimental cross sections also can be reproduced with a constant p-d cross section, independent of the momentum transfer q.

In summary, we have found evidence that the 0^+, $T=1$ state at 1.74 MeV excitation energy in ^{10}B is excited in the reaction $^{12}C(e,e'd)$ through the mechanism of deuteron integration. If further theoretical study about the possible contributions of two-step processes indeed supports the dominance of the proposed deuteron-integration mechanism, we may, by use of this reaction, be able to investigate correlated p-n pairs in ^{12}C which are not in a deuteron quantum state, and thus to obtain complementary information about correlations in the ^{12}C nucleus. The prospect then would be application of this method to other nuclei as well.

We would like to thank Professor H. Arenhövel for the calculation of the electrodisintegration cross sections. This work was supported in part by the Stichting voor Fundamenteel Onderzoek der Materie (FOM), which is financially supported by the Nederlandse organisatie voor Wetenschappelijk Onderzoek (NWO), by the National Science Foundation, by the U.S. Department of Energy, and by the Jeffress Memorial Trust.

[1]P. H. M. Keizer *et al.*, Phys. Lett. **157B**, 255 (1985).
[2]R. Ent *et al.*, Phys. Rev. Lett. **57**, 2367 (1986).
[3]M. Bernheim *et al.*, Phys. Rev. Lett. **46**, 402 (1981).
[4]S. Boffi, C. Giusti, and F. D. Pacati, Nucl. Phys. **A386**, 599 (1982).

[5]M. Rai, D. R. Lehman, and A. Ghovanlou, Phys. Lett. **59B**, 327 (1975).

[6]B. F. Gibson and D. R. Lehman, Phys. Rev. C **29**, 1017 (1984).

[7]S. Frullani and J. Mougey, Adv. Nucl. Phys. **14**, 1 (1985).

[8]S. Barshay, Phys. Rev. Lett. **17**, 49 (1966).

[9]C. de Vries *et al.*, Nucl. Instrum. Methods Phys. Res. **223**, 1 (1984).

[10]L. Lapikás and P. K. A. de Witt Huberts, J. Phys. (Paris), Colloq. **45**, C4-57 (1984).

[11]G. van der Steenhoven *et al.*, Phys. Rev. Lett. **57**, [illegible] (1986).

[12]W. Fabian and H. Arenhövel, Nucl. Phys. **A314**, 253 (1979); H. Arenhövel, private communication.

[13]S. Boffi, C. Giusti, F. D. Pacati, and S Frullani, Nucl. Phys. **A319**, 461 (1979).

[14]F. Hinterberger *et al.*, Nucl. Phys. **A111**, 265 (1968).

[15]E. Descroix *et al.*, Nucl. Phys. **A438**, 112 (1985).

Reaction ^{6}Li$(e,e'd)^4$He and the α-d Momentum Distribution in the Ground State of ^{6}Li

R. Ent, H. P. Block, J. F. A. van Hienen, and G. van der Steenhoven
Natuurkundig Laboratorium, Vrije Universiteit, 1007 MC Amsterdam, The Netherlands

J. F. J. van den Brand, J. W. A. den Herder, E. Jans, P. H. M. Keizer, and L. Lapikás, E. N. M. Quint, P. K. A. de Witt Huberts
National Instituut voor Kernfysica en Hoge-Energiefysica, Sektion K, 1009 AJ Amsterdam, The Netherlands

B. L. Berman, W. J. Briscoe, C. T. Christou, and D. R. Lehman
Department of Physics, The George Washington University, Washington, D.C. 20052

and

B. E. Norum[(a)] and A. Saha
Department of Physics, University of Virginia, Charlottesville, Virginia 22901
(Received 26 June 1986)

The α-d momentum distribution in the ground state of ^{6}Li has been measured in parallel kinematics with the reaction ^{6}Li$(e,e'd)^4$He in the momentum range $0 < p_m < 270$ MeV/c. The reaction can be described by a direct coupling of the virtual photon to a deuteron in ^{6}Li. The results agree well with the predictions of a three-body αNN model of ^{6}Li.

PACS numbers: 25.30.Fj, 21.60.Gx, 25.10.+s, 27.20.+n

Correlations between nucleons bound in a nucleus play an important role in nuclear physics, e.g., in alpha decay and in pion absorption. Although single-nucleon densities have been studied extensively with stripping and pickup reactions and more recently with the $(e,e'p)$ reaction,[1] little is known about two- (or more-) nucleon density functions. Some information has been obtained from knockout reactions with hadrons, especially from the (p,pd) reaction.[2] However, the results of such experiments are hard to interpret because of both uncertainties in the reaction mechanism and distortion effects in the entrance and exit channels.[3] Electron-induced knockout reactions, like $(e,e'd)$, suffer from fewer uncertainties because the electromagnetic interaction which drives the reaction is known, and the only important distortion effects occur between the hadronic particles in the final state.

The only $(e,e'd)$ measurements with a reasonable energy resolution have been performed on ^{6}Li at Saclay[4] and on ^{3}He at the National Instituut voor Kernfysica en Hoge-Energiefysica Sektion K (NIKHEF-K).[5] However, the energy of the outgoing deuterons in the ^{6}Li experiment was rather low, resulting in large rescattering effects, and only a limited momentum range was investigated. In the experiment reported here we have studied the reaction ^{6}Li$(e,e'd)^4$He at higher deuteron energies with good resolution over a large momentum interval and have compared the extracted α-d momentum distribution with model predictions.[6]

The ^{6}Li nucleus is an excellent candidate for such a comparison because the tight binding of ^{4}He and the small separation energy between the α and the deuteron in ^{6}Li suggest a description of this nucleus as an α-d cluster or as an αpn three-body system. In either approach the Pauli principle plays an important role. In cluster models antisymmetrization leads to an effective α-d wave function that has a $2S$ form, i.e., a wave function that possesses a node, independent of whether the relative-motion wave function is chosen to have $1S$ (no node) or $2S$ character before antisymmetrization.[7] Likewise, three-body models of ^{6}Li, which go beyond cluster-model and resonating-group work[7,8] in that the dynamics are not reduced to effective two-body dynamics, predict an effective S-wave α-d wave function of the $2S$ form.[9-11] The structure of this wave function is reflected in the α-d momentum distribution in ^{6}Li. Thus a determination of this distribution constitutes a test of three-body models of ^{6}Li.

If one assumes that the virtual photon couples quasielastically to the deuteron[5] and that one can neglect the D-wave component in the $^6\text{Li} \rightarrow \alpha + d$ vertex,[6,9,11] the coincidence cross section for the $(e,e'd)$ reaction in the plane-wave impulse approximation (PWIA) can be written[12] as

$$d^6\sigma/d\mathbf{e}'d\mathbf{p} = K\sigma_{ed}S(E_m,p_m), \tag{1}$$

where $\mathbf{e}'$ is the momentum of the outgoing electron, $\mathbf{p}$ is the momentum of the outgoing deuteron, K is a kinematical factor, and σ_{ed} is the elastic electron-deuteron cross section, corrected for the (small) off-shell effects according to the current-conservation prescription of de Forest.[13,14] The dependence of the cross section on σ_{ed} will be discussed below. The spectral function $S(E_m,p_m)$ is the probability of finding a deuteron with energy $-E_m$ and momentum p_m in the target nucleus. For a transition to a bound state one can define the momentum den-

© 1986 The American Physical Society

sity distribution $\rho(p_m)=\int_{\Delta E_m} S(E_m,p_m)dE_m$, which is the Fourier transform of, in our case, the effective α-d wave function $\Psi_{\alpha\text{-}d}(R)$:

$$\rho(p_m)=\left|\int e^{-i\mathbf{p}_m\cdot\mathbf{R}}\Psi_{\alpha\text{-}d}(R)d\mathbf{R}\right|^2, \qquad (2)$$

where R is the α-d relative coordinate.

Inclusion of the interaction between the deuteron and the α particle in the final state can be incorporated approximately by the change of ρ in Eq. (2) into the distorted momentum distribution $\rho^D(\mathbf{p}_m,\mathbf{p})$, which now also depends on the momentum of the outgoing deuteron. The distortions can be described by replacement of the plane wave for the deuteron, which is used in Eq. (2), by an optical-model wave function.

The ^{6}Li$(e,e'd)$ experiment was performed at the NIKHEF-K electron accelerator. The experimental setup, which includes two magnetic spectrometers, was the same as has been used for $(e,e'p)$ experiments.[15] Identification of the outgoing deuterons and rejection of other particles was accomplished by pulse-height discrimination in two scintillators behind the multiwire drift chambers in the focal plane of the hadron spectrometer. The target was a self-supporting foil of thickness 13.0 mg/cm^2, enriched to 98.7% in ^{6}Li. The energy of the incoming electrons was 480 MeV. The range in missing momentum covered in the experiment was $-50<p_m<270$ MeV/c, with parallel kinematics ($\mathbf{p}\parallel\mathbf{q}$, $p_m=p-q$). The outgoing deuteron energy was such as to yield an α-d center-of-mass energy $E_{\text{c.m.}}$ of 45 MeV for the data with p_m up to 120 MeV/c, 55 MeV for $120<p_m<230$ MeV/c, and 70 MeV for $120<p_m<270$ MeV/c.

The data analysis included subtraction of accidental coincidences and unfolding of the radiative tail (see Ref. 15 for details). An E_m spectrum for $80<p_m<120$ MeV/c is shown in Fig. 1. Except for the peak corresponding to the ground state of ^{4}He, the spectrum is consistent with zero up to the breakup threshold of ^{4}He. The resolution is 250 keV, which is almost completely due to variation in energy loss in the target. The momentum distribution for the transition to the ground state of ^{4}He is shown in Fig. 2. The curves are the results of calculations in which we used the "repulsive" α-d wave fun of Parke and Lehman.[11] (Using the "attractive" function of Ref. 11 gives an almost equivalent, though slightly poorer, description.) The PWIA curve shows a maximum at $p_m=0$ and a minimum (at $p_m=145$ MeV/c) characteristic of a 2S-type wave function. The other curves are the results of distorted-wave impulse-approximation (DWIA) calculations for the relevant deuteron energies. Because our data were obtained at different values of $E_{\text{c.m.}}$, we used the global optical-model parameter set of Hinterberger *et al.*[16] As can be seen from the difference between the PWIA and DWIA curves, distortion effects are relatively small at low p_m. This can be understood from the fact that the data at small p_m are sensitive mainly to the wave function at large values of R, where the optical-model potential (OMP) is weak. However, at larger p_m the minimum which exists in the PWIA curve is almost completely filled in because the contributions from the nuclear interior, which are responsible for the minimum, are strongly suppressed by the absorptive part of the OMP. The overall agreement in shape between the data and the DWIA calculation is rather good. It seems that a little more strength around $p_m=0$ is needed in the calculation. In this region use of a different OMP changes the calculated cross sections by only a few percent, while in the

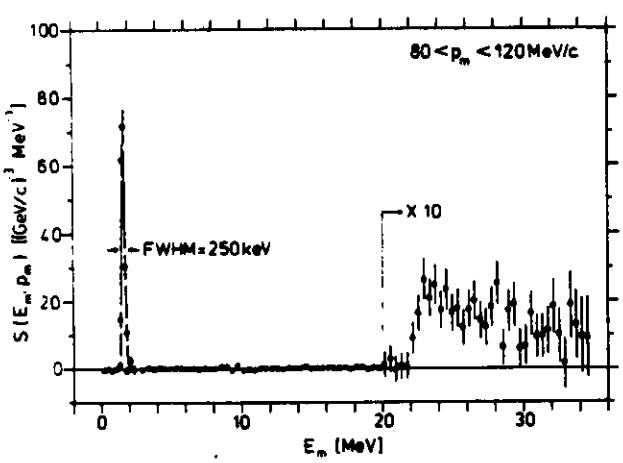

FIG. 1. Missing-energy spectrum of the ^{6}Li$(e,e'd)$ reaction.

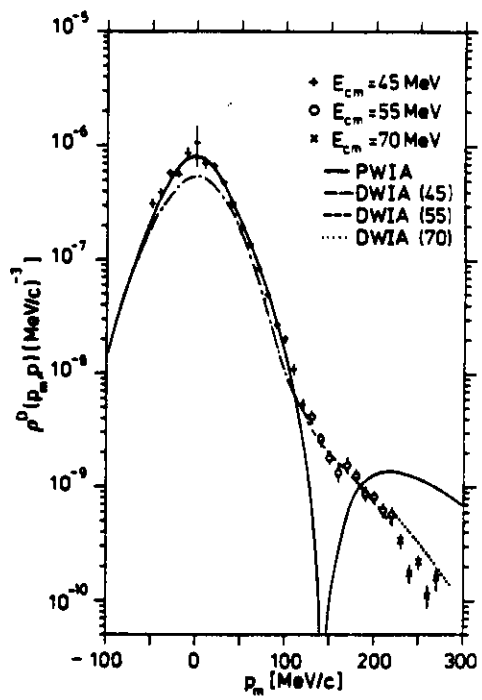

FIG. 2. Measured momentum distribution for the reaction ^{6}Li$(e,e'd)^4$He(g.s.) compared with the results of DWIA calculations, which use the "repulsive" wave function of Re DWIA curves are for the indicated center-of-mass en Each datum point represents an average over a 10-MeV/c bind.

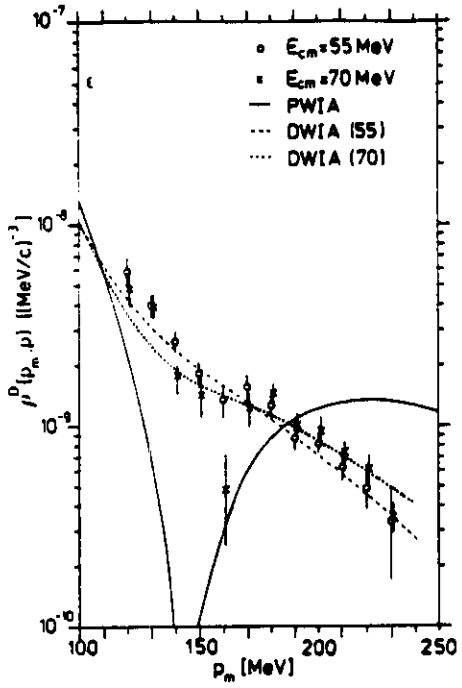

FIG. 3. Momentum distribution for the reaction ^{6}Li$(e,e'd)^4$He(g.s.) for $120 \leq p_m \leq 230$ MeV/c, measured at two α-d center-of-mass energies. DWIA curves are for the indicated center-of-mass energies. Each data point represents an average over a 10-MeV/c bin.

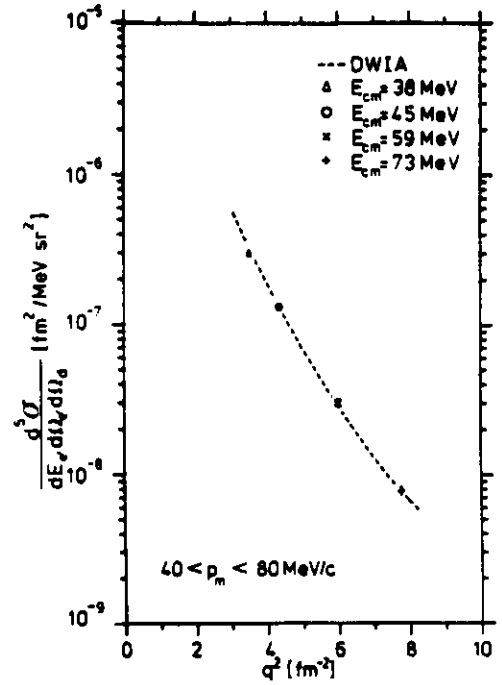

FIG. 4. Measured cross sections for the reaction ^{6}Li$(e,e'd)^4$He(g.s.) as a function of the momentum transfer squared. The dashed curve indicates the expected behavior (normalized at the highest q) of the cross section for direct deuteron knockout, corrected for distortion effects.

high-p_m region it yields effects of up to 30%.

The α-d probability in the ground state of ^{6}Li from the three-body calculations is $P=0.616$ (Ref. 11). The data yield $P=0.73$, which was obtained by integration of the measured momentum distribution (extrapolated to infinity) after correction of it for distortion effects. The statistical and extrapolation uncertainty is 0.03. The uncertainty due to target thickness, solid angle, etc., is about 0.04. The uncertainty from the description of the distortion effects with the optical model is estimated to be 0.07. Values of P from the ^{6}Li(p,pd) reaction[2] obtained by normalization of a calculated momentum distribution at $p_m=0$ to the data range from 1.08 to 1.35.

In order to investigate the region of the minimum more thoroughly, data for $120 < p_m < 230$ MeV/c were obtained as well for $E_{c.m.}=70$ MeV, in which case the distortion effects are expected to be smaller than for $E_{c.m.}=55$ MeV. The two data sets are compared in Fig. 3. Although the separate data points exhibit overlapping error bars, the higher-$E_{c.m.}$ data tend towards the PWIA curve, i.e., the 70-MeV points are systematically lower at $p_m \sim 160$ MeV/c and higher at $p_m \sim 200$ MeV/c, in agreement with the DWIA calculations.

It should be mentioned that the data cannot be described by assumption of a $1S$-type α-d wave function, because a $1S$ wave function yields a momentum distribution that decreases smoothly at $p_m \sim 150$ MeV/c, in contrast with the data, which show a change of slope (Figs. 2 and 3). It should be noted that in the reaction ^{6}Li$(p,pd)^4$He the various distortions completely hide the $1S$ or $2S$ character of the α-d wave function.[3] Clearly, the $(e,e'd)$ reaction has the advantages that the electron can probe the nuclear interior and that only one distorting interaction is present.

We explicitly checked the assumption that the coincidence cross section follows σ_{ed} as a function of q [Eq. (1)]. Therefore data were taken for four values of q between 370 and 550 MeV/c, with p_m kept constant at 60 MeV/c. The measured cross sections are compared with $K\sigma_{ed}$ in Fig. 4. The change of the coincidence cross section by a factor of nearly 40 is, within the error bars ($<10\%$), accounted for by the change in σ_{ed} (of a factor of 10) and K over this range of q. Since $E_{c.m.}$ changes with q (because p_m is kept constant and $\mathbf{p} \parallel \mathbf{q}$), the distortions change also, but this change is not large at this value of $p_m (\sim 30\%)$. The curve for $K\sigma_{ed}$ includes a correction for this effect. The variation in σ_{ed} is almost completely due to its Coulomb part, as the kinematics of our data points were such that the transverse contribution is $\sim 15\%$ at the highest-q point and much less for the other points. It is hard to imagine that a different reaction process would yield the observed q dependence. For instance, sequential knockout $(e,e'p)(p,d)$ is expected to follow approximately $K\sigma_{ep}$, which changes by only a factor of 5 in the q range of our data points. Thus it can be concluded that the $(e,e'd)$ reaction on ^{6}Li proceeds pri-

marily via quasielastic deuteron knockout, akin to what has been found for the ^{3}He(e,$e'd$) reaction.[5]

In summary, the reaction ^{6}Li(e,$e'd$)^{4}He allows one to determine the α-d momentum distribution in the ground state of ^{6}Li. The reaction can be described by a direct coupling of the virtual photon to a deuteron in ^{6}Li. A three-body model for ^{6}Li gives a good description of the data. The data clearly illustrate the $2S$ character of the α-d relative wave function, as required by antisymmetrization.

This work was supported in part by the Stichting voor Fundamenteel Onderzoek der Materie, which is financially supported by the Nederlandse Organisatie voor Zuiver Wetenschappelijk Onderzoek, by the National Science Foundation, by the U.S. Department of Energy, and by the Jeffrefs Memorial Trust.

---

[a]Currently on leave at CEBAF, Newport News, VA 23606.

[1]L. Lapikás, Nucl. Phys. **A434**, 85C (1985).

[2]P. Kitching *et al.*, Phys. Rev. C **11**, 420 (1975); W. Dollhopf *et al.*, Phys. Lett. **58B**, 425 (1975); D. Albrecht *et al.*, Nucl. Phys. **A338**, 477 (1980).

[3]R. E. Warner *et al.*, Nucl. Phys. **A422**, 205 (1984), and **A443**, 64 (1985).

[4]J. P. Genin *et al.*, Phys. Lett. **52B**, 46 (1974).

[5]P. H. M. Keizer *et al.*, Phys. Lett. **157B**, 255 (1985).

[6]C. T. Christou *et al.*, Phys. Rev. C **31**, 250 (1985).

[7]Yu. A. Kudeyarov, V. G. Neudatchin, S. G. Serebryakov, and Yu. F. Smirnov, Yad. Fiz. **6**, 1203 (1967) [Sov. J. Nucl. Phys. **6**, 876 (1968)]; I. V. Kuryumov, V. G. Neudatchin, and Yu. F. Smirnov, Phys. Lett. **31B**, 426 (1970); Yu. A. Kudeyarov, I. V. Kerdymov, V. G. Neudatchin, and Yu. F. Smirnov, Nucl. Phys. **A163**, 316 (1971).

[8]Y. C. Tang, K. Wildermuth, and L. D. Pearlstein, Phys. Rev. **123**, 548 (1961).

[9]D. R. Lehman and M. Rajan, Phys. Rev. C **25**, 2743 (1982).

[10]D. R. Lehman, Phys. Rev. C **25**, 3146 (1982).

[11]W. C. Parke and D. R. Lehman, Phys. Rev. C **29**, 2319 (1984).

[12]S. Frullani and J. Mougey, Adv. Nucl. Phys. **14**, 1 (1985).

[13]T. de Forest, Jr., Nucl. Phys. **A392**, 232 (1983).

[14]R. Ent, NIKHEF-K Report No. 85-15, 1985 (unpublished).

[15]L. Lapikás and P. K. A. de Witt Huberts, J. Phys. (Paris) **45**, C4-57 (1984).

[16]F. Hinterberger *et al.*, Nucl. Phys. **A111**, 265 (1968).

Nuclear Physics A508 (1990) 433c-444c
North-Holland

RECENT RESULTS FROM (e,e'X) REACTIONS ON ^{4}He.

Eddy JANS

National Institute for Nuclear Physics and High-Energy Physics, section K (NIKHEF-K), Postbus 4395, 1009 AJ Amsterdam, The Netherlands

Coincidence cross sections for the ^{4}He(e,e'p), ^{4}He(e,e'd)^{2}H and ^{4}He(e,e't)^{1}H reaction have been measured under various kinematical conditions. In the impulse approximation they can be related to either the single-nucleon or the multi-nucleon momentum density distribution. The data are compared to microscopic calculations of the reaction cross section that include final-state interaction effects and meson exchange currents.

1. INTRODUCTION

Studies on few body systems are characterized by an enormous effort from both theoreticians and experimentalists to obtain reliable and mutually consistent results. In the sector of (e,e'p) related topics two new results merit to be mentioned: i) a longitudinal-transverse separation of the coincidence cross section[1] on ^{4}He and ii) the recent continuum Faddeev calculations of Tjon and van Meijgaard[2] which permit an interesting comparison with the ^{3}He(e,e'p)pn results of Jans et al.[3], covering excitation energies of the residual pn-system up to 80 MeV. However, in this contribution I will report on an experimental investigation of various ^{4}He breakup channels. The following reaction channels have been measured: ^{4}He(e,e'p), ^{4}He(e,e'd)^{2}H and ^{4}He(e,e't)^{1}H, which will be discussed in the sections 3 to 5. In section 2 an introduction to the theoretical aspects of electrodisintegration of ^{4}He is given. A summary is given in section 6.

2. ELECTRODISINTEGRATION MEASUREMENTS OF ^{4}He.

In the plane wave impulse approximation (PWIA) the (e,e'p) coincidence cross section can be related to the energy (E_m) and momentum (p_m) distribution of the initial proton[4] through:

$$d^6\sigma/de'd\Omega_{e'}dp'd\Omega_{p'} = k\,\sigma_{ep}(Q)\,S(E_m,p_m), \qquad (1)$$

in which k is a kinematical factor and σ_{ep} represents the off-shell electron-proton cross section, for which the current conserving expression σ_{cc1} of de Forest[5] is employed. The four-momentum transfer is denoted by Q, while the spectral function $S(E_m,p_m)$, which contains the nuclear structure information, can be compared with theoretical results from four-nucleon system calculations that use realistic NN-interactions.

For instance spectral functions have been calculated by Schiavilla et al.[6] using the variational Monte Carlo (VMC) method for the Urbana potential to which the model-VII three-nucleon interaction was added. This calculation yields 28.2 ± 0.4 MeV for the ^{4}He binding energy in good agreement with the experimental value of 28.3 MeV. The theoretical result for the r.m.s. charge radius is 1.62 fm versus 1.67 ± 0.01 found experimentally. In order to obtain spectral function values the overlap $\langle\Psi_{A-1}|\Psi_A\rangle$ between the initial (A) and final (A-1) wave function, has been

0375-9474 / 90 / $3.50 © Elsevier Science Publishers B.V.
(North-Holland)

calculated using a Monte Carlo method.

Using the ATMS (Amalgamation of Two-body correlation into the Multiple Scattering process) four-nucleon wave function of ref. 7, obtained for the Reid Soft Core potential, Morita et al.[8] have also calculated p-t and d-d momentum density distributions.

The distortion of the outgoing proton can be accounted for in the optical potential framework. In that case the spectral function of expression 1 can be approximated by a distorted spectral function $S^D(E_m, p_m, p')$, which also depends on the momentum p' of the knocked out proton.

Recently Laget and Schiavilla[9] have extended the existing diagrammatic approach for describing the (e,e'p) reaction on ^{2}H and ^{3}He to ^{4}He. This approach permits the separate microscopic calculation of each process as shown in Fig. 1.

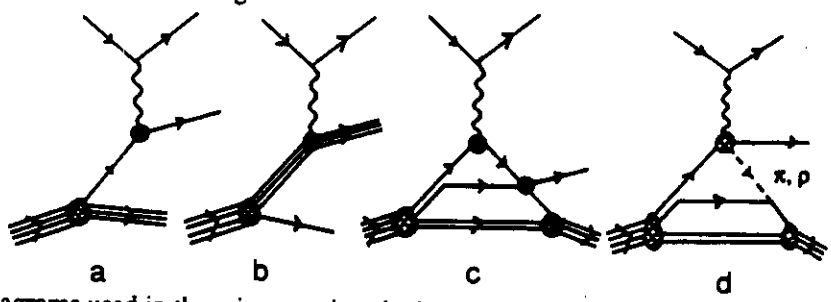

Fig. 1: Diagrams used in the microscopic calculation of the cross section of the ^{4}He(e,e'p) reaction. a) pure PWIA process. b) recoil term. c) single nucleon-nucleon rescattering. d) meson-exchange contribution.

In addition to the pure PWIA process (diagram a in Fig. 1) the contribution due to anti-symmetrization of the final-state wave function (diagram b) also has to be considered. At the γ-(A-1) vertex the free ^{3}H form factors, as experimentally determined by Juster et al.[10], are used. Corrections to this PWIA picture arise from

i) final state interactions of the emerging nucleon with the residual nucleus (FSI, diagram c). This single nucleon-nucleon rescattering process is accounted for by considering S, P and D scattering matrix elements while permitting the active nucleon pair to be in a T=0 or T=1 state. Therefore the various overlap integrals of the 3-body and 4-body variational wave-function components for each contributing angular momentum value have been calculated.

ii) coupling of the virtual photon to mesonic currents in the nucleus (MEC, diagram d). The exchange of π and ρ mesons is considered.

In the following sections I will compare the aforementioned calculations to the experimental results.

3. PROTON MOMENTUM DISTRIBUTION IN ^{4}He OBTAINED WITH THE ^{4}He(e,e'p) REACTION

The first set of experimental cross sections has been obtained at NIKHEF-K in (q,ω)-constant kinematics[11], at a proton-triton center-of-mass energy $T_{pt\text{-}CoM}$ of 75 MeV.

kin I:	q=431 MeV/c	$10 < p_m < 210$ MeV/c
kin II:	q=250 MeV/c	$110 < p_m < 350$ MeV/c

The virtual-photon polarization parameter amounts to 0.48 and 0.80 for kinematics I and II,

respectively. An E_m-spectrum at p_m = 35 MeV/c is displayed in Fig. 2.

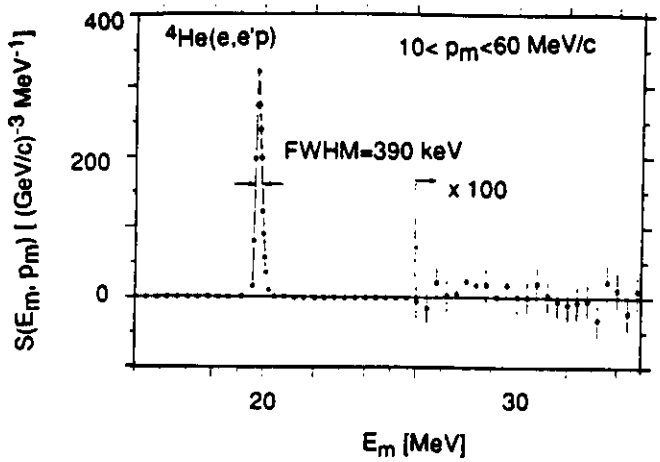

Fig 2: Missing-energy spectrum of the ^{4}He(e,e'p) reaction measured in kinematics I after random subtraction, phase space correction and radiative unfolding.

The momentum dependence of the cross section for the ^{4}He(e,e'p)^{3}H reaction is obtained by integrating over the missing-energy region that covers the (p+t) final state. The resulting five-fold differential cross section $d^5\sigma/de'd\Omega_{e'}d\Omega_{p'}$ for kinematics I is compared with the microscopic calculation of Laget and Schiavilla for the Urbana + model-VII three-nucleon interaction in Fig. 3.

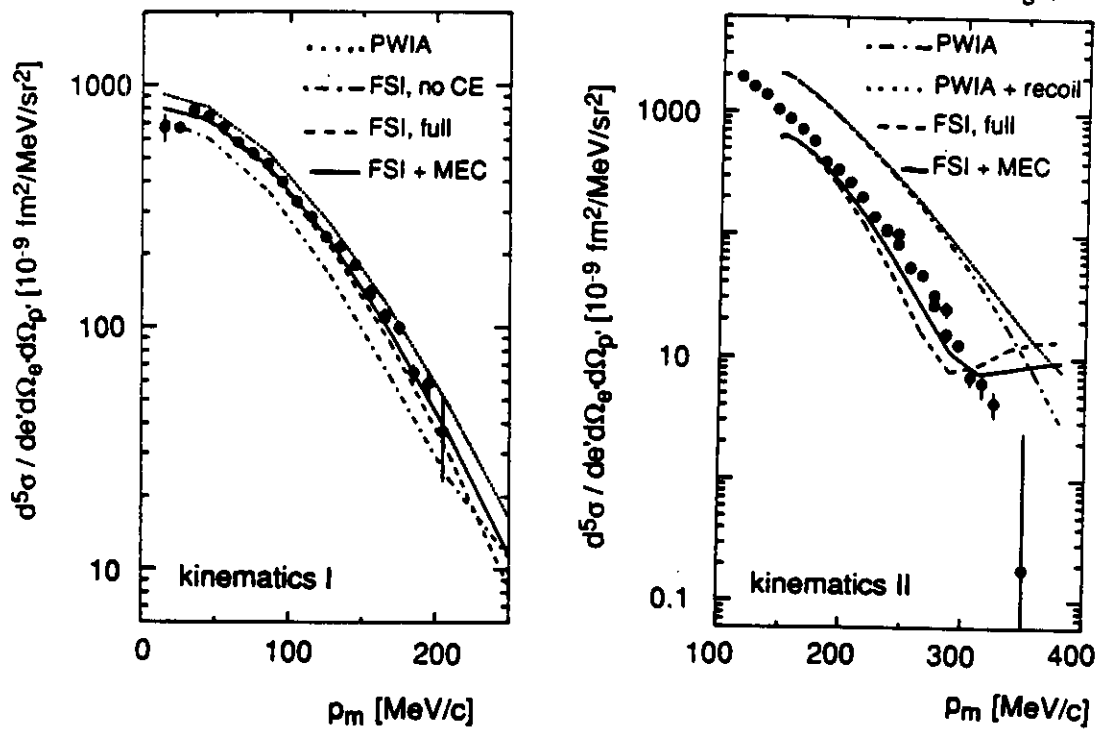

Fig 3: Five-fold differential cross section for the ^{4}He(e,e'p)^{3}H reaction in kinematics I (left) and kinematics II (right) measured at NIKHEF-K. For an explanation of the curves see text.

The dotted curve represents the PWIA calculation, which predicts a spectroscopic strength for the

pt-channel of 75-80% of the total Z=2 sum rule, when integrated up to momenta > 400 MeV/c. The dashed and dash-dotted curves show the results including FSI effects, with and without the (e,e'n)(n,p) charge-exchange contribution respectively. The full curve accounts for all FSI and MEC contributions. Apparently the charge exchange part of diagram c of figure 1 is crucial to obtain a good description of the data of kinematics I. In figure 3 the data of kinematics II are compared with the same microscopic calculation. Here the dot-dashed and dotted curves represent the contribution of diagram a (pure PWIA) and diagram a+b (pure PWIA + recoil contribution) respectively. The recoil contribution, which is negligible at low missing momenta, becomes quite important at p_m>300 MeV/c. The dashed and full curve represent the complete FSI and complete FSI + MEC calculation. In this kinematics the reduction of the cross section due to proton rescattering is not compensated by an increase due to the charge-exchange process as is the case in kinematics I. This is due to the much smaller transverse component in the electromagnetic interaction in kinematics II. The full calculation correctly describes the slope of the data between p_m=150 and 300 MeV/c, but is too small by ≈ 20%. This observation is confirmed by other ^{4}He(e,e'p) data[12] taken under various kinematic conditions at comparable three-momentum transfer values. At missing momenta above 300 MeV/c the interference of the various amplitudes causes the calculation to flatten off much more than the data. Nevertheless the model accounts for the major part of the deviations from PWIA both in kinematics I and II.

This leads to the conclusion that the q=431 MeV/c data, and to a lesser extent the q=250 MeV/c data, can correctly be described in the impulse approximation with the VMC four-nucleon wave function obtained with the Urbana + model-VII three-nucleon interaction.

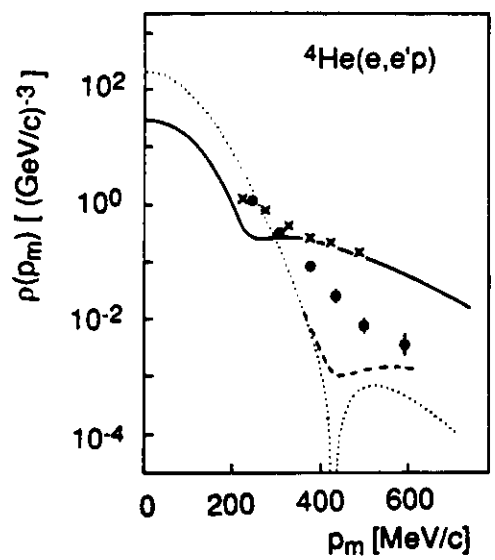

Fig 4: The circles represent the momentum distribution of the (p+t)-breakup of ^{4}He measured at Saclay. The dotted curve is the (p+t) prediction of the ATMS method of ref. 8., while the dashed curve is Laget's calculation including FSI and MEC corrections. The crosses represent the data of the complete breakup channel and the solid curve corresponds to the ATMS calculation.

Various calculations[6,8,13] have indicated that the effects of short-range correlations between nucleons will mainly be manifest at both high missing momenta (p_m>400 MeV/c) and high missing energy values (E_m>40 MeV). Recently a ^{4}He(e,e'p) experiment has been performed at Saclay that

probes this kinematic region. In figure 4 the momentum distribution of both the (p+t)-breakup and complete (2p+2n) breakup channel is plotted. Clearly above 350 MeV/c the continuum is the dominant reaction channel, as correctly predicted by the plane wave ATMS calculation[8]. The PWIA calculation for the (p+t)-channel of Morita et al. predicts a second maximum around 500 MeV/c due to correlations, but underestimates the cross section dramatically. When FSI and MEC effects are accounted for, as done by Laget and Schiavilla, the calculated values are still up to an order of magnitude smaller than the experimental results. So the diagrammatic model that describes the ^{4}He(e,e'p)^{3}H data below p_m=300 MeV/c within 20%, deviates considerably at missing momenta well above the Fermi momentum, where the differences between various nucleon-nucleon interactions are expected to show up most.

The energy distribution of the continuum strength is related to the underlying mechanism by which it is generated. In figure 5 the missing-energy spectra measured at p_m=275 and 487 MeV/c are shown.

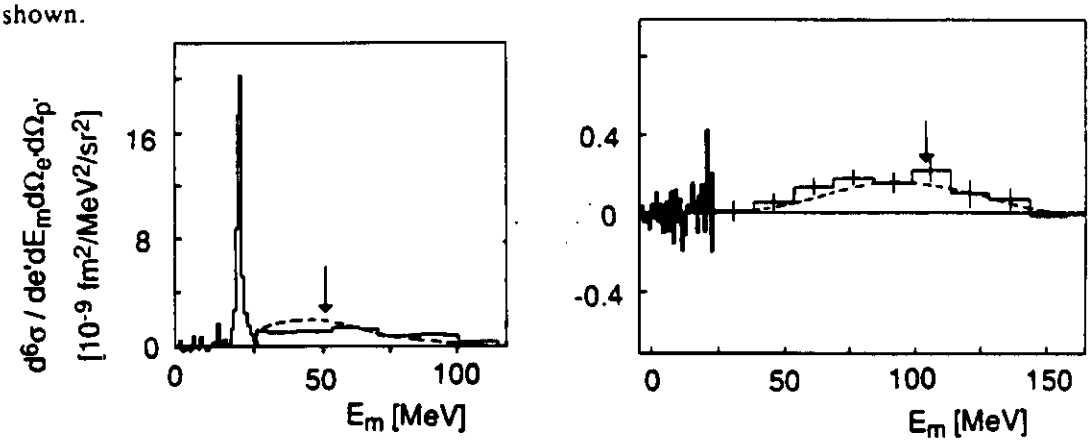

Fig 5: Missing-energy spectrum of the ^{4}He(e,e'p) reaction obtained at missing momentum values p_m=275 (left) and 487 MeV/c (right) for the center of the continuum. The dashed curve is the result of the complete calculation of Laget and Schiavilla.

Clearly the location of the strength depends on the missing momentum value probed. The following tentative explanation for this effect can be formulated as follows: two nucleons are at rest, the other two have opposite momentum p_m. After the reaction one of the latter two is ejected with momentum p_m+q, while the remaining three nucleons recoil with momentum -p_m. The missing energy at which this process will show up is indicated by an arrow in figure 5. Apparently the location of the observed strength can be attributed to coupling of the virtual photon to a correlated nucleon pair. When the nuclear dynamics is taken into account, as does the calculation of Laget via the momentum distributions of the various reaction channels, spreading of the strength takes place, as illustrated by the dashed curve. So the initial-state wave function does contain a sufficiently large amount of correlations to explain the experimentally observed strength.

To summarize the ^{4}He(e,e'p) results: data obtained in quasi-elastic kinematics at missing momenta smaller than 300 MeV/c can correctly be described by the VMC wave function calculated for the Urbana + model-VII three-nucleon interaction when accounting for FSI and MEC effects in the diagrammatic approach of Laget. At high missing momenta (350<p_m<600 MeV/c), where differences

between NN-interactions are expected to show up, the same calculation underestimates the data up to an order of magnitude. The continuum results at $250<p_m<500$ MeV/c, which are sensitive to short-range correlations, have the correct amplitude and missing energy distribution.

4. ELECTRO-INDUCED DEUTERON EMISSION FROM ^{4}He: THE ^{4}He(e,e'd)^{2}H REACTION

Due to the tight binding of the four-nucleon system, which reflects itself in e.g. the large removal energy of the first nucleon (20 MeV) and the small rms radius of 1.67 fm, short-range correlations are expected to play an important role in the wave function of ^{4}He. The study of correlation phenomena via multi-nucleon coincidence reactions, like ^{4}He(e,e'NN) and ^{4}He(e,e'dN), forms an important part of the future research programs of the c.w. electron beams that are presently under construction at CEBAF, Mainz and NIKHEF. However a subset of these correlations can already be studied with present day facilities with the (e,e'd) reaction, which has the advantage that only one hadronic particle has to be detected. In analogy with (e,e'p), the cross section for quasi-elastic deuteron knockout can be approximated by

$$d^6\sigma/de'd\Omega_e dp_d'd\Omega_{d'} = k\,\sigma_{ed}(Q)\,S^D(E_m,p_m,p_d'), \qquad (2)$$

where σ_{ed} is the off-shell electron-deuteron cross section and $S^D(E_m,p_m,p_d')$ the distorted spectral function that depends on the the initial (p_m) and final (p_d') deuteron momentum.

Predictions of the d-d component in the ^{4}He wave function are available from calculations of Schiavilla et al.[6] and Morita et al.[8] using the VMC and ATMS method respectively. However, before a reliable interpretation of the momentum distribution of $\langle\Psi_d|\Psi_{^4He}\rangle$ can be given, the quasi-elastic deuteron-knockout mechanism of the ^{4}He(e,e'd) reaction has to be investigated first. For that purpose the description of the coincidence cross section as in expression 2 has been tested at NIKHEF-K. Measurements were performed at a constant p_m-acceptance (100-150 MeV/c) and at a constant $T_{dd\text{-}CoM}$=35 MeV, for three-momentum transfers q, varying from 270 to 440 MeV/c. Deuterons were separated from protons by ΔE-E correlations in the two scintillators layers in the QDQ spectrometer. An E_m-spectrum measured at q = 270 MeV/c is shown in Fig. 6.

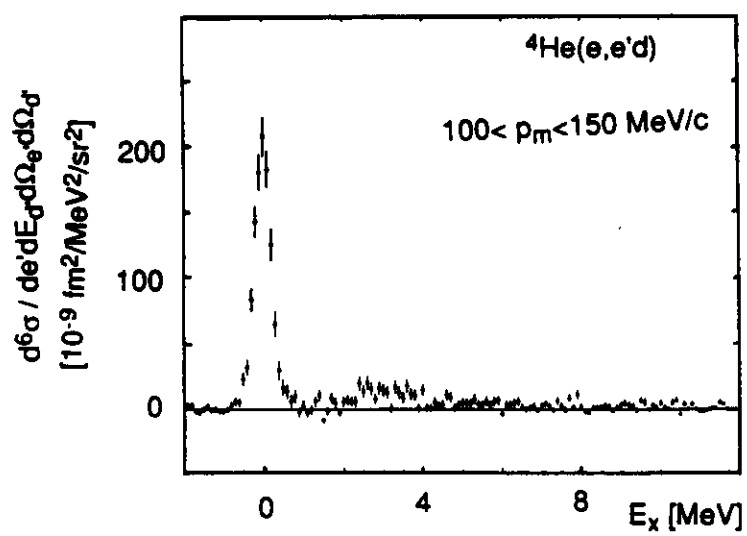

Fig 6: Excitation-energy spectrum of the ^{4}He(e,e'd) reaction obtained at q=270 MeV/c.

The cross section for the $^4He(e,e'd)^2H$ process was obtained by integrating over the missing-energy region that covers the (^2H+d) final state. Due to the resolution of 0.5 MeV the $^4He(e,e'd)^2H$ process is clearly separated from the $^4He(e,e'd)pn$ continuum. Although the d-d center-of-mass energy is kept constant, relative FSI effects have to be calculated because the angle between $\mathbf{p_m}$ and $\mathbf{p_{d'}}$ changes from one kinematics to the other. These distortion effects were calculated with the factorized DWIA code PEEP[14] using the bound-state wave function of ref. 8, obtained with the ATMS method for the Reid Soft Core potential. The d-d optical potential was constructed by double folding the JLM effective nucleon-nucleon interaction[15]. The calculated ratio of distorted over undistorted spectral function varies by 30% over the measured momentum transfer interval.

When quasi-elastic deuteron knockout is the reaction mechanism and FSI effects are correctly described, the experimental fall-off of the coincidence cross section should essentially be given by the decrease of the elastic deuteron form factor times the kinematical factor k of expression 2. In figure 7 a calculation of the cross section using the free deuteron form factor and corrected for FSI effects is shown together with the data. The theoretical cross section decreases with a factor 23 over the experimentally covered Q^2-region, while the data only drop by a factor of 10.

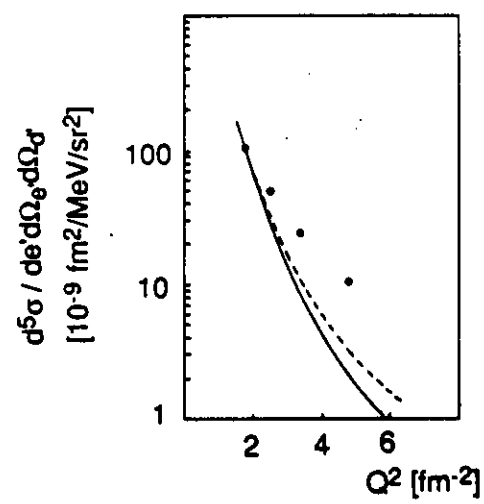

Fig 7: Five-fold differential cross section of the $^4He(e,e'd)^2H$ reaction as a function of the four-momentum transfer squared. The dashed curve is calculated with the free deuteron form factor. The solid curve represents Morita's calculation that accounts for a realistic spatial distribution of the pn-pair in ^4He. The curves have been normalized to the lowest Q-point.

This difference might be due to the fact that the spatial distribution of a pn-pair in ^4He is quite different from that in a free deuterium nucleus, which has a rms radius of 2.10 fm. To calculate this effect Morita has performed a microscopic calculation of the transition matrix element due to charge interaction for the $^4He(e,e'd)^2H$ reaction. For the initial state he used his full ATMS wave function, in which correlations between the nucleons due to the RSC potential are included via two-body correlation functions in the trial wave function. The result of Morita's calculation, that accounts for a realistic spatial distribution of the pn-pair in ^4He and that has been corrected for FSI effects, is

represented by the solid curve in figure 7. It describes the data even worse, so still some important ingredients are missing. Possible candidates are i) the amount of high-momentum components in the relative wave function of pn-pairs in ^{4}He and ii) two-step processes like (e,e'p)(p,d), which have to be calculated before the deuteron momentum distribution in ^{4}He, which was also measured, can be interpreted.

5. ELECTRO- INDUCED TRITON EMISSION FROM ^{4}He: THE ^{4}He(e,e't)^{1}H REACTION

Similar to the mechanism described in section 3 where detection of knocked out protons was undertaken to study the proton channel in ^{4}He, detection of recoiling tritons can also be performed to study the ^{4}He(e,e'p)^{3}H breakup channel. This technique is in principle very useful to study the high-momentum components of the p-t wave function because the single triton rate is an order of magnitude smaller than the proton rate in the corresponding (e,e'p) kinematics. The signal to noise ratio of the recoil measurements will therefore be accordingly higher. However, direct coupling of the virtual photon to a triton cluster and two-step processes leading to an emerging triton will also contribute to the (e,e't) cross section. Therefore the reaction mechanism was investigated by measuring (e,e't) cross sections at constant triton missing momenta for three-momentum transfers q varying from 250 up to 450 MeV/c. The corresponding kinematics are shown in figure 8.

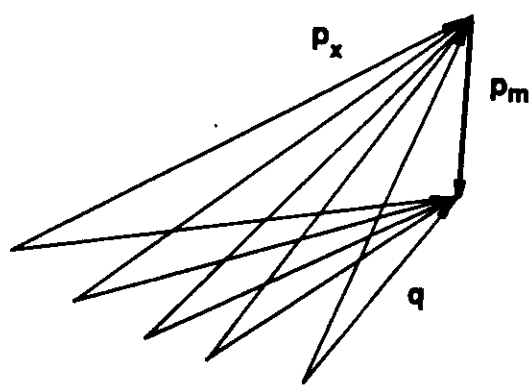

Fig 8: Orientation of the relevant momenta of the ^{4}He(e,e't) experiment.

Since the central missing energy, triton missing momentum and $T_{pt\text{-}CoM}$ were fixed at 20 MeV, 180 MeV/c and 40 MeV respectively, the outgoing triton momentum varied from 414 up to 528 MeV/c. A missing energy spectrum obtained in the q=250 MeV/c kinematics is shown in figure 9. When a quasi-elastic triton knockout mechanism is assumed the cross section can be written analogous to previous expressions as:

$$d^6\sigma/de'd\Omega_e dp_t'd\Omega_{t'} = k\ \sigma_{et}(Q)\ S^D(E_m,p_m,p_t')\,. \qquad (3)$$

where σ_{et} represents the off-shell electron-triton cross section for which the form factor data of Juster et al.[10] have been taken.

The spectral function at p_m=180 MeV/c is taken from the VMC calculation of Schiavilla et al., corrected for FSI effects in the DWIA formalism using the energy-dependent set of optical potential parameters as determined by van Oers et al.[16] The Q-dependence of the data, together with the

theoretical prediction, is shown in figure 10. The data drop by a factor of 11.6 ± 1.9 while the calculated cross section decreases by a factor 154 over the Q^2-range under investigation. Clearly the calculation in which the virtual photon is assumed to couple to a triton with free triton properties, cannot describe the data correctly.

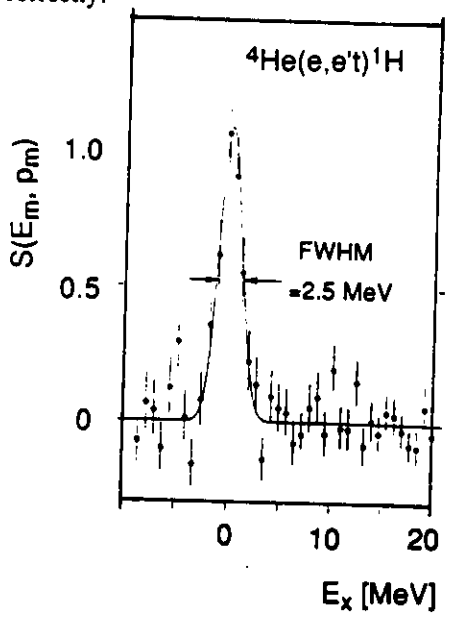

Fig 9: Excitation-energy spectrum of the ^{4}He(e,e't) reaction obtained at q=250 MeV/c.

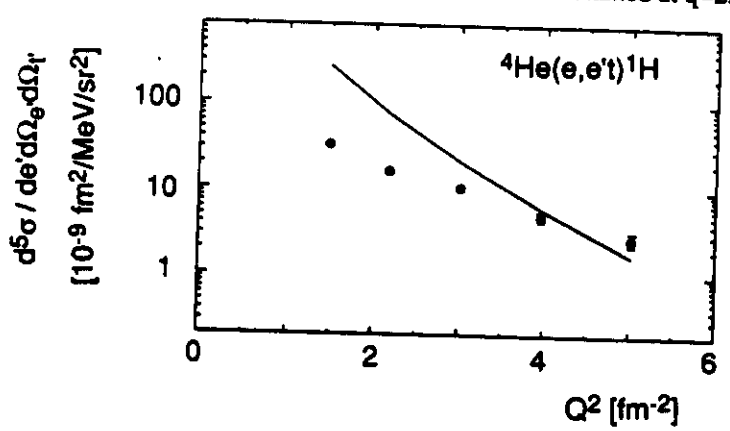

Fig 10: Five-fold differential cross section of the ^{4}He(e,e't)^{1}H reaction as a function of the four-momentum transfer squared. The solid curve represents the DWIA prediction according to expression 3.

Laget also calculated the cross section for the kinematics represented in figure 8. After transformation by means of phase space Jacobians, the curves of figure 11 result. The triton momenta correspond in the pure PWIA to high recoil momenta of the ^{4}He(e,e'p)^{3}H reaction (diagram a in Fig. 1). The dotted curve corresponds to this calculation with only coupling to the proton, the probability of which is evidently very small at these high proton missing momenta. The dot-dashed curve accounts for diagram a and b in figure 1, illustrating the fact that the recoil term is indeed quite

important in these kinematics. The dashed curve is the result of the coherent sum of diagram a and c indicating that the effect of final state interactions is very important. Finally the full curve accounts for all four diagrams of figure 1, but clearly fails to describe even qualitatively the ^{4}He(e,e't) data.

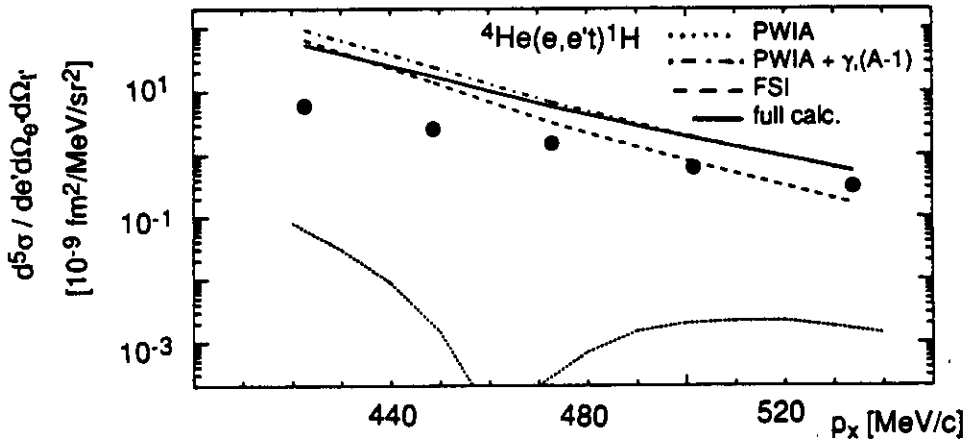

Fig 11: Five-fold differential cross section of the ^{4}He(e,e't)^{1}H reaction as a function of the triton momentum. The various curves correspond to calculations of Laget and Schiavilla.

In summary, studies of the mechanisms of the ^{4}He(e,e'd) and ^{4}He(e,e't) reactions by measuring the Q-dependence of the cross section yielded results that can not be explained until now by theoretical calculations. The effect of two-step processes like (e,e'p)(p,d) and (e,e'p)(p,t) on the cross sections needs to be investigated first.

6. SUMMARY

A number of ^{4}He(e,e'p) data sets, collected under various kinematical conditions have been discussed in this contribution. Cross sections of the ^{4}He(e,e'p)^{3}H reaction, probing initial proton momenta up to 300 MeV/c, that were collected at three-momentum transfer values of 250 and 431 MeV/c have been compared to calculations using the VMC four-nucleon wave function obtained with the Urbana + model-VII three-nucleon interaction. The data can correctly be described when FSI and MEC effects are accounted for by means of the diagrammatic approach of Laget and Schiavilla. However, at much higher missing momenta (300-600 MeV/c) the same calculation underestimates the experimental cross section for the (p+t)-breakup channel by up to an order of magnitude.

Short-range correlations between nucleons reflect themselves in the high missing-energy region of the four-body breakup channel at high missing momenta. The aforementioned microscopic calculation correctly describes both the experimentally determined spreading of this continuum strength and its location as a function of missing momentum. Within this approach the initial-state wave function seems to contain a sufficient amount of correlations, but too many high momentum components in the (p+t)-channel.

Nucleon cluster knockout studies as ^{4}He(e,e'd) and ^{4}He(e,e't) reveal a four-momentum transfer dependence of the cross section that cannot be explained by present-day calculations. A better understanding of the reaction mechanism is clearly needed, a goal that might be reached via an

estimate of the contribution of two-step processes like (e,e'p)(p,d) and (e,e'p)(p,t).

ACKNOWLEDGEMENTS

The results on ^{4}He that have been discussed in this contribution have been collected thanks to the effort of a large group of people working at NIKHEF-K and Saclay. However, I would like to thank especially Jo van den Brand and Rolf Ent part of whose thesis work is contained in section 3 and 5, and 4. Alain Magnon and Hiko Morita are gratefully acknowledged for supplying me with results prior to publication.

This work is part of the research program of the National Institute for Nuclear Physics and High-Energy Physics (NIKHEF, section K) made possible by the financial support from the Foundation for Fundamental Research on Matter (FOM) and the Netherlands' Organization for the Advancement of Research (NWO).

REFERENCES

1) A. Magnon et al., Phys. Lett. B222 (1989) 352

2) J.A. Tjon and E. van Meijgaard, private communication

3) E. Jans et al., Nucl. Phys. A475 (1987) 687

4) S. Frullani and J. Mougey, Adv. in Nucl. Phys. 14 (1984) 1

5) T. de Forest, Nucl. Phys. A392 (1983) 232

6) R. Schiavilla, V.R. Pandharipande and R.B. Wiringa, Nucl. Phys. A449 (1986) 219

7) H. Tanaka, Nucl. Phys. A328 (1979) 454

8) H. Morita et al., Progr. of Theor. Phys. 79 (1988) 863

9) J.M. Laget and R. Schiavilla, private communication

10) F.P. Juster et al., Phys. Rev. Lett. 55 (1985) 2261

11) J.F.J. van den Brand et al., Phys. Rev. Lett. 60 (1988) 2006

12) J.F.J. van den Brand, Ph. D. thesis University of Amsterdam (1988), unpublished

13) M.Strikman and C. Ciofi degli Atti, private communication

14) S. Boffi, C. Giusti, F.D. Pacati and S. Frullani, Nucl. Phys. A319 (1979) 461

15) J.P. Jeukenne, A. Lejeune and C. Mahaux, Phys. Rev. C16 (1977) 80

16) W.T.H. van Oers et al., Phys. Rev. C25 (1982) 390

NUCLEAR RESPONSE FUNCTIONS AT LARGE ENERGY AND MOMENTUM TRANSFER†

W. Bertozzi[1], R.W. Lourie[3] and E.J. Moniz[1,2]

[1] *Bates Linear Accelerator Center*
Department of Physics and Laboratory for Nuclear Science
Massachusetts Institute of Technology
Cambridge, MA 02139 USA

[2] *Institut für Theoretische Physik*
Universität Erlangen-Nürnberg
D8520 Erlangen, Germany

and

[3] *Department of Physics and Institute of Nuclear and Particle Physics*
University of Virginia
Charlottesville, VA 22901 USA

To appear as a chapter in the book
Modern Topics in Electron Scattering
Edited by B. Frois and I. Sick

---

† This work supported in part by the U.S. Department of Energy under contracts DE-AC02-76ER03069 (WB and EJM) and DE-FG05-90ER40570 (RWL) and the Alexander von Humboldt Foundation (EJM).

NUCLEAR RESPONSE FUNCTIONS AT LARGE ENERGY AND MOMENTUM TRANSFER†

W. Bertozzi[1], R.W. Lourie[3] and E.J. Moniz[1,2]

[1] *Bates Linear Accelerator Center*
Department of Physics and Laboratory for Nuclear Science
Massachusetts Institute of Technology
Cambridge, MA 02139 USA

[2] *Institut für Theoretische Physik*
Universität Erlangen-Nürnberg
D8520 Erlangen, Germany

[3] *Department of Physics and Institute of Nuclear and Particle Physics*
University of Virginia
Charlottesville, VA 22901 USA

I. Introduction

Quasifree nucleon processes are expected to dominate the nuclear electromagnetic response function for large energy and momentum transfers, i.e., for energy transfers large compared with nuclear single particle energies ($\omega \gtrsim 50$ MeV) and momentum transfers large compared with typical nuclear momenta ($|\vec{q}| \equiv q \gtrsim 400$ MeV/c). The inclusive spectra shown in Figure 1[1] [2] qualitatively confirm this idea. The two prominent bumps are located at energy losses corresponding to quasifree elastic scattering from nucleons and to quasifree Δ-excitation. The quasifree peak is centered at an energy loss approximately equal to that for elastic scattering on free nucleons and has a width which reflects the ground state momentum distribution of nucleons, a fact exploited some time ago to extract nuclear Fermi momenta[3] in reasonable agreement with expectations based upon the nuclear density. The increased broadening of the quasifree peak with increasing target mass number A, as seen in Figure 1(a), follows from such considerations. The Δ-excitation peak practically scales with A; indeed, the basically identical cross sections in the Δ-region for the mirror pair ^{3}H and ^{3}He, as seen in Figure 1(b), shows the dominance of the purely isovector Δ-excitation process. The peak is clearly broadened with respect to that measured for hydrogen, resulting both from Fermi broadening and from dynamical processes which we discuss later. Figure 2 shows the missing energy spectrum[4] for longitudinal and transverse proton knockout from ^{12}C in parallel kinematics (i.e., the proton is emitted along $\vec{q}$). The electron kinematics are close to the quasifree peak. The longitudinal

† This work supported in part by the U.S. Department of Energy under contracts DE-AC02-76ER03069 (WB and EJM) and DE-FG05-90ER40570 (RWL) and the Alexander von Humboldt Foundation (EJM).

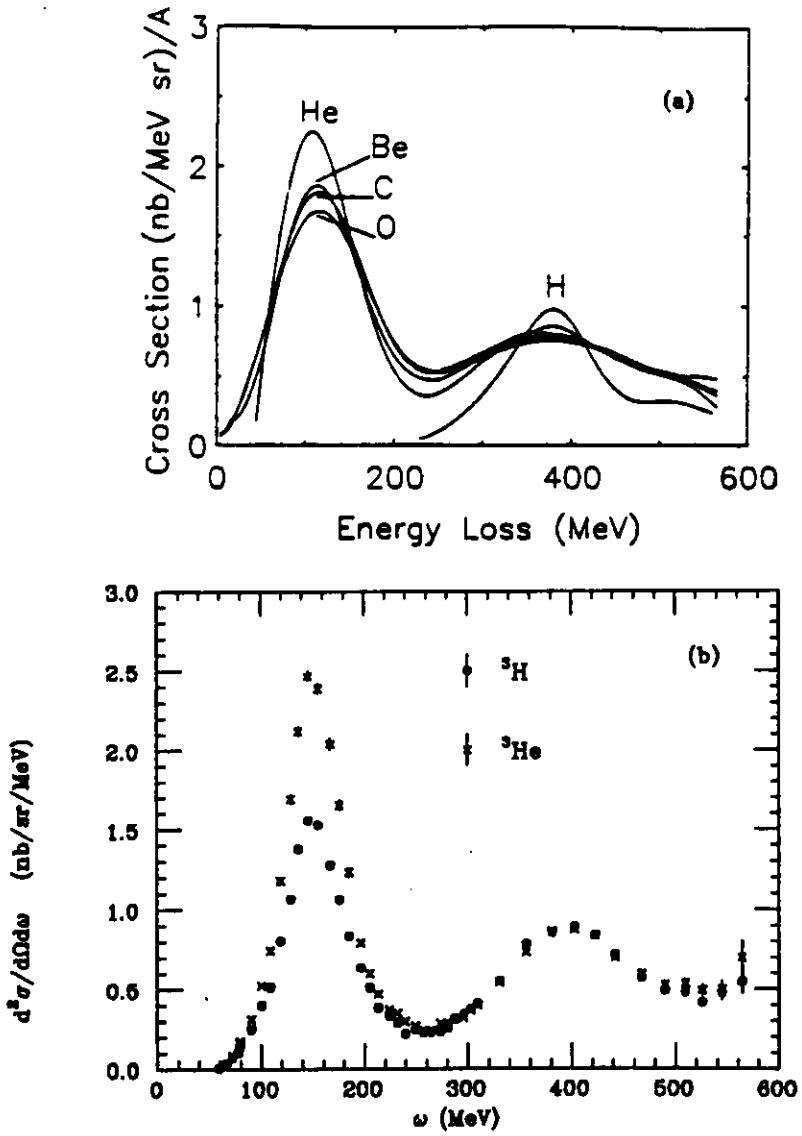

Figure 1. *a) Inclusive quasielastic electron scattering from various light nuclei when E_0 = 730 MeV and θ = 37°.*[1] *b) Inclusive (e,e′) spectra from ^3H and ^3He for E_0 = 651 MeV and θ = 54°.*[2]

spectrum has a clear quasifree character in that the entire strength is located in the p- and s-shell peaks. This general success of the quasifree picture suggests that "single particle properties" of the nucleus can be examined quantitatively, including properties such as nucleon momentum distributions, modified in-medium nucleon structure, or Δ-spreading widths in the nucleus. Such studies have formed the basis for a major program of (e,e′p) coincidence experiments at Saclay, Bates and NIKHEF. These studies reveal explicitly the "discrete" nuclear shell structure, and quantitative tests of mean field theory have resulted; e.g., spectroscopic information such as occupation probabilities and the momentum distribution of nucleons in specific orbits. Such results will be described extensively elsewhere in this volume.

Despite this evident success of the quasifree picture in providing the basic framework for discussing and understanding the large-ω, large-q nuclear response, the limits of this picture have also become quite clear. The "dip" region of the inclusive response function

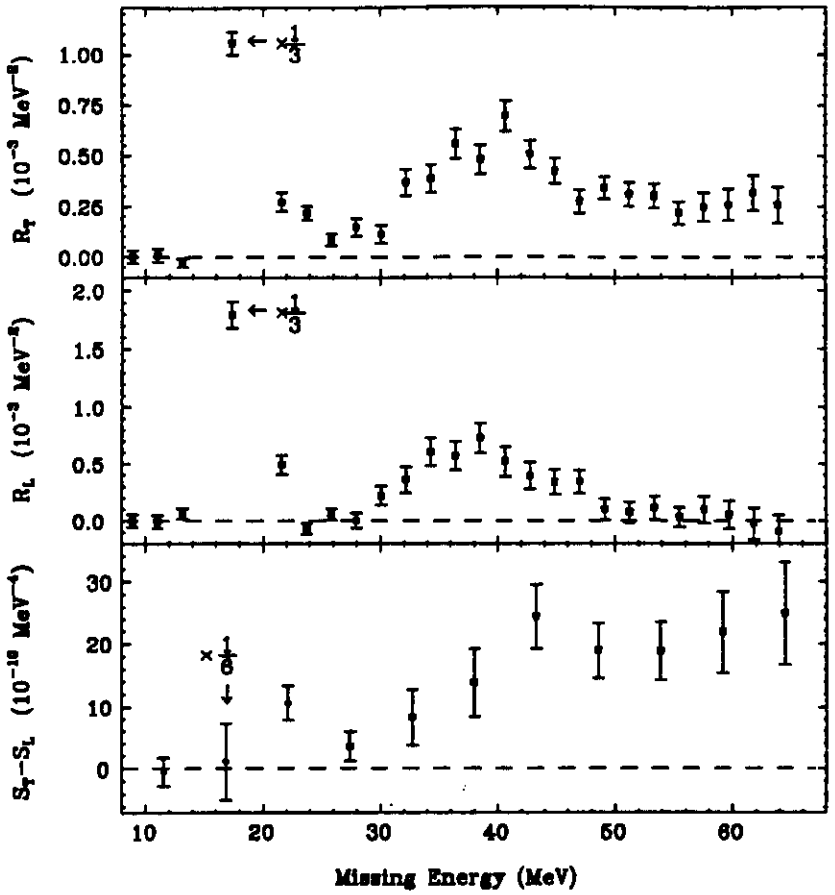

Figure 2. *Separated $^{12}C(e,e'p)$ response functions and their difference for kinematics near the quasielastic peak: q = 400 MeV/c and ω = 120 MeV.*[4] *Transverse (top) and longitudinal (middle) response functions and the difference in the spectral functions (bottom) vs. missing energy.*

(i.e., the region between the quasifree and Δ-excitation peaks seen in Figure 1) has long been recognized as having substantially too much strength to be reconciled with a one-body process. There is a similar excess of strength on the low-ω side of the quasielastic peak. The longitudinal quasielastic response function, whose integrated strength is subject to the charge sum rule (within "conventional" nuclear models), is known experimentally to have significant missing strength, at least for A$\geq$12. The ratio of transverse and longitudinal response functions does not agree with quasifree expectations. In contrast to the longitudinal response, the transverse response in Figure 2 shows considerable additional strength well beyond the s-shell knockout peak, characteristic of a non-quasifree process. Consequently, it is clear that two-body, and possibly many-body, effects must come into play. These may be associated with nuclear ground state correlations not contained in the mean field picture, with final state interactions (FSI), or with explicit involvement of sub-nucleon degrees of freedom (e.g., multi-body currents or modified nucleon structure). The focus of our review will be presentation of the evidence for such effects.

In Chapter II, we present a selected set of inclusive and coincidence data, principally for A=3 and A=12 targets. These data will serve to define the limits of the quasifree picture more quantitatively than was done above. In Chapter III, we extend the discussion to encompass specific dynamical mechanisms thought to be important in going beyond

the quasifree picture.

II. Quasifree Processes in Light Nuclei

As suggested above, the quantitative shortcomings of the quasifree picture came into sharper focus only with the experimental separation of the longitudinal and transverse response functions. The underlying framework is provided by the familiar plane wave Born approximation Rosenbluth formula for inclusive scattering

$$\frac{d^2\sigma}{d\Omega d\omega} = \sigma_M \left\{ \left(\frac{Q^2}{q^2}\right)^2 R_L(q,\omega) + \left[\frac{1}{2}\left(\frac{Q^2}{q^2}\right) + \tan^2\theta/2\right] R_T(q,\omega) \right\} \tag{1}$$

where σ_M is the Mott cross section, ω is the electron energy loss, and $Q^2 = (q^2 - \omega^2)$ is the four-momentum transfer squared. Separation of the response function is particularly informative because R_L and R_T are sensitive to rather different physics beyond quasielastic scattering. In particular, the transverse response function is sensitive to the "long range" aspects of sub-nucleon degrees of freedom, namely pion exchange and Δ-excitation. Consequently, R_L, which basically samples the nuclear charge response, is preferable for quantitative tests of the wavefunction, particularly those emphasizing short-range properties (e.g., nucleon-nucleon correlations). In addition, the integral over all energy transfer of the charge response function is subject to the Coulomb sum rule

$$C(q) = \int_{0+}^{\infty} \frac{R_L(q,\omega)}{|\bar{F}_N(Q^2)|^2}\, d\omega = Z\left[1 - F_{el}^2(q)\right] + Z(Z-1)C^{(2)}(q) \quad , \tag{2}$$

where the integration starts at inelastic threshold, the (measured) nuclear elastic form factor (with the proton form factor divided out) is denoted by F_{el}, the denominator of the integrand consists of the square of nucleon form factors modified by a relativistic correction,[5] and $C^{(2)}(q)$ is the Fourier transform of the proton-proton correlation function:

$$\begin{aligned} C^{(2)}(q) &= \int d\vec{r}_1 d\vec{r}_2\, e^{i\vec{q}\cdot(\vec{r}_1-\vec{r}_2)} \left[\rho^{(2)}(\vec{r}_1,\vec{r}_2) - \rho(\vec{r}_1)\rho(\vec{r}_2)\right] \\ &= \rho^{(2)}(\vec{q},-\vec{q}) - F_{el}^2(q) \quad . \end{aligned} \tag{3}$$

The two-body and one-body densities are determined by the many-body ground state wavefunction $\Psi_0(\vec{r}_1,\ldots,\vec{r}_A)$:

$$\begin{aligned} \rho^{(2)}(\vec{r}_1,\vec{r}_2) &= \int d\vec{r}_3 \ldots d\vec{r}_A\, |\Psi_0(\vec{r}_1,\ldots,\vec{r}_A)|^2 \\ \rho(\vec{r}_1) &= \int d\vec{r}_2\, \rho^{(2)}(\vec{r}_1,\vec{r}_2) \quad . \end{aligned} \tag{4}$$

Thus, the sum rule measures the nuclear charge Z modified by correlation effects, which are expected to be fairly small at large momentum transfer. Note that the applicability of free-space nucleon form factors is explicitly assumed in performing the integral in Equation (2). It is also important to stress that $C(q)$ is a static quantity, determined entirely by the nuclear ground state wavefunction, and is thus considerably easier to calculate theoretically than the dynamic response function $R_L(q,\omega)$.

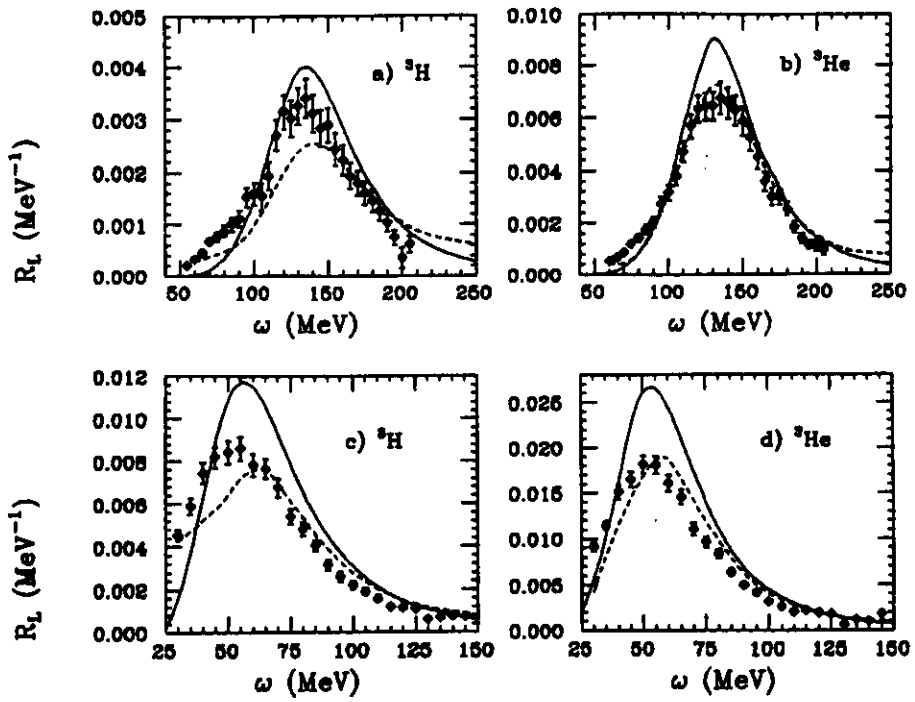

Figure 3. *The longitudinal response functions*[2] *for A=3.* ^3H *at* $|\vec{q}|$*=500 MeV/c (a) and 300 MeV/c (c).* ^3He *at* $|\vec{q}|$*=500 MeV/c (b) and 300 MeV/c (d). The solid (dashed) curves are the calculations of the Hannover*[6] *(Illinois*[7]*) group.*

1. The A=3 System

We start our more detailed review of the data by considering the A=3 system for several reasons. For such a light system, the theoretical formalism is more developed, allowing more quantitative comparison with experiment than is possible for heavier nuclei. Coulomb corrections are clearly less problematical in extracting the experimental data. The availability of data on both members of the isotopic mirror pair ^{3}H and ^{3}He presents insights into the reaction dynamics. The average density in the A=3 system is approximately a quarter of nuclear matter density (i.e., roughly half that of light and medium weight nuclei) and thus large enough to support at least some of the two-body processes which may be suggested in heavier nuclei.

A. Inclusive Scattering

The ^{3}H and ^{3}He longitudinal[2] and transverse[8] response functions for q = 300 and 500 MeV/c are shown in Figures 3 and 4. We start with a discussion of the longitudinal response.

The longitudinal response functions shown in Figure 3 clearly have the general characteristics expected for quasielastic scattering. The free nucleon recoil energies for q = 300 and 500 MeV/c are 47 and 125 MeV, respectively. The response functions scale with Z to a very good approximation. The Coulomb sum rule obtained by integrating over energy transfer is shown in Figure 5.[2][9] The contribution to the integral coming from the energy transfer region beyond the last data point is determined by adding an exponential tail fit to

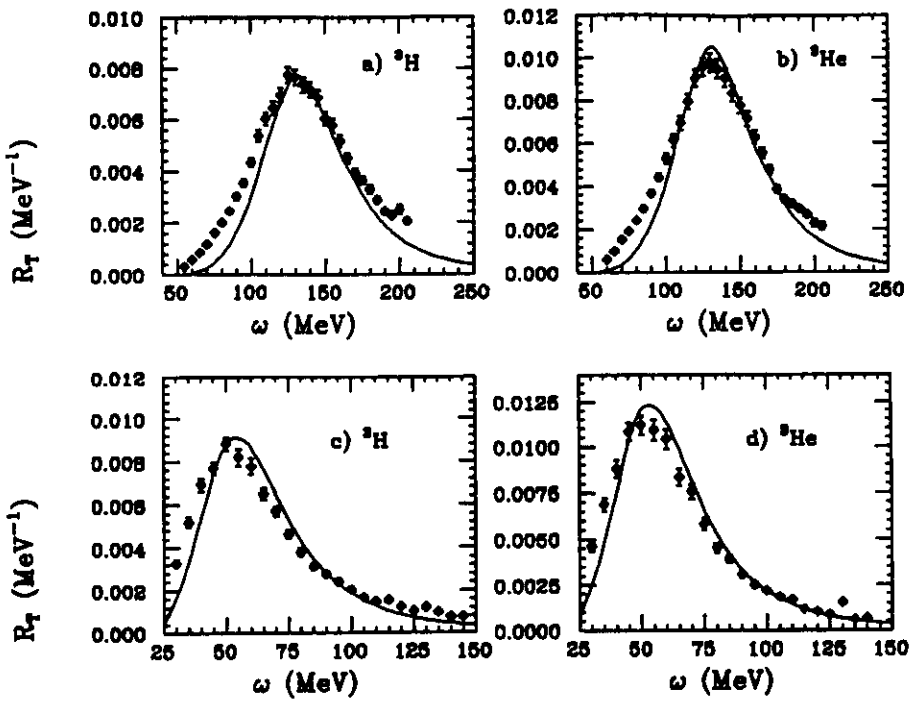

Figure 4. *The transverse response functions*[2] *for A=3.* ^3H *at* $|\vec{q}|$*=500 MeV/c (a) and 300 MeV/c (c).* ^3He *at* $|\vec{q}|$*=500 MeV/c (b) and 300 MeV/c (d). The curves show the calculations of the Hannover group.*[6]

the last few data points. The resulting tails are consistent with the energy-weighted sum rule analysis of Schiavilla *et al.*[10] and, for momentum transfers greater than 300 MeV/c, the contribution to the sum from the extrapolation is less than five percent.[11] Using Equations (2) and (3), Beck[11] has extracted the proton-proton density shown in Figure 6. The calculation shown[12] is based on solution of the three-body Faddeev equations using the Argonne v_{14} NN potential and the Urbana model-VII three-nucleon interaction. The qualitative behavior of the data is reproduced, although the data suggest that the coordinate space density at very small proton-proton separations might be smaller than that calculated.

The comparison between theory and experiment is far less favorable for the dynamic response function itself. Neither the Illinois calculations[7] (dashed curves) nor those of the Hannover group[6] (solid curves) shown in Figure 3 can reproduce the distribution of strength, particularly for ^{3}H. Given the impressive success of the Illinois calculation discussed above for the sum rule, we assume that the problem resides in the approximate form taken for the final states (recall that the sum rule needs only the exactly calculated ground state wavefunction). They have constructed the final states by successive orthogonalization, apparently leading to significant errors for the three-body continuum. Since the contributing ^{3}H final states are essentially all in the three-body continuum (in contrast to the substantial p-d channel for ^{3}He), we assume that this is the origin of the problem rather than any breakdown of the underlying "conventional" picture of nuclear dynamics. However, there is also a persistent underestimation of the low-ω strength, in both R_L and R_T, that appears to result from the neglect, in plane wave impulse approximation (PWIA)

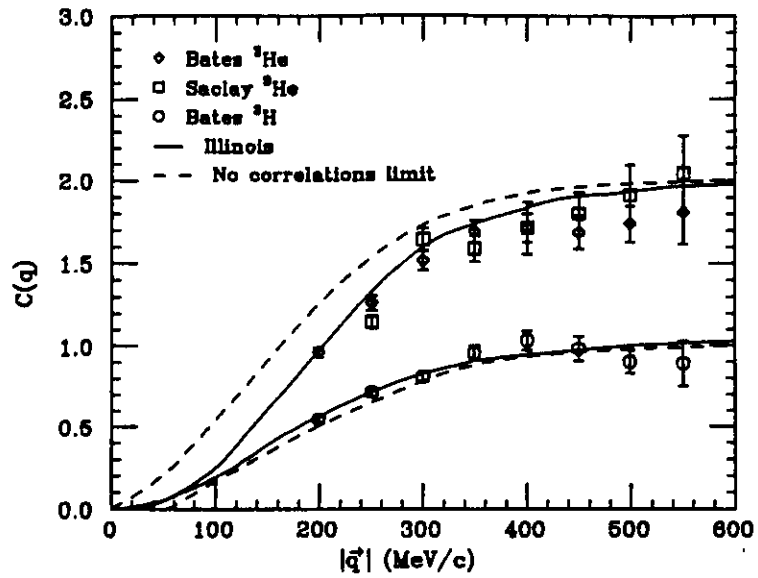

Figure 5. *The Coulomb Sum Rule in the three-body systems.*[2][9]

plus FSI calculations, of the (e,e′d) contribution to the p-d breakup channel (this problem remains even in high Q^2 data on ^{3}He(e,e′) measured at SLAC).[13] This effect appears to be reasonably well understood theoretically as will be seen below. Nevertheless, complete solution of the continuum three-body problem remains an important theoretical goal for permitting precision tests of the underlying dynamics.

B. Coincidence Studies

Given the apparent success in describing static ground state correlations for A=3, we turn to ^{3}He(e,e′p) coincidence studies.[14] By measuring the momentum and energy of the outgoing nucleon, additional information can be obtained concerning the reaction dynamics and target structure. This is indicated schematically in Figure 7.

In the plane wave impulse approximation, the inclusive cross section is proportional to the nuclear spectral function times an (off-shell) electron-nucleon cross section:

$$\begin{aligned}\sigma_{PWIA} &= \int d\vec{p}\, dE\, \sigma_{eN}\, S(\vec{p},E)\, \delta\left(\omega + E - \sqrt{M^2 + (\vec{p}+\vec{q})^2}\right) \\ &\approx \sigma_{eN}\, R(q,\omega) \quad .\end{aligned} \tag{5}$$

The spectral function gives the probability to find a nucleon with momentum $\vec{p}$ and energy E in the nucleus; the integral over energy gives the momentum distribution:

$$n(p) = \int dE\, S(\vec{p},E) \quad . \tag{6}$$

We show the results of a Faddeev calculation[6] of the ^{3}He spectral function in Figure 8.

Note that there is substantial strength out to and beyond 100 MeV of excitation energy and that the large E tail is especially pronounced for large momenta. This may

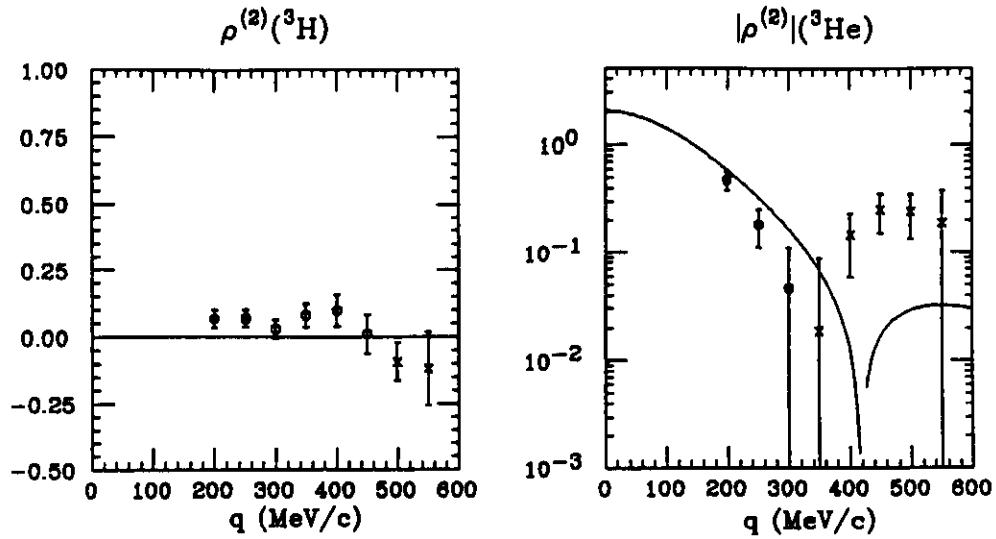

Figure 6. *Proton-proton density in ^3H and ^3He extracted[11] from data of ref.[2]. Crosses indicate negative density.*

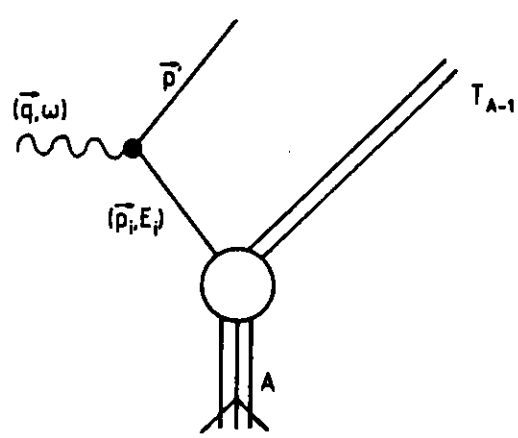

Figure 7. *Schematic illustration of the impulse approximation for (e,e′p).*

be seen more easily in Figure 9, where we show the momentum distribution[15] obtained by integrating the spectral function over a finite energy interval:

$$n(p, E_{max}) \equiv \int_0^{E_{max}} dE\, S(\vec{p}, E) \quad . \tag{7}$$

For momenta above 300 MeV/c, a substantial fraction of the total strength lies at large excitation energy. This is consistent with the picture that the largest momenta are generated by "back-to-back" short range collisions of two nucleons, so that the excitation energy is effectively the energy of the recoiling partner; e.g., for $p = 2$ fm^{-1}, the nucleon kinetic energy is greater than 80 MeV.

Marchand *et al.*[14] investigated this experimentally through the ^{3}He(e,e′p) reaction, separating the two-body pd final state and the three-body continuum states. They extracted the missing energy spectra and the momentum distributions shown in Figure 10. The missing energy spectra indeed show considerable strength in the three-body breakup regime. The centroid of the strength moves to larger missing energy as the missing momentum increases, suggestive of the picture described above. The momentum distributions

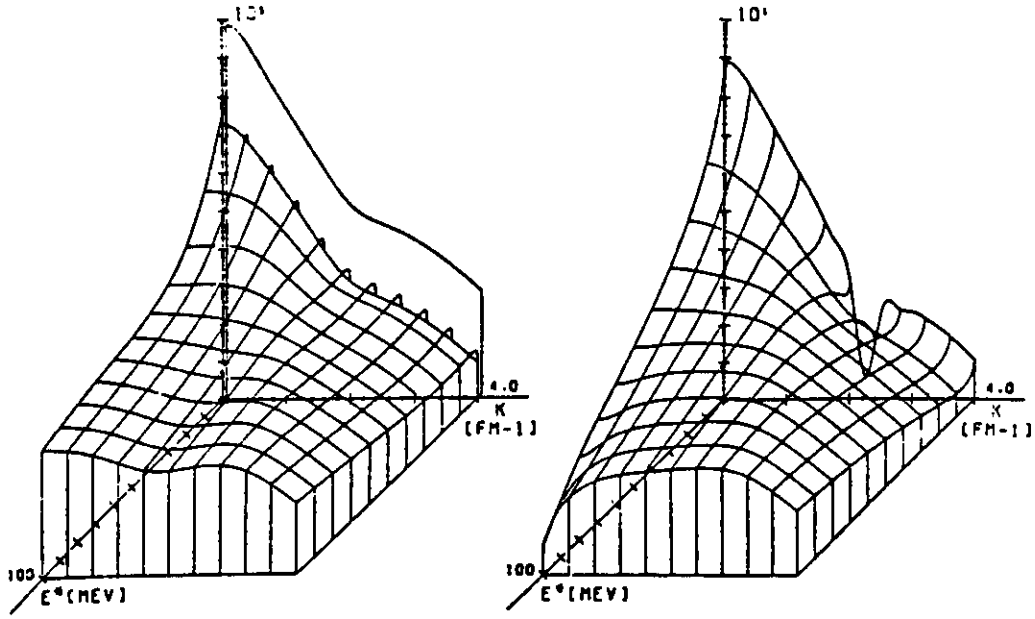

Figure 8. *Spectral function for ^{3}He.[6] The left (right) panel is for T=0 (T=1). The solid line at low E in the T=0 channel is the two-body p+d breakup.*

extracted from the two-body breakup channel fall rapidly, in quantitative agreement with expectations based upon the Faddeev wavefunction. However, for momenta above ~300 MeV/c, the momentum distribution extracted from the three-body channel is dominant and follows very closely the momentum distribution extracted from deuteron electrodisintegration.

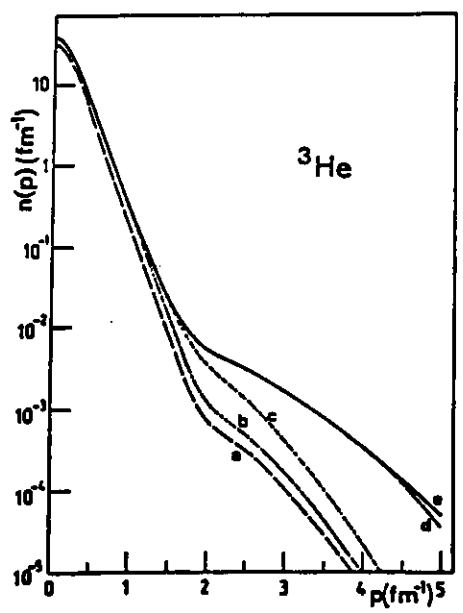

Figure 9. *The proton momentum distribution in ^{3}He.[15] Curve (a) shows the contribution of the two-body p+d breakup channel while curves (b), (c) and (d) result from integrating the continuum strength up to 12, 50 and 300 MeV respectively. The full n(p) obtained by integrating to infinity is indicated by the solid curve (e).*

Recall that the PWIA underestimated the inclusive cross section in ^{3}He at low ω. This is the region near $x = 2$, i.e., which kinematically corresponds to quasifree deuteron

knockout. There are then two coherent mechanisms present in the two-body breakup channel. The dominance of the coupling to nucleon pairs that emerge as deuterons has been observed at NIKHEF in the ^{3}He(e,e'd) reaction.[16] The data at a fixed $|\vec{q}|$=380 MeV/c are shown as a function of initial momentum in Figure 11. The calculations by van Meijgaard and Tjon[17] that treat the direct deuteron knockout mechanism describe the data quite well while the pure PWIA result (not shown) is three orders of magnitude lower. All of the results support the picture based upon Figures 8 and 9. Weighing both the inclusive and coincidence data, we can conclude that a rather satisfactory understanding of the basic reaction-dynamics and A=3 correlation structure has been achieved within the conventional framework when modern nuclear forces are employed.

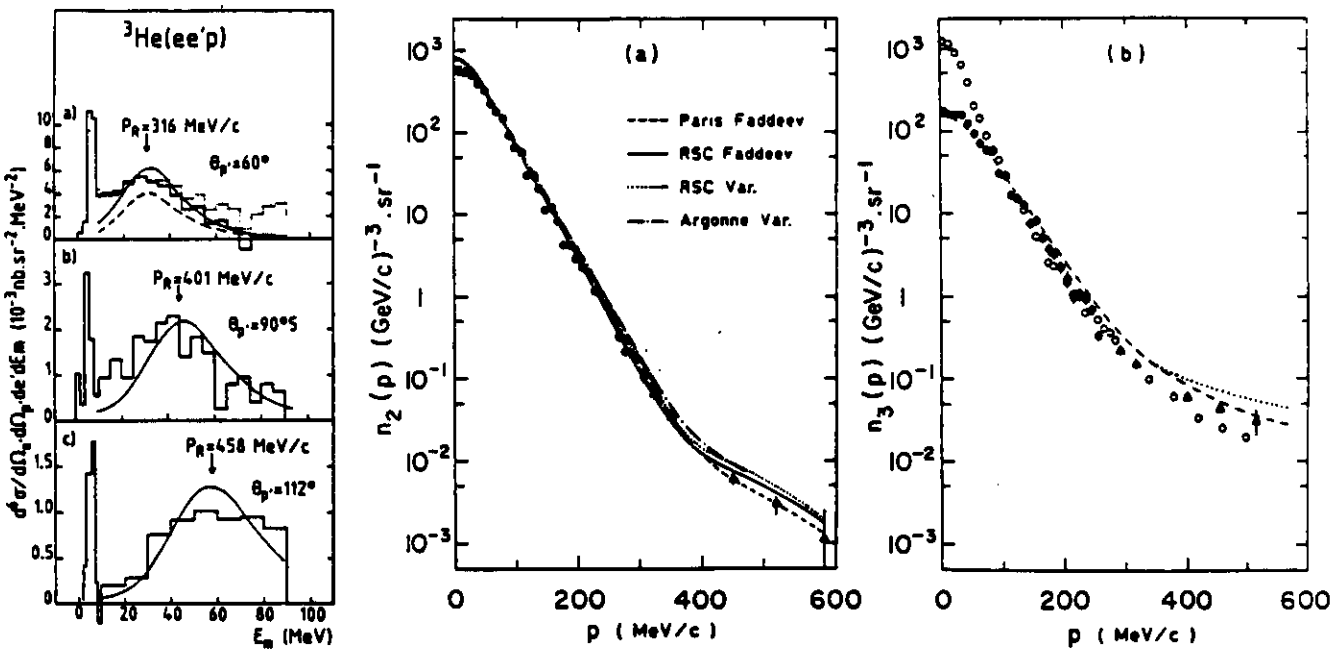

Figure 10. *Left: Missing energy spectra for the ^{3}He(e,e'p) reaction. Right: The experimental proton momentum distribution for the two-body (a) and three-body (b) breakup channels in ^{3}He.*[14][18] *Note the dominance of the three-body breakup channel for large momenta and its similarity to the deuteron electrodisintegration data (open circles).*[19]

2. A=12

Anchored by our phenomenological understanding of the general features of the A=3 response, we turn our attention to heavier nuclei, where many-body effects may be expected to be more prominent. A number of inclusive and coincidence experiments have by now been carried out at Saclay, Bates and NIKHEF on various nuclei, and we must be selective in presenting data. We shall focus on ^{12}C, a target for which all three laboratories have contributed to an extensive data set. The global features of the response are best known experimentally for this case. Other data will be introduced when needed to emphasize new phenomena.

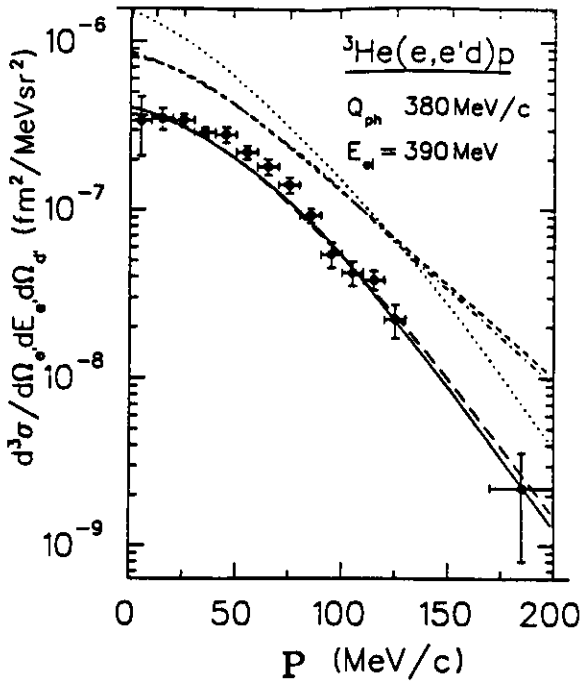

Figure 11. *The ^{3}He(e,e'd) cross section vs. initial momentum at a fixed momentum transfer of 380 MeV/c.*[16] *Curves are from ref.*[17]

A. Inclusive Scattering

Figure 12 shows the longitudinal and transverse ^{12}C inclusive response function[20] for three different momentum transfers. For convenience, these are shown as functions of the scaling variable y.[21] For a nonrelativistic Fermi gas, this is just the longitudinal component of the struck nucleon's momentum

$$y_{nr} = \frac{\omega - q^2/2M}{q/M} \quad , \tag{8}$$

and the Fermi gas response function (for $q \geq 2k_F$) can then be written in the scaling form

$$\frac{q}{M} R_{FG}(q,\omega) = f(y) \equiv \int_{|y|}^{\infty} p dp\, n(p) \quad . \tag{9}$$

To set a scale, we note the width of the Fermi gas quasielastic peak at half-maximum $\Delta y = \sqrt{2}k_F \approx 300$ MeV/c for ^{12}C, in reasonable agreement with the f_L shown in Figure 12. Extensive discussions about corrections to this oversimplified y-scaling analysis are summarized elsewhere in this volume. Our only point here is to emphasize that the kinematic analysis at the root of the scaling seen in the quasielastic region clearly argues for a simple quasielastic reaction dynamics. For example, ω at $y = 0$ differs by more than a factor of two for $q = 400$ and 600 MeV/c, and the peak heights have been scaled by q. The inapplicability of the scaling analysis to the dip and Δ regions are, of course, expected.

The first major problems appear in addressing the magnitude of the response functions. The integral of the longitudinal response function is to be compared with Equation (2). For ^{12}C, it falls short of the "no-correlations sum rule" by about 20%; the shortfall may be even larger for heavier nuclei, as seen in Figure 13.[20][22] Uranium seems not to follow the general pattern established by the other heavy nuclei.

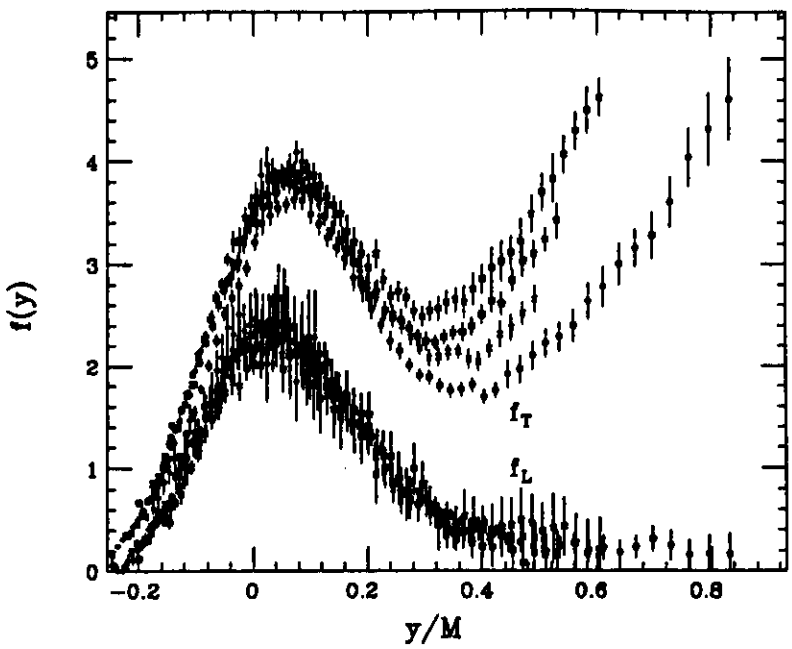

Figure 12. *Longitudinal and transverse scaling functions in $^{12}C(e,e')$[21] for momentum transfers of 400, 450, 500, 550 and 600 MeV/c.*

These discrepancies are well beyond any realistic expectation about the effect of correlations (assuming that the all of the longitudinal strength is included in the experimental integrals) and so lead to two generic classes of attempts at explanation. One approach argues that appreciable response function strength is spread out over a much greater region of energy transfer than anticipated on the grounds of single particle models. Mechanisms such as final state interactions and short-range correlations would work in this direction. The conclusion would then be that the missing longitudinal strength has escaped detection. The only data[23] which have explored far into the tail region are shown in Figure 14; the solid lines represent tails consistent with energy-weighted sum rules. An estimate based on the data would assign an additional 0.00±0.05 to the sum rule in ^{12}C and 0.03 ± 0.04 in ^{56}Fe. This can be compared with the expectations from the theoretical tails of an additional ~ 0.1 in ^{12}C and ~ 0.2 in ^{56}Fe although, as can be seen in Figure 14, these tails are not significantly above the data. Baran *et al.*[23] tentatively conclude that insufficient strength has been found to resolve the sum rule problem, but we feel that additional experiments will be needed to make this conclusive.

The second general approach lies in questioning the validity of the conventional framework and thus of the sum rule, Equation (2). The possibility of increased in-medium proton size has been suggested in this context. We shall evaluate the status of both approaches in the next chapter, but must present additional data before drawing far-reaching conclusions about breakdown of the traditional framework. The considerable success witnessed in describing the A=3 system reinforces this caution.

The second problem posed by Figure 12 lies in the ratio of the transverse and longitudinal response functions. The scaling functions $f_{L,T}(y)$ were defined[21] so that they

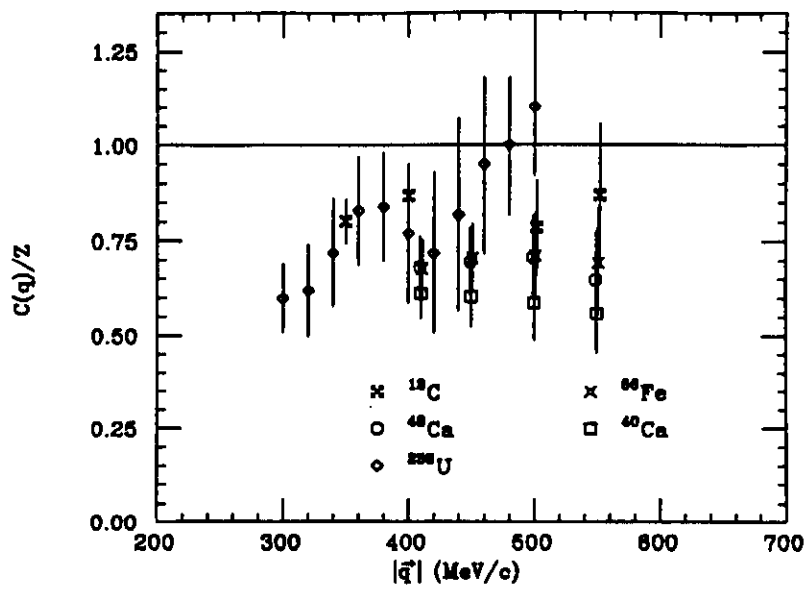

Figure 13. *The Coulomb Sum, divided by Z, for a variety of heavier nuclei.*[20][22]

would be equal if the impulse approximation were valid:

$$\begin{aligned} R_L^{nuclear} &\propto \left(Z R_L^{proton} + N R_L^{neutron}\right) f(y) \\ R_T^{nuclear} &\propto \left(Z R_T^{proton} + N R_T^{neutron}\right) f(y) \quad . \end{aligned} \tag{10}$$

The dip and Δ cross sections clearly suggest a background underneath the quasifree peak in $f_T(y)$ which is not related to quasielastic scattering. However, even if this is subtracted by assuming a reasonable extrapolation from the higher energy loss data, the residual transverse response would be roughly 25% bigger than the longitudinal response at the quasielastic peak. (We must caution, however, that one cannot simply add one-body and two-body mechanisms in the inclusive response.) It is interesting to note that $f_L < f_T$ appears to "turn on" at A=4 as shown by the ^{3,4}He data in Figure 15.[24] Theoretically, the need for extra transverse strength in A= 4 was pointed out by Schiavilla in a sum-rule analysis of the A= 2, 3 and 4 systems.[25]

The dip and Δ regions are seen from Figure 12 to be essentially entirely transverse. We also see from Figure 1(a) that for $A \geq 4$ the yield in the dip region is only weakly A-dependent. However, it, like f_T/f_L, increases rapidly from A=2 to A=4.[26]

The quasifree picture clearly assigns the Δ excitation strength to the transverse response function. Figure 16 shows the entire Δ region,[1] together with a Δ-hole calculation[27] constrained by pion scattering. The substantial spreading of the Δ peak in comparison with that seen for hydrogen is reproduced, although too little strength is predicted throughout the Δ-region. We will return to a more detailed discussion about this calculation in the next chapter. Nevertheless, it is clear that the major discrepancy appears in the dip region where the one-body quasifree processes are small. The large excess strength obviously suggests that other degrees of freedom are at work, perhaps two- or multi-body processes. The failure of meson exchange currents[28] (MEC) and Δ-hole[27] calculations to sufficiently augment the strength in the dip region points to the involvement of new cur-

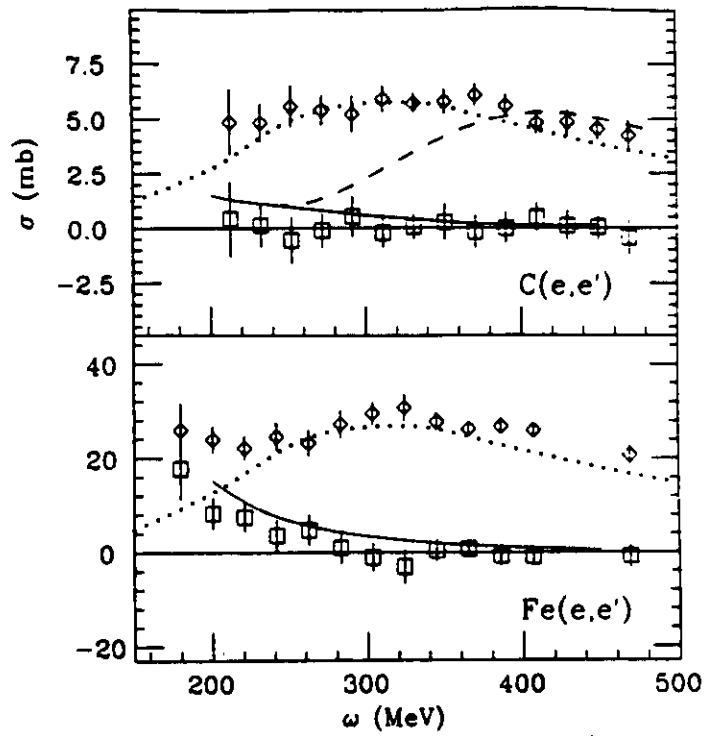

Figure 14. *Cross sections for longitudinal (squares) and transverse (diamonds) photon absorption vs. photon energy. The data are from NPAS and span the energy range from the dip region to beyond the Δ resonance.*[23]

rents and/or reaction mechanisms. The purely transverse nature of the strength suggests the involvement of pions in the multi-nucleon processes.

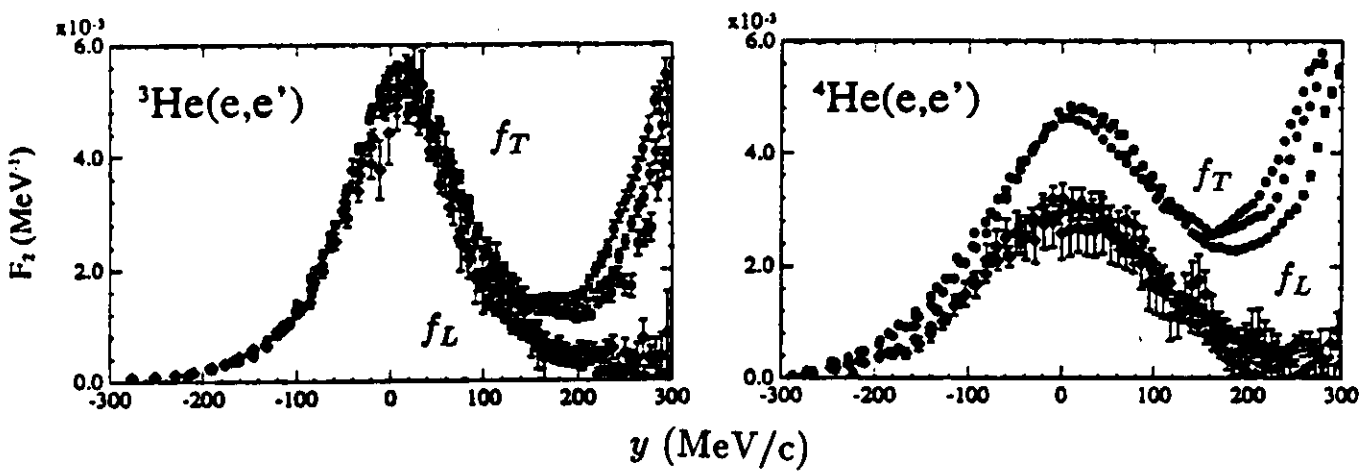

Figure 15. *Longitudinal and transverse scaling functions in ^{3,4}He for $400 < q < 600$ MeV/c.*[24]

In summary, the inclusive data present a host of problems already for a nucleus as light as ^{12}C. Qualitatively, all of these problems persist (and are sometimes quantitatively more severe) for heavier systems and may, to a large extent, already be present for ^{4}He![24] We obviously must look at the phenomenology of coincidence cross sections for additional insight into the reaction processes.

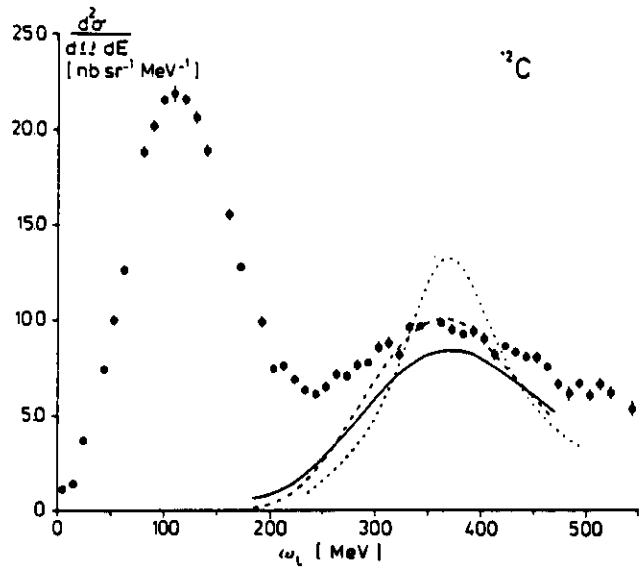

Figure 16. *Δ-hole calculations[27] of $^{12}C(e,e')$ at $E_0 = 730$ MeV and $\theta_e = 37°$. Solid curve: Full calculation including Δ spreading potential, long-dashed curve: no spreading potential, short-dashed curve: sum of free nucleon cross sections.*

B. Coincidence Studies

Figures 2, 17 and 18 show the missing energy spectra[4] [29][30] for $^{12}C(e,e'p)$ for $q \approx 400$ MeV/c as one passes over the dominant features of the response function. The missing energy is defined simply as $E_m = (\omega - T_p)$, where T_p is the kinetic energy of the detected proton. All three spectra are in parallel kinematics (i.e., the proton emitted along $\vec{q}$), so there are no interferences between longitudinal and transverse responses. Each of the three figures corresponds to a fixed electron kinematics: Figure 2 is close to the quasielastic peak ($y/M \approx 0.1$); Figure 17 is in the dip region ($y/M \approx 0.35$); Figure 18 is in the Δ region ($y/M \approx 0.75, 1.1$). See Figure 12 to relate y to the various response function features.

The longitudinal response seen in Figure 2 looks quite simple. The p-shell and s-shell removal peaks are seen clearly and there is no additional strength visible above 45 MeV missing energy. The s-shell hole is appropriately broadened because of its large excitation energy. In other words, the response looks appropriately one-particle-like, although, as already pointed out for the inclusive response, the strength is somewhat too low. The transverse response is quite different in that, in addition to p-shell and s-shell strength, there is a substantial continuum extending to the largest missing energies measured. The difference of the two responses is also shown. Recall from Figure 12 that the transverse response is about 50% larger than the longitudinal for these electron kinematics. Yet the difference spectrum is consistent with no single particle structure at all, as would be expected in impulse approximation. Given the error bars, one could not rule out ~15% greater transverse p-shell strength and some hint of excess transverse s-shell strength as well. Nevertheless, it is clear that these single particle responses, particularly the p-shell, are much closer to the impulse approximation L/T ratio than are the inclusive spectra. It should also be noted that the ratio of transverse to longitudinal inclusive scaling functions, $f_T(y)/f_L(y)$, can be made consistent with these data by simply extending the flat transverse yield to about 80 MeV in missing energy, about 15 MeV beyond the

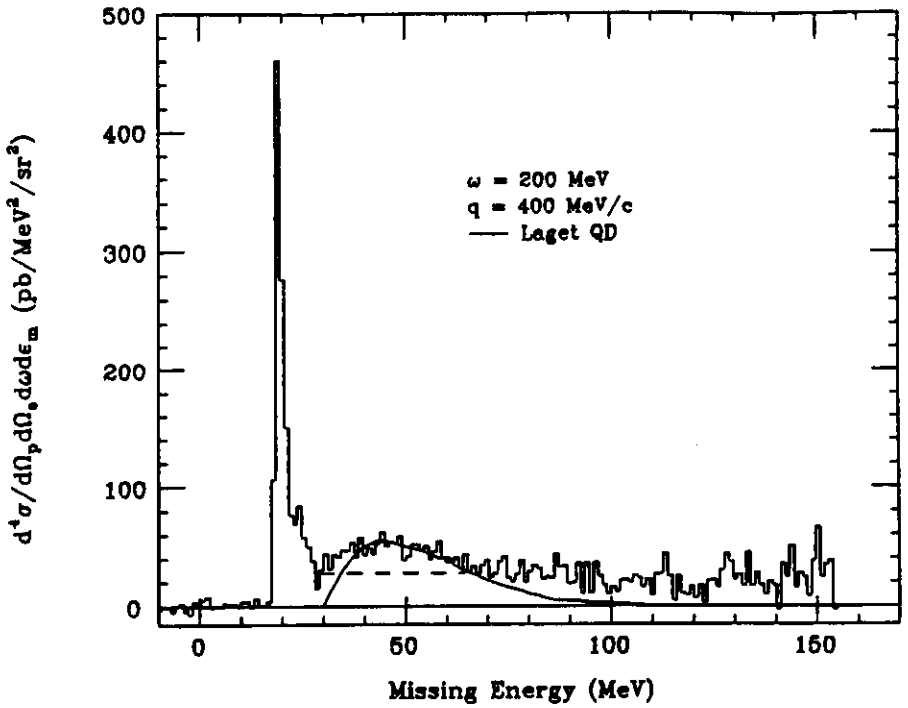

Figure 17. *Missing energy spectrum for $^{12}C(e,e'p)$ in the dip region.*[27] *The area above the dashed line is attributed to $1s_{1/2}$ proton knockout while the solid curve shows the quasideuteron model result of Laget.*[29]

measurement, but allowed by the kinematics with $\omega = 120$ MeV. If the angular distribution (relative to $\vec{q}$) of the supposed two-body transverse piece is broader than the one-body (e,e'p) distribution, then a lesser extension of the data in E_m is required.

The important role played by the continuum is evidenced by the observation that the difference shown in Figure 2 starts increasing above $E_m = 28$ MeV, the threshold for two-nucleon emission. A measurement of ^{12}C(e,e'p) at NIKHEF[30] confirms the increased transversality and its missing energy dependence. This effect has also been observed in another NIKHEF experiment[31] on ^{6}Li(e,e'p) where the 2N threshold is only 8 MeV compared to 28 MeV in carbon. The NIKHEF results are shown in Figure 19. In all cases, the increased transversality is associated with the two-nucleon knockout threshold. One concludes that the dominant part of the inclusive differences resides in the additional two- (or many-) body strength. Near the quasifree peak, the influence of MECs and the Δ are even smaller than in the dip region so again new processes, essentially entirely of transverse character, are likely to be required. It is not unreasonable to associate them with the same processes responsible for the excess yield in the dip region.

The Q^2 dependence of the L/T ratio has also been investigated for the $1p_{3/2}$ knockout from ^{12}C. The data[4][32] (and similar data for ^{6}Li) are shown in Figure 20. The plot shows $R_G \equiv [(2M^2q^2/Q^2)(R_T/R_L)]^{1/2}$, which is just equal to $\mu_p = 2.79$ in impulse approximation. Clearly, the data favor a value 15% to 20% above the impulse value.

Turning to the dip region data of Figure 17, we recall that the inclusive data already determine the response function here to be almost purely transverse. We again see a large

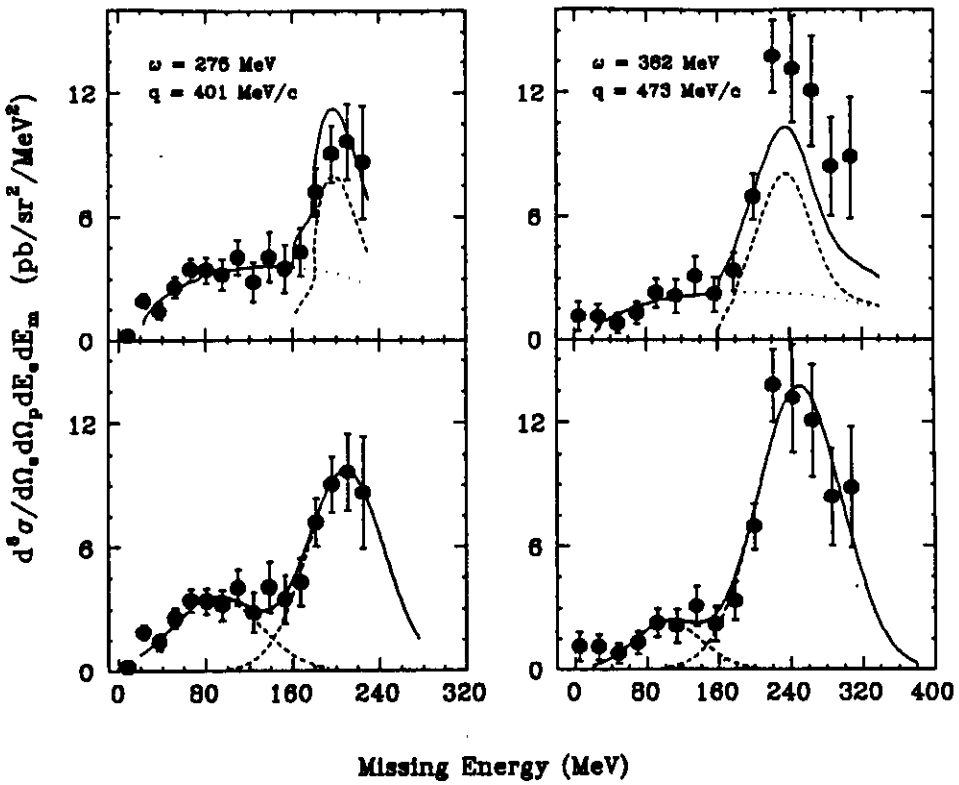

Figure 18. *Missing energy spectra obtained in the region of the Δ resonance.*[30] *Kinematics I (left) corresponds to a point approximately halfway between the dip region and the Δ peak while kinematics II (right) are at the maximum of the peak. In the lower half of the figure the curves are Gaussian fits while the upper half shows the results of a quasifree pion production calculation (dashed) along with the phase space for two nucleon knockout (dotted) and their sum (solid).*

missing energy tail extending to the limits of the data. The area above the dashed curve is attributed to $1s_{1/2}$ knockout. We shall argue in the next chapter that the solid curve indicates the region in missing energy populated by any two-body process, so that three- (or more-) body currents must be dominating the highest missing energy response and indeed making a substantial contribution to the total.[35]

The missing energy spectra in the Δ-region, Figure 18, show two distinct peaks. The left hand panel, kinematics I, corresponds to electron kinematics halfway between the dip and peak; the right hand panel, kinematics II, corresponds to the peak. The dashed curves are Gaussian fits to the data. The peak for $E_m \geq 160$ MeV, that is, for a missing energy greater than the pion mass, follows the kinematics of quasifree Δ production and decay $\gamma^* + N \rightarrow \Delta \rightarrow N + \pi$. The lower missing energy peak does not permit a pion in the final state and follows the kinematics of direct emission of a correlated pair; this is the "quasideuteron" mechanism $\gamma^* +$ "d" $\rightarrow n + p$. The quasideuteron peak is relatively more important for lower energy transfer. It is similar to the two-body pion absorption process studied extensively with pion beams. The pion absorption studies have revealed a large component of multi-nucleon absorption,[36] reminiscent of the result described above in the dip region. We also note that the results of Figure 18 are quantitatively very similar to the results of Homma *et al.*[37] and Kanazawa *et al.*[38] using tagged photons. Kanazawa

et al.[38] performed coincidence studies of $(\gamma, p\gamma), (\gamma, p\pi), (\gamma, pn)$ and (γ, pp). They found that (γ, pn) dominates the character of the small peak we call the quasideuteron peak. The large peak we associate with Δ production and pion emission indeed results predominantly in p-π pairs.

In the upper half of Figure 18, the data for the two kinematics are compared with an estimate[30] assuming quasifree delta production. That is, they assume

$$\sigma(e, e'p) = K\sigma'_{eN} S(p, E) \quad , \tag{11}$$

where K is a kinematic factor and σ'_{eN} is derived from the free nucleon processes $\gamma_v + p \rightarrow p + \pi^\circ$ and $\gamma_v + n \rightarrow p + \pi^-$ assuming only the M1 Δ amplitude. The results are shown by the dashed curves. They are considerably below the experimental yields. Although the Born terms and the E2 and other contributions to the Δ are neglected, these contributions roughly cancel the effect of neglecting final state proton absorbtion which is about 30-40%. A reasonable conclusion is that there is an additional process in the pion production region. This is supported by the significant yield in the (γ, pn) channel observed in this region.[38]

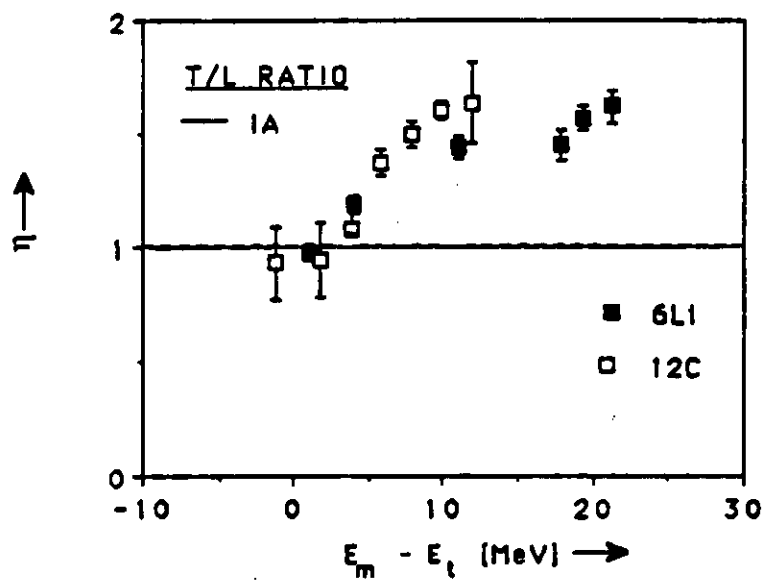

Figure 19. *Ratio of the transverse to longitudinal response function in* ^{12}C[32] *and* ^{6}Li[33] *vs. distance from two-nucleon emission threshold.*

The highest momentum transfer (e,e'p) data measured to date are at $q \approx 1$ GeV/c. The data[39] are shown in Figure 21. The higher energy loss data, $\omega = 470$ MeV, are very close to the quasielastic peak, while the $\omega = 330$ MeV data are about halfway down the low energy loss side of the peak. For these high momentum transfers, it must be noted that the cross sections are mostly transverse. The p- and s-shell knockout peaks are seen clearly and, once again for transverse response functions, an appreciable high missing energy tail is seen. The high missing energy strength ($50 \leq E_m \leq 150$ MeV) grows with q, increasing from 30% of the "one-body" yield at $q = 600$ MeV/c[40] to over 50% at $q = 1000$ MeV/c. Note, however, that no increased yield is seen at pion production threshold, implying that the tail of the Δ is unimportant and that any appreciable pion production must be a quasifree process and would occur only for $\omega \gtrsim 550$ MeV at $q = 1$ GeV/c.

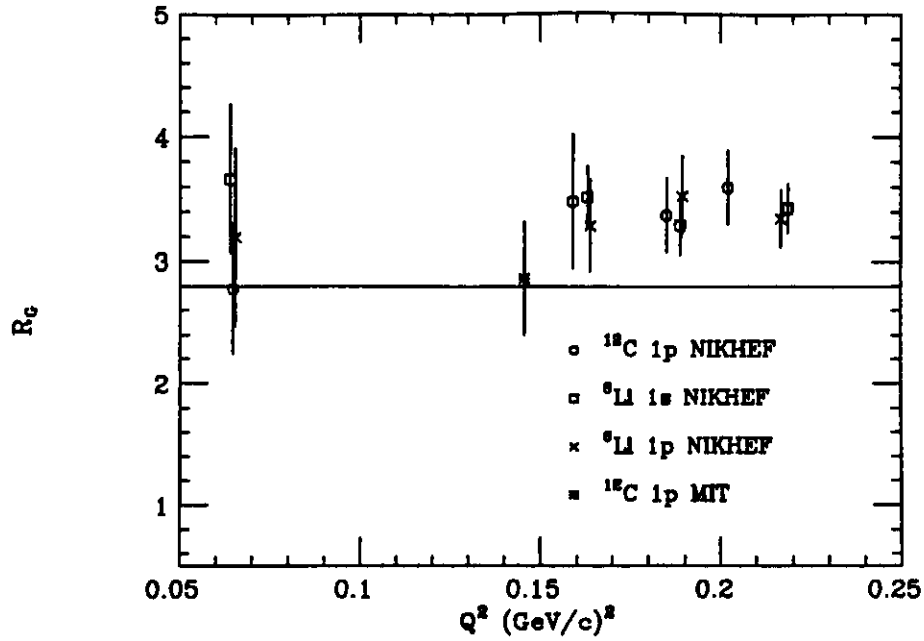

Figure 20. *Experimental results*[4][34] *of longitudinal/transverse separations in (e,e'p) on* ^{12}C *and* ^6Li *expressed as the ratio* R_G *(see text). The solid line indicates the free nucleon value of 2.79.*

These data provide a large lever arm for testing the q-dependence of the single particle process in comparison to quasifree expectations. The results are shown in Figure 22 for both ^{12}C[4][29][39][40] and ^{40}Ca.[41] Obviously, the data are consistent with an impulse approximation q-dependence, although the total strength is considerably below that of the simple shell model. At a purely phenomenological level, this result presents a major problem for the "swollen nucleon" hypothesis, since the central feature of that hypothesis is an accelerated falloff of nucleon form factors in the medium with respect to that in free space. We note that the data points for the s-shell in ^{12}C were obtained by summing the strength up to 45 MeV, where R_L goes to zero at q = 400 MeV/c. It is likely that non-one-body processes are still present beneath the s-shell and, if they could be removed, would lower the (predominantly) transverse "pure" s-shell data.

In concluding this chapter, we summarize the principal features uncovered by the global phenomenology of inclusive and coincidence experiments at large energy and momentum transfer for A$\geq$12:

(i) There is substantial missing strength in the experimentally measured longitudinal response, both inclusive and exclusive. The available coincidence measurements are characteristic of a single particle picture for the longitudinal response.

(ii) The transverse/longitudinal ratio is larger than predicted by the impulse approximation. In the quasielastic regime, the inclusive ratio is ~50% larger for ^{12}C at $q \approx 500$ MeV/c. However, the single particle piece measured in (e,e'p) is no more than ~20% larger, with the additional transverse strength generated by a two- or multi-body process. This reflects new currents and/or reaction processes, perhaps related to the multi-nucleon modes of pion absorption.

(iii) The single particle part of the nuclear response is evident in (e,e'p) experiments

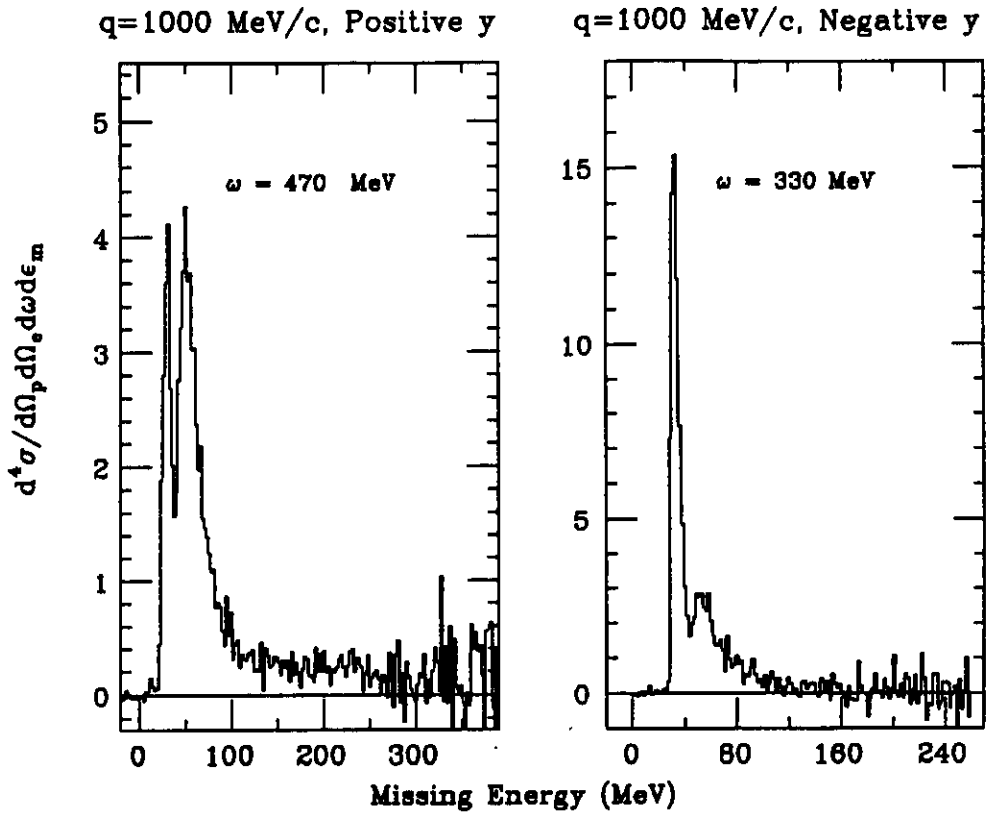

Figure 21. *Preliminary missing energy spectra*[39] *from* $^{12}C(e,e'p)$ *at* $|\vec{q}|$ *=1000 MeV/c. The spectrum on the left was obtained on the high-*ω *side of the quasielastic peak (positive y) while the one on the right is on the low-*ω *(negative y) side.*

carried out to the highest momentum transfers, ~1 GeV/c. The q-dependence is consistent with that of the impulse approximation, casting doubt on the simple "swollen nucleon" hypothesis.

(iv) In the dip region, we see a transverse strength appreciably larger than that explainable by the tails of one-body processes. The (e,e'p) missing energy spectrum indicates a strong multi-nucleon process, again suggestive of a pionic process.

(v) In the Δ region, we again see both the one-body quasifree process $\gamma^* + N \rightarrow \Delta \rightarrow N + \pi$ and a large multiparticle/pion annihilation process, at least part of which is associated with the quasideuteron process $\gamma^* +$ "d" $\rightarrow \Delta N \rightarrow np$.

(vi) Therefore, multi-nucleon processes are pervasive across the entire transverse response function while the much more kinematically limited longitudinal response function data show a dominant single particle character.

III. Dynamical Processes

A number of dynamical processes have been suggested as accounting for part of the difficulty summarized above. We give here an overview of several of these processes.

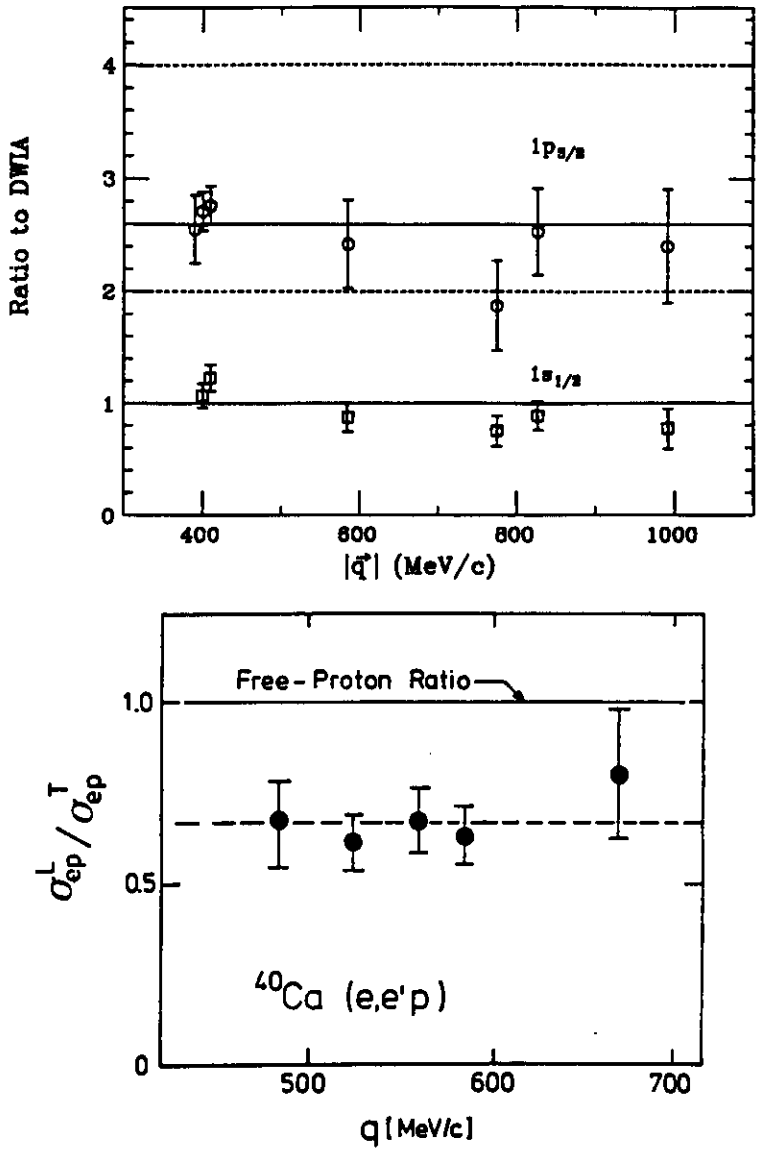

Figure 22. *Top: Ratio to DWIA calculations of the (e,e'p) cross sections for* $1p_{3/2}$ *and* $1s_{1/2}$ *proton knockout from* ^{12}C.[4][29][39][40] *The solid lines are a one-parameter fit to the data while the dashed line indicate the values expected on the basis of the simple shell model. Bottom: Ratio of longitudinal to transverse response in* $^{40}Ca(e,e'p)$.[41]

1. Final State Interactions

A. Quasielastic Region

We start our discussion of final state interactions by looking in the quasielastic region. Final state interactions of the knocked out nucleon with the residual nucleus are clearly of major importance for describing the (e,e'p) process. Attenuation of the "elastic" wave-function, as described by the optical potential, greatly reduces the cross section to specific hole states; this attenuation clearly becomes larger as the nuclear size increases. A direct (e,e'p) measurement of this was carried out;[42] the results, shown in Figure 23, indicate

a "mean free path" of about 5 fm, as expected. In fact, one gains some confidence in the various analyses since DWIA analyses of the (e,e'p) data, using realistic nuclear optical potentials, find missing shell model strength consistent with the missing longitudinal inclusive strength.

In contrast to this explicit account of final state interactions in the coincidence channel, almost all discussions of the inclusive response functions are based upon the impulse approximation. Since the inclusive response function is essentially a total cross section for (virtual) photon absorption, it is clear that final state interaction effects will not be nearly so dramatic as in the exclusive channel; the approximate scaling of the quasielastic cross section with the atomic number bears this out. Nevertheless, final state interactions do influence the inclusive cross section, and we examine their effect with respect to quasifree expectations for three problems: suppression of the longitudinal response function, the continuum yield in (e,e'p) and the enhanced transverse/longitudinal ratio.

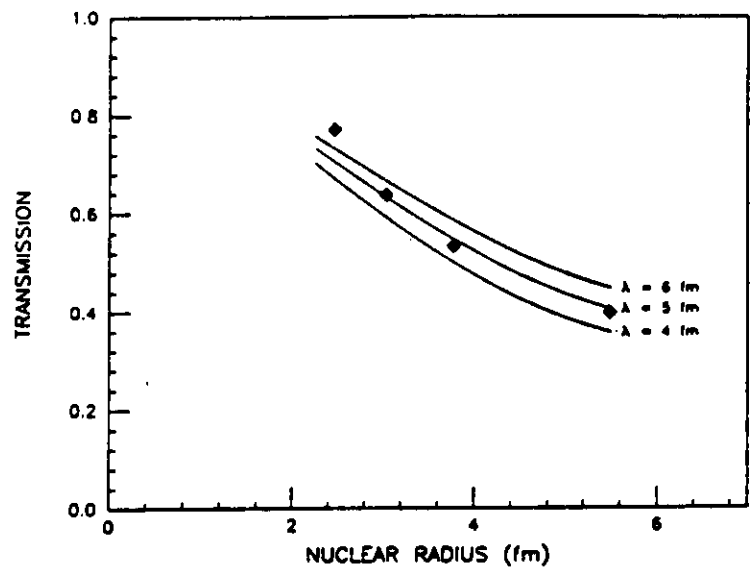

Figure 23. *Proton transmission, defined as the ratio of the (e,e'p) to the (e,e') cross section, vs. nuclear radius.*[42] *The solid curves represent classical attenuation calculations for three values of the nucleon mean free path.*

The suppression of the inclusive response function by final state interactions is most easily seen in the Green function approach.[43] The idea is to use the fact that the response function/total cross section can be rewritten via the optical theorem in terms of the elastic (virtual) photon forward scattering amplitude:

$$\begin{aligned} R(q,\omega) &\equiv \langle 0|\rho_q^\dagger \delta(\omega - H)\rho_q|0\rangle \\ &= -\frac{1}{\pi}\mathrm{Im}\langle 0|\rho_q^\dagger G(\omega)\rho_q|0\rangle \quad . \end{aligned} \tag{12}$$

The Green function for propagation in an optical potential can now be introduced[43] in a manner which preserves the sum rule but, of course, changes the response function. In order to get a qualitative idea about the effects, we make a crude evaluation of Equation

(12) in the Fermi gas model modified by optical absorption:[44]

$$R(q,\omega) = -\frac{1}{\pi}\mathrm{Im}\int^{k_F} \frac{d\vec{k}}{\Omega_F} \frac{\theta(|\vec{k}+\vec{q}|-k_F)}{\omega + k^2/2M - (|\vec{k}+\vec{q}|^2/2M - i|\vec{k}+\vec{q}|/2M\lambda)} \quad , \qquad (13)$$

where $\Omega_F \equiv (4\pi/3)k_F^3$. Here we have simply modified the knocked out particle's energy by adding an imaginary piece reflecting final state optical absorption; λ is the nuclear mean free path. The resulting modification of the Fermi gas response function is shown in Figure 24 as a function of λ.[44]

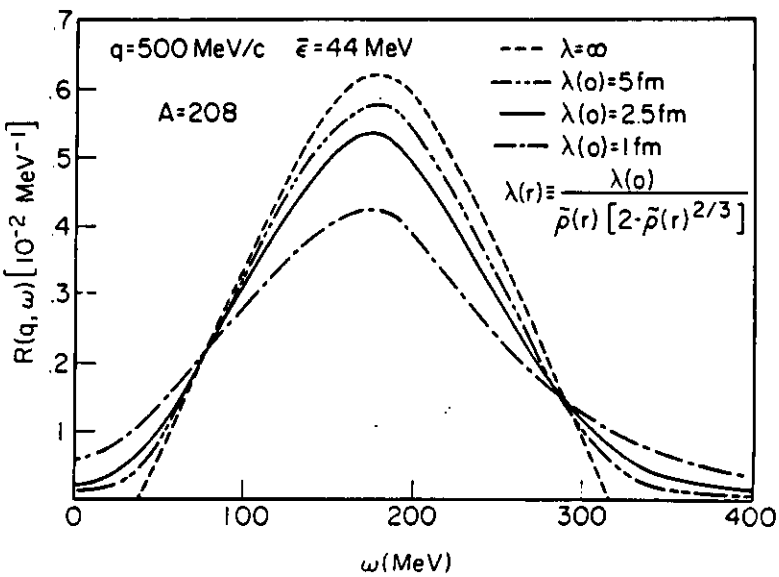

Figure 24. *Quasielastic response function for various values of the nucleon mean free path* λ.[44]

The width of the noninteracting Fermi gas response function is characterized by qk_F/M. As is evident from Equation (13), the final state interaction smears the response function over an energy loss interval characterized by $q/M\lambda$. Consequently, the dimensionless parameter $(k_F\lambda)^{-1}$ determines the spreading effect. This parameter is only weakly A-dependent (for A$\geq$12). For $\lambda \sim 5$ fm, the spreading leads to a reduction in the peak height of about 5% to 10%. Obviously, a long tail is added to the response function, suggesting that some of the strength is indeed experimentally inaccessible. It is clearly important to include this effect in quantitative analyses of the missing strength, although equally clearly it cannot resolve the entire problem.

We have seen that all ^{12}C(e,e'p) spectra exhibit significant strength in the missing energy continuum. One might suspect that "trivial" FSI effects such as two-body NN scattering, i.e., (e,e'p) followed by (p,p'), or intranuclear cascades could be responsible since such processes produce a continuous distribution of proton energies. It turns out, however, that they can account for only a small fraction ($\sim$ 10%) of this strength as can be seen in Figure 25. In that figure, the q = 585 MeV/c missing energy spectrum[40] is shown (on a greatly expanded vertical scale) along with two classical estimates of the strength expected from nucleon rescattering. One result, indicated by the solid line, is the result from the intranuclear cascade code MECC-7.[45] The other, dashed curve is

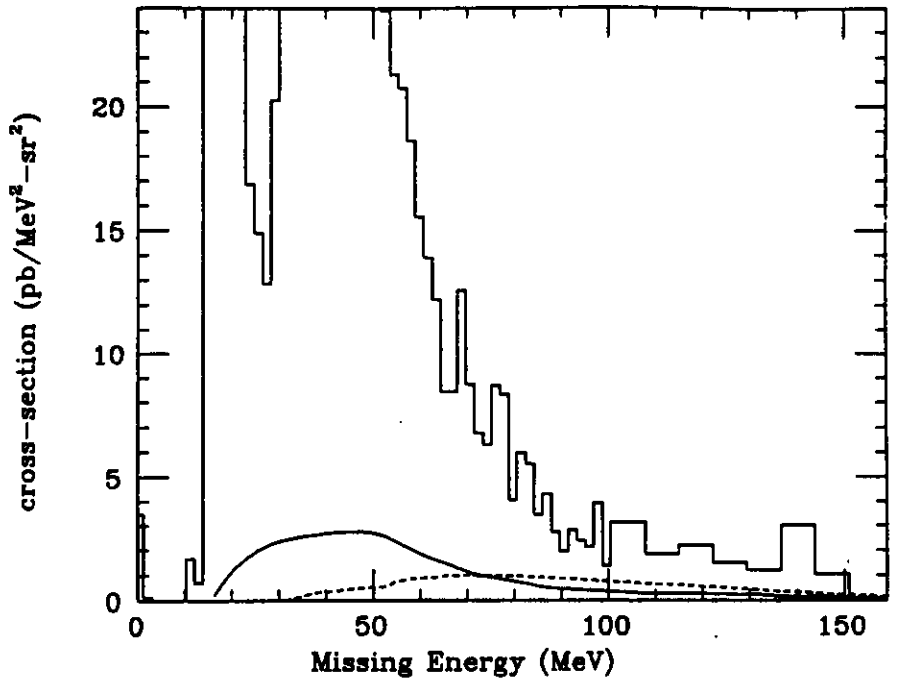

Figure 25. *Nucleon rescattering contribution to the missing energy spectrum at q = 585 MeV/c and ω = 210 MeV.*[40] *Solid curve: Results of intranuclear cascade code MECC-7. Dashed curve: Result using measured 200 MeV $^{12}C(p,p')$ data.*

produced by employing 200 MeV ^{12}C(p,p′) data[46] to describe the rescattering via the two-step process (e,e′p)(p,p′). Neither approach results in appreciable strength in the missing energy continuum and these effects are even smaller in the higher q data. In any event, they are unlikely to affect preferentially the transverse response.

We next turn to the transverse/longitudinal ratio in quasifree knockout. Recall from Figure 20 and from the hand-waving arguments concerning the "one-body part" of the transverse response function of Figure 12 that enhancements of this ratio on the scale of 20% have been observed. Final state interactions can affect this ratio through spin-dependence. Several groups[47][48] have now evaluated the effects of the optical potential spin-orbit coupling and find effects of about this magnitude for (e,e′p). Some results[34][49][50] are shown in Figure 26. The rapid variation in the calculations seen at some values of Q^2 reflects the structure of the specific single particle orbit being studied. Qualitatively, we see that the transverse/longitudinal ratio for the quasifree (e,e′p) process can be reasonably well understood in a straightforward manner. Whether a similar mechanism can account for the inclusive "one-body" ratio is unclear; of course, this ratio is not rigorously well defined, since "one-body" and "two-body" parts can interfere in the inclusive response function. In any event, we repeat that the overall strength cannot be reproduced simply through the inclusion of final state interactions.

B. Dip Region

We turn next to the issue of final state interactions in the dip region. Recall that the issue here is the large transverse inclusive strength compared with expectations based

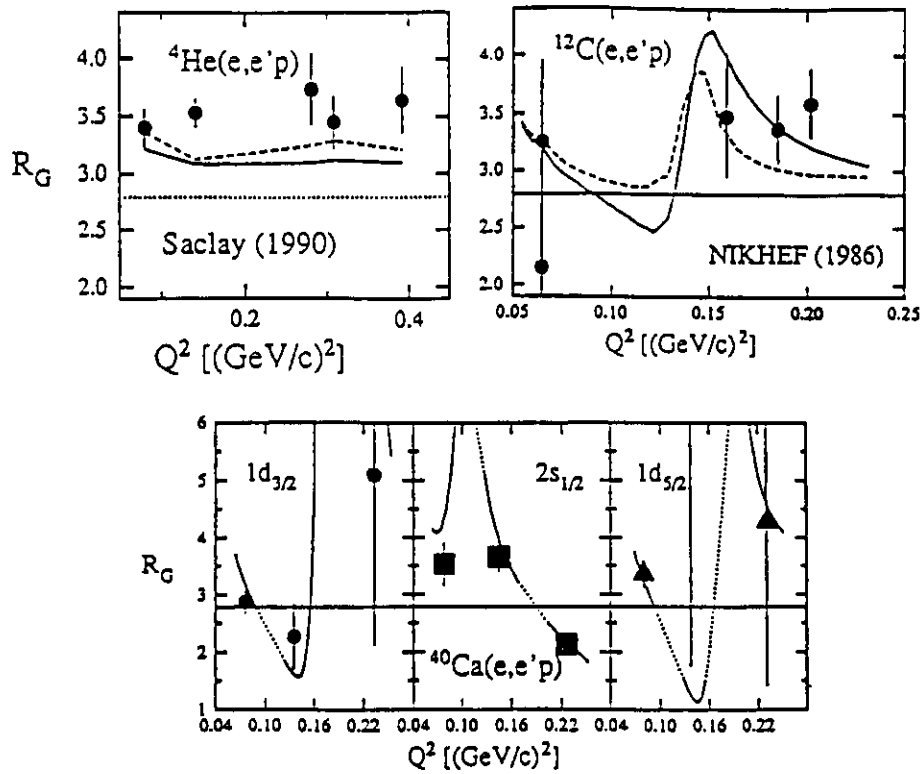

Figure 26. *The ratio R_G in ^4He,[50] ^{12}C,[34] and ^{40}Ca.[49] The calculations in ^4He are from Laget[51] (dashed) and Schiavilla[52] (solid). Curves from the Pavia group[47] are shown for ^{12}C and ^{40}Ca. In ^{12}C, two versions of the (e,p) cross section were used.*

upon a one-body picture and the supporting (e,e'p) missing energy spectrum shown for parallel kinematics in Figure 17. A natural question to ask is whether final state interactions can populate this large missing energy regime for these non-quasielastic kinematics. One suspects the answer is negative on purely phenomenological grounds, since the longitudinal response function does not have comparable strength. Takaki[35] confirms this in a fully quantum-mechanical calculation. While Figure 17 shows a typical cross section of 30 pb/Mev^2/sr^2 beyond the hole region, Takaki[35] finds a cross section of only about 2 pb/MeV^2/sr^2 from final state interactions. Further, longitudinal and transverse contributions are nearly equal. This is consistent with experiment. It is worth noting that the quantum-mechanical aspect of the calculation is important because of intermediate off-shell propagation. Defining the kinematics as in Figure 27, we can expand the T-matrix as:

$$\begin{aligned} T &= T_1 + T_2 + \dots \\ &= \phi(\vec{p} - \vec{q}) + \int d\vec{r}' d\vec{r} e^{-i\vec{p}\cdot\vec{r}'} V(r') G_p^0(\vec{r}' - \vec{r}) e^{i\vec{q}\cdot\vec{r}} \phi(r) + \dots \quad , \end{aligned} \tag{14}$$

where ϕ is the proton bound state wavefunction and the single-particle Green function is:

$$G_p^0(\vec{r}' - \vec{r}) = \int \frac{d\vec{p}'}{(2\pi)^3} \frac{e^{i\vec{p}'\cdot(\vec{r}'-\vec{r})}}{\epsilon_p^+ - \epsilon_{p'}} \quad . \tag{15}$$

To make a crude estimate, we use the eikonal approximation with $\hat{q} = \hat{p} = \hat{z}$ and further assume that V and ϕ are approximately constant over length L in the nucleus.

Then the double scattering contribution is:

$$T_2 \approx -i\frac{M}{2p}\Omega\phi\, V L\, \beta\left((p-q)L\right) \quad , \tag{16}$$

where

$$\begin{aligned}\beta(\tilde{y}) &= \frac{2}{L^2}\int_0^L dz' \int_0^{z'} dz\, e^{i(q-p)z} \\ &= \frac{2}{\tilde{y}^2}\left[1 + i\tilde{y} - e^{i\tilde{y}}\right] \\ &\approx \begin{cases} 1, & \tilde{y} \to 0; \\ 2i/\tilde{y}, & \tilde{y} \to \infty; \end{cases}\end{aligned} \tag{17}$$

where $\tilde{y} = (q-p)L$ and Ω is the nuclear volume. Note that $(p-q)$ is just the scaling variable y, for large momentum transfer. Far off the quasielastic peak, as in the dip region, $\tilde{y}$ becomes large and off-shell propagation in the intermediate propagation is important.

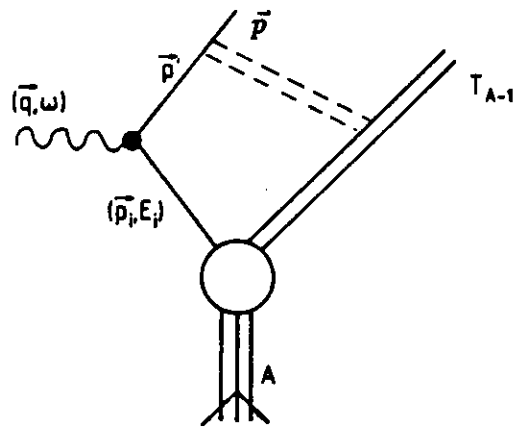

Figure 27. *FSI kinematics.*

Takaki further analyzed the phenomenology of the missing energy spectrum in the dip region. The arguments are essentially kinematic. For parallel kinematics, the two-body process is very restricted by energy and momentum conservation. This is most easily seen by considering virtual photon absorption on two nucleons at rest. For parallel kinematics, energy and momentum conservation give

$$\begin{aligned} y = \frac{2M\omega - q^2}{2q} &= -\frac{p_1 p_2}{q} \\ p_1 + p_2 &= q \quad , \end{aligned} \tag{18}$$

where $p_{1,2}$ are the final nucleon momenta (along $\hat{q}$). This is easily solved to give

$$p_{1,2} = \frac{q}{2} \pm \sqrt{\left(\frac{q}{2}\right)^2 + qy} \quad . \tag{19}$$

Clearly, if y is positive, as for the dip region, the faster nucleon goes forward, the slower backward. Thus, an (e,e'p) parallel kinematics measurement of such a two-body process will yield only low missing energies. For negative y, both nucleons can go forward and

one could then detect nucleons under both large and small missing energy conditions. To make this somewhat more quantitative, Takaki[35] made a simple zero range estimate with harmonic oscillator target wavefunctions. The shape of the missing energy spectrum for the kinematics of Figure 17 is shown by the solid curve in Figure 28. This is essentially the same as the solid line in Figure 17. The lesson is that the shape of the missing energy spectrum for a two-body process in parallel kinematics is largely determined by kinematics and the nucleon wavefunction. Different two-body dynamical mechanisms (final state interactions, exchange currents,...) will determine the normalization. However, we are now left with the conclusion that the large strength seen in Figure 17 at large missing energy, say $E_m \gtrsim 80$ MeV, cannot be explained by any two-body process. This same conclusion also applies to the high-q data nearer to the quasielastic peak.

Clearly, an n-body process, with n$\geq$ 3, will not have the kinematic constraints of the two-body process and should be peaked (perhaps weakly) in the parallel direction. In order to get an idea about the missing energy distribution, Takaki again made a zero-range estimate, now for a generic three body process. The missing energy distribution, arbitrarily normalized, is also shown in Figure 28. It peaks at $E_m \approx 140$ MeV and, as can be seen from Figure 17, has the right shape to "explain" the observed parallel kinematics spectrum. Needless to say, we have offered no suggestion as to what mechanism might be responsible, other than that the transverse nature suggests a pionic process. In this spirit, Takaki also evaluated the missing energy distribution for pion production followed by absorption of the pion. This is also shown in Figure 28. Of course, with $\omega = 200$ MeV, there is little phase space for on-shell pion production and this process is unlikely to be significant.

The kinematic conditions discussed above force the two-body process to large angles with respect to $\hat{q}$ for large missing energy. Takaki's result[35] for various missing energies is shown in Figure 29. Clearly, the angular shape of the two-body process may be used at modest missing energy (i.e., below that at which the three-body process dominates) to test the phenomenology. Using the calculated angular distributions and making an assumption about the final nucleon multiplicities, Takaki integrates the (e,e'p) cross sections, normalized in parallel kinematics, to obtain the inclusive dip region cross section. Within the framework of these crude estimates, he finds an inclusive cross section that indeed is comparable with that measured and further that the two-body and three-body contributions are comparable.

To summarize the results of this subsection, we find that final state interactions alone cannot account for the data; some two-body process of transverse nature is also playing a major role. Phenomenological analysis further indicates that a substantial part of the inclusive cross section actually arises from a three- (or more) body process. The nature of these mechanisms is not understood.

C. Δ Region

Finally, we turn to final state interactions in the Δ region. We shall be very brief here, since another contribution to this volume[53] will discuss this in greater depth. Analyses of pion-nucleus scattering in the Δ-hole model[54] have established that Δ propagation in the nuclear medium is subject to a significant spreading interaction. At nuclear matter density, the imaginary spreading potential, $\mathrm{Im}\, V_{sp} \approx -50$ MeV, is comparable to the free

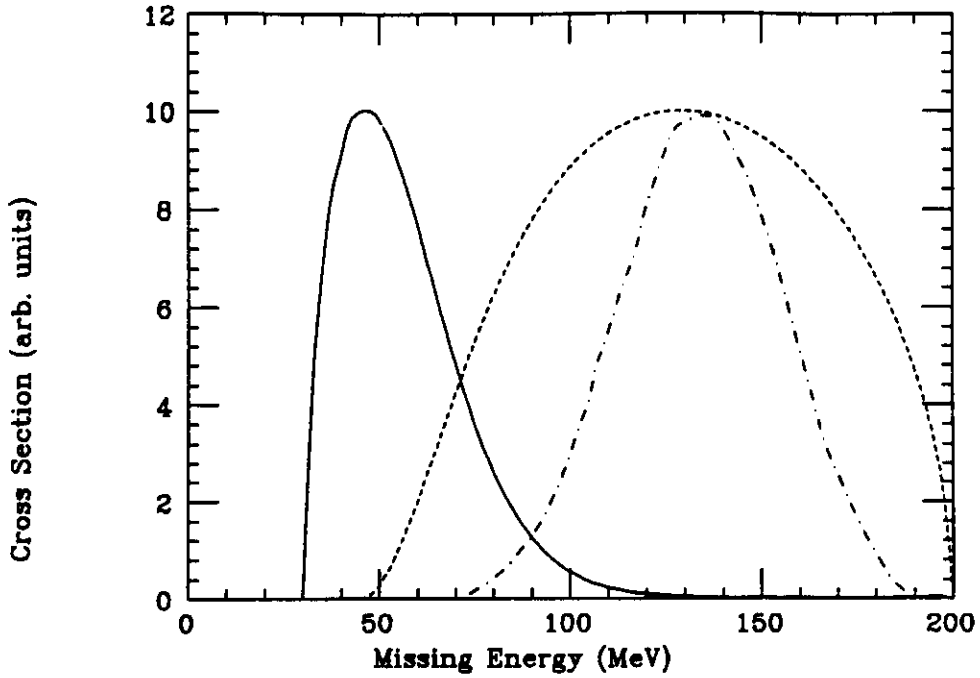

Figure 28. *Missing energy spectra in parallel kinematics (q = 400 MeV/c, ω = 200 MeV) as calculated by Takaki.*[35] *The solid (dashed) curve indicates the two (three) nucleon zero-range mechanism and the dot-dashed curve is the pion production/absorption result.*

Δ half-width. This suggests that another decay channel is comparable to the quasifree process. Indications are that the additional dynamical process is principally pion absorption through $\Delta N \rightarrow NN$. Indeed, this process also appears to shows up strongly in the (e,e'p) data, as discussed in Chapter II. The spreading effect on the (e,e') inclusive cross section[27] is shown in Figure 16. The indication seems to be that there is yet additional strength, transverse in nature. The coincidence data demonstrate that this additional strength is likely to be many-body in character. As we have seen, such additional strength seems to enhance the transverse response function in all the kinematic regions we have examined.

2. In-Medium Hadron Structure

As discussed already, the idea that a "swollen" nucleon in the medium could account for the missing longitudinal strength was introduced some time ago.[55] That is, increasing the nucleon radius would concomitantly make the proton charge form factor fall off more rapidly with momentum transfer. The longitudinal discrepancy would then grow dramatically with q. As seen in Chapter II, the subsequent (e,e'p) data do not support a dramatic effect of this type. Also, we stress again the A=3 results, both the sum rule and the (e,e'p) data. The swollen nucleon hypothesis rests on a mean field idea, with the size increase essentially proportional to the local density. However, the ratio of the average nuclear density to nuclear matter density is roughly 1/4 for A=3, 1/2 for A=12 to 40, and 3/4 for A=208. The A=3 sum rules are understood at the few percent level with "conventional" dynamics, so an entirely new mechanism would have to become operative at larger A in order to produce effects on the scale of the missing sum rule strength. This cannot

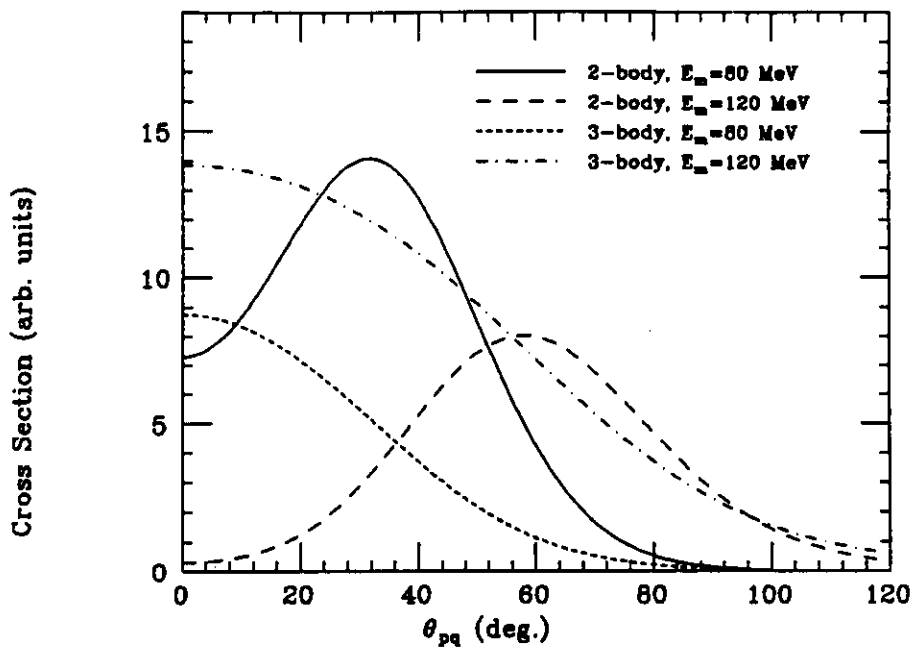

Figure 29. *Angular distributions of two- and three-nucleon knockout for $^{12}C(e,e'p)$ in the dip region as calculated by Takaki.*[35]

be ruled out. Indeed, total cross sections for pion absorption on nuclei have suggested just such a dramatic change in going from A=3 to A=4 (as did the behavior of f_L and f_T in (e,e')[24]). The two-nucleon absorption mode appears to scale with the number of isoscalar pairs, but the ^{4}He total absorption cross section measurement of Baumgartner *et al.*[56] suggested that a very large multinucleon absorption mechanism appeared for A$\geq$4. However, a recent measurement[57] of the $\pi^{\pm}$-^{4}He absorption cross section obtained in a counter experiment by adding all integrated partial cross sections has yielded a much smaller total cross section and specifically a relatively small multinucleon cross section (~70% of the 120 MeV total absorption cross section comes from quasifree absorption on T=0 pairs). Still, recent results on heavier nuclei (e.g., ^{6}Li[58] and ^{58}Ni[59]) support the notion of a significant multi-body mechanism giving on the order of half the total absorption cross section in the resonance region. Further experiments with large acceptance detectors are needed to clarify this situation.

Returning to the issue of modified in-medium hadron structure, we note that several groups have tried to provide a dynamical explanation of such modifications. For example, Bernard and Meissner[60] have used a generalized Nambu-Jona-Lasinio model, and Brown and Rho[61] a chiral bag. A common theme is reduction of in-medium vector meson masses proportional to the local density, thereby leading to a reduced in-medium nucleon form factor. At half nuclear matter density, they typically find $m_V^*/m_V \approx 0.9$, leading to a reduction of the q = 500 MeV/c longitudinal response function by ~10%. The authors argue that their results are supported by other successful applications of the same model, but two problems remain. The momentum transfer dependence indicated in Figure 22 needs to be understood. The success in describing the A=3 results within the conventional framework argues strongly against a simple mean field modification of hadron properties.

3. Correlations

Up to this point, our discussion of dynamical mechanisms has implicitly assumed a mean field description of the nuclear ground state. Residual interactions clearly modify the spectral function, depleting orbits below the Fermi level and shifting strength to higher energy. A schematic representation of occupation numbers as a function of binding energy is shown in Figure 30.[62] Although there is no clear separation between the two, short-range and long-range correlations are often addressed separately. Nuclear matter calculations tend to emphasize the effects of the short-range NN repulsion in shifting spectral strength to very high excitation energy, while RPA calculations highlight the role of long range correlations in "smearing" the Fermi surface.

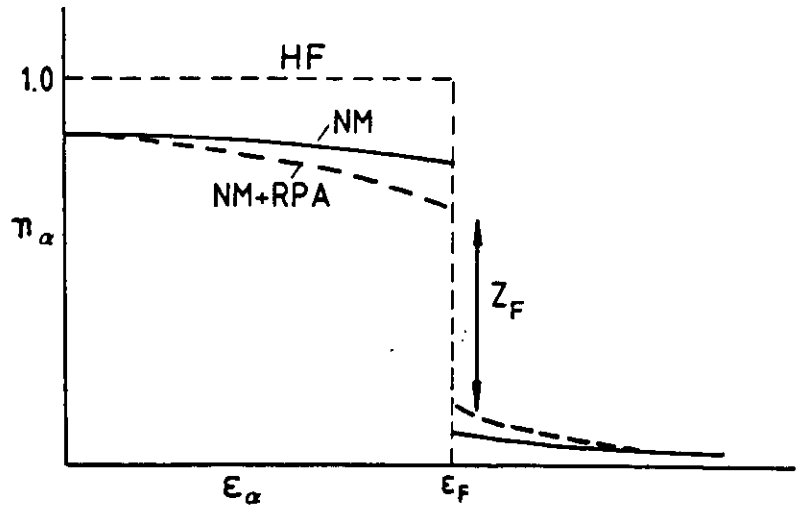

Figure 30. *Schematic behavior of occupation number vs. distance from the Fermi surface for Hartree-Fock (HF), nuclear matter with correlations (NM) and finite nuclei (NM+RPA).*[62]

As suggested by Figure 30, the depletion of the Fermi sea is rather considerable. The systematics of inelastic electron scattering, both to discrete nuclear states (e.g., to the "stretched" configurations) and to the continuum support this. For example, we show in Figure 31 the $^{12}C(e,e'p)^{11}B$ spectrum with very good missing-mass resolution measured at NIKHEF.[63] The fragmentation of the p-shell hole strength is seen very clearly. The relative strength of the three low-lying odd-parity states is reasonably consistent with the expectations based on Cohen-Kurath wavefunctions. However, the total occupation strength is almost a factor of two below expectations, $\sum_\alpha n_\alpha$ (p-shell protons)$\approx$ 2.2.[63] Similar high resolution measurements have been performed at NIKHEF for nuclei as heavy as ^{208}Pb. The overall spectroscopic strength for valence orbits[64] is summarized in Figure 32. Clearly, the strength close to the Fermi surface falls with increasing A and reaches approximately 50% for A=12 to 208. Therefore, even if the correlation effects have a comparatively small effect on the longitudinal sum rule, we obviously cannot rule out significant redistribution of strength in the dynamic response function. A major issue is the excitation energy distribution of the spectral function strength above the Fermi level.

Buballa *et al.*[65] have performed a continuum RPA calculation of the ^{12}C response functions. It is crucial that they use finite-range forces, including a tensor force, and include exchange terms. A zero-range force would produce totally unrealistic effects at the

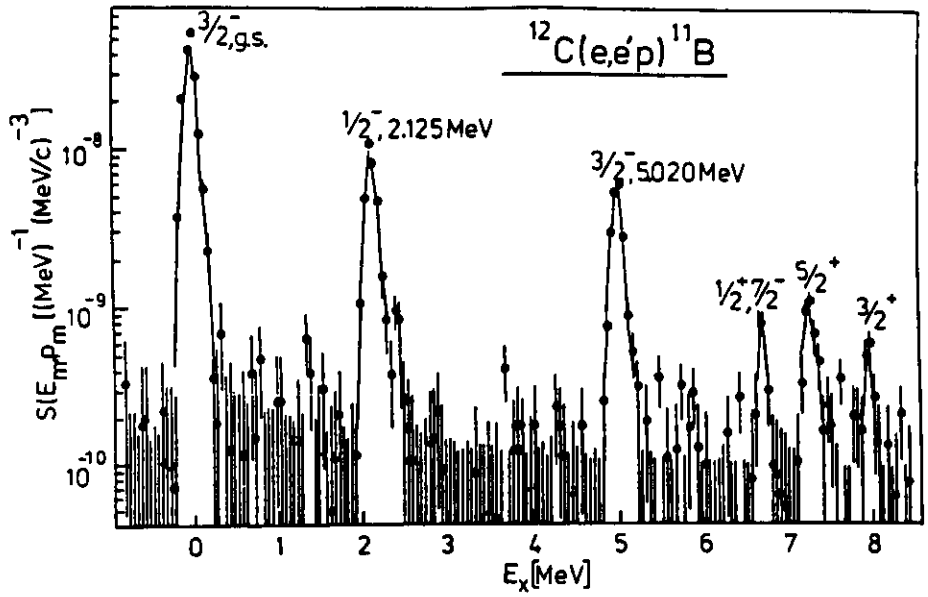

Figure 31. *High-resolution $^{12}C(e,e'p)$ missing energy spectrum from NIKHEF.*[63]

momentum transfers of relevance here. Their results for the longitudinal and transverse inclusive response functions at $q = 500$ MeV/c are shown in Figure 33. In the longitudinal response, they find a reduction of the quasielastic peak by about 8% in comparison with the result obtained in the absence of residual interactions. The principal effect here is particle-hole rescattering through the exchange terms, since the relevant exchange momentum transfer can still be small at large q. In contrast, the transverse response function shows essentially no suppression. The residual interaction is dominated by the tensor force at large q and is therefore strongly repulsive. The strength is pushed to somewhat higher energy transfer and coherence effects reduce the spreading. These coherence effects can be thought of as vertex corrections arising from particle-hole interactions. They change the p-h state spreading from the simple sum of particle and hole widths. The longitudinal response function is not strongly affected by these vertex corrections, since the long-range bubble-type corrections of relevance are ineffective at large momentum transfer. On the other hand, ladder-type particle-hole interactions are significant for the transverse response, which is primarily sensitive to the nuclear spin density. These effectively short-range interactions persist to higher momentum transfer and thus affect the transverse response in the relevant kinematic regime. As has long been known in the context of giant resonance spreading widths,[66] these vertex corrections tend to cancel the spreading due to self-energy (or optical potential) effects, thus enhancing the transverse response function relative to the longitudinal. Note that these calculations[65] contain no two- or many-body currents which we have seen from the (e,e'p) data are certainly needed to obtain the full response function. Thus, two results emerge from this study. First, the longitudinal response function is modestly "spread" by RPA correlations. Second, the transverse/longitudinal ratio is increased slightly from the impulse value primarily through the residual p-h tensor force.

We next address the issue of short-range correlations. We repeat that there is no clear separation between this discussion and that above (i.e., there is likely to be some amount of both double-counting and undercounting!). Our goal here remains the more limited one of gaining a semi-quantitative understanding of how various dynamical processes

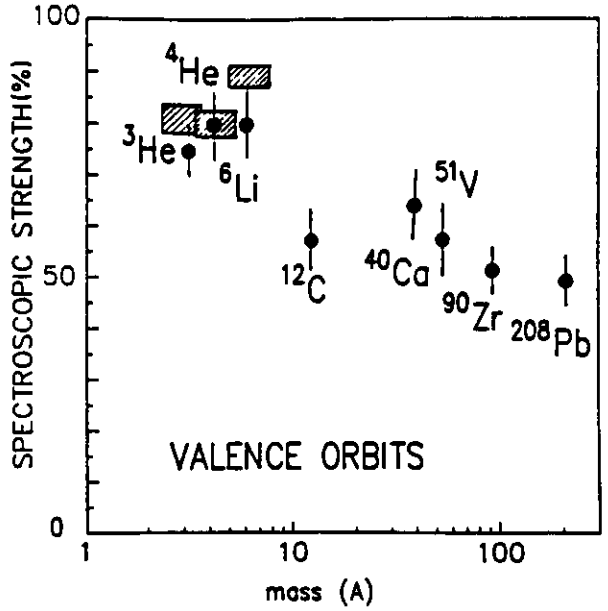

Figure 32. *Spectroscopic strength for valence orbitals vs. atomic number.*[64]

may influence the nuclear large momentum transfer, large energy transfer electromagnetic response.

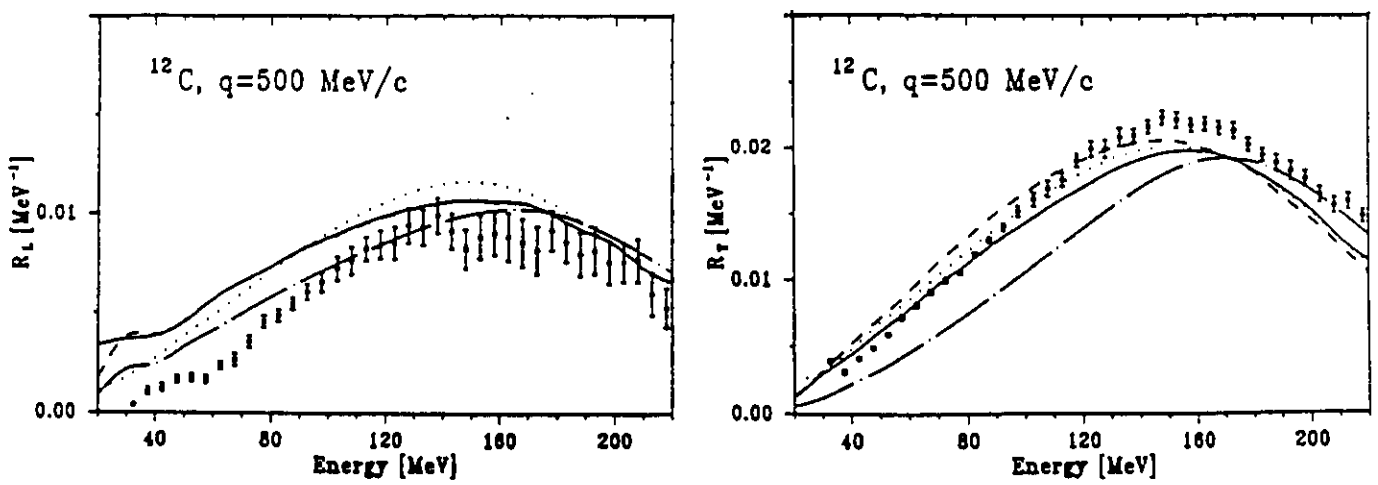

Figure 33. *Longitudinal and transverse response functions of ^{12}C from the continuum RPA calculation of Buballa et al.*[65] *Dotted line: free response. Solid line: full result. Dashed line: no tensor force. Dash-dot line: zero-range force.*

Our discussion centers about the impulse approximation schematically summarized by Equation (5). In particular, we must understand the spectral function at large p and E. The momentum distribution calculated in a Brueckner-Bethe-Goldstone expansion[67] is shown in Figure 34. For momenta $\gtrsim$300 MeV/c, the shape of $n(k)$ is approximately the same for all nuclei; there is a roughly exponential fall-off $\exp(-k/k_0)$ with $k_0 \approx$ 120 MeV/c. This is consistent with the idea that very high momentum components

are generated principally by short-range two-nucleon collisions. As discussed in Section II.1.B for ^{3}He, this suggests that the energy dependence of the spectral function at fixed large momentum should reflect the dominance of hard "back-to-back" collisions. Several groups[68][69] have shown this; we show the result of Ji and McKeown[68] in Figure 35. The peak corresponds to the recoil energy of the partner nucleon, shifted by a separation energy. For the purposes of a simple evaluation of Equation (5), we parameterized the spectral function of Reference[68] and chose a normalization

$$\int_{k_F}^{\infty} d\vec{k}\, n(k) = 0.2 \quad , \tag{20}$$

which is perhaps slightly larger than indicated by microscopic nuclear matter calculations using realistic forces. Our schematic response function is shown in Figure 36 for $q = 400$ MeV/c (the integral over energy transfer is unity). The Fermi gas result has been multiplied by 0.8, and the remaining strength has been incorporated through Equation (5). In addition, we have for comparison evaluated the tail contribution neglecting the full energy dependence of the spectral function; that is, we replace $E \to M - \bar{\epsilon}$, with $\bar{\epsilon} = 40$ MeV, in the energy-conserving delta function of Equation (5). Note that this additional approximation of neglecting the energy dependence results in more than half the "correlation strength" reappearing under the Fermi gas quasielastic peak, thereby considerably reducing the correlation effect on the inclusive response. On the other hand, the full impulse approximation calculation shifts the strength to considerably higher energy. The average energy transfer for the "correlation strength" is

$$\bar{\omega} \approx T(\bar{k}) + T\left(\sqrt{\bar{k}^2 + q^2}\right) \quad , \tag{21}$$

where $T(k)$ is the nucleon kinetic energy for momentum k and $\bar{k}$ is the average momentum in the correlation tail, $\bar{k} \approx 500$ MeV/c. Clearly, almost the entire correlation strength is pushed beyond the quasifree region for $q = 400$ MeV/c, indeed, nearly half of it resides in the experimentally inaccessible region $\omega > 400$ MeV (although, of course, the sum rule is still obeyed). The tail is "buried" under the Δ peak and never exceeds 10% of the Fermi gas peak, making experimental measurement of the longitudinal part difficult. Thus, the energy dependence of the spectral function for $k \gtrsim 300$ MeV/c results in a significant "suppression" of the quasielastic peak in impulse approximation. Note, however, that Equation (21) implies, for $q \lesssim M$, a rather slow shift of the correlation strength with increasing q relative to the shift of the one-body quasifree strength. Consequently, the reduction of the quasielastic peak height will be less effective as q increases.

Reduction of the quasielastic contribution has been observed in experiments at the Yerevan Electron Synchrotron.[70] Their results are displayed in Figure 37 which shows the spectrum of scattered electrons gated on fast (high momentum) protons detected at different angles with respect to $\vec{q}$. Note how the quasielastic peak disappears as the proton angle increases, leaving a rather flat distribution of the scattered electrons in ω.

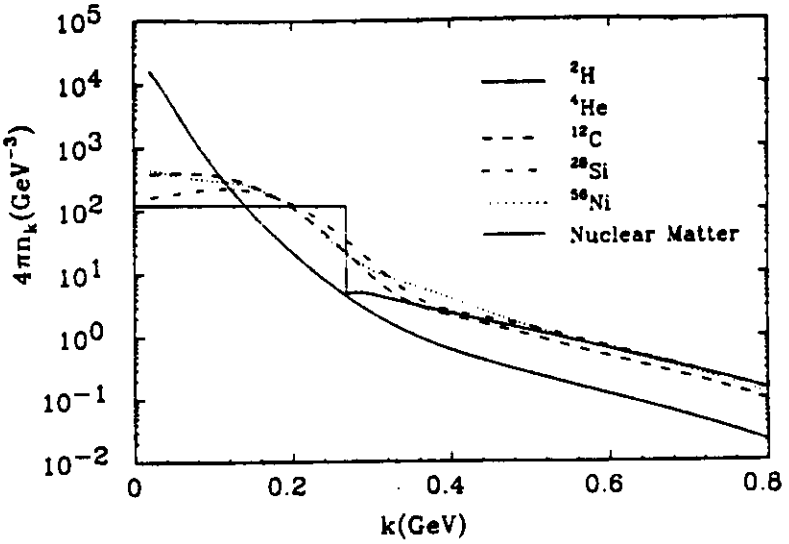

Figure 34. *Nucleon momentum distributions from Brueckner-Bethe-Goldstone expansion.*[67]

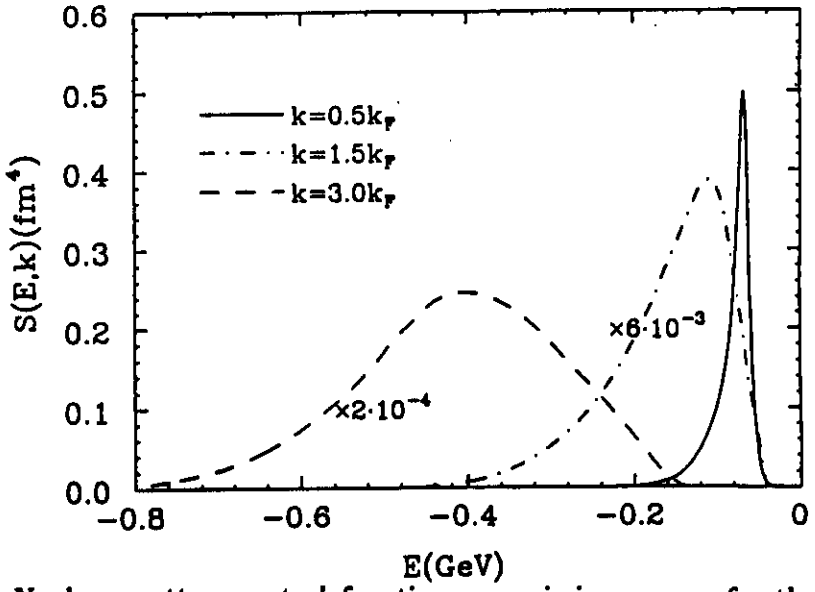

Figure 35. *Nuclear matter spectral function vs. missing energy for three values of the initial momentum.*[68]

4. Off-Shell Form Factors and Relativistic Theories

Apart from our brief description of microscopic attempts to generate a density dependent nucleon "swelling", our discussion has been cast in the framework of nonrelativistic many-body theory. It is clear that we would like to have a relativistic many-body theory, perhaps a renormalizable field theory based upon meson and nucleon degrees of freedom (quantum hadrodynamics, QHD) and ultimately a description in terms of QCD. The latter appears well beyond reach at this time. In this section, we summarize briefly attempts based upon hadronic degrees of freedom. Regrettably, we shall see that the theory has not developed to the point where quantitative comparisons with data can be made. We note, however, that the experimental studies are inexorably moving on to probe the nuclear response at momentum transfers comparable to or greater than the nucleon mass, so

that theoretical progress in developing a relativistic theory will be essential for meaningful quantitative comparison with data.

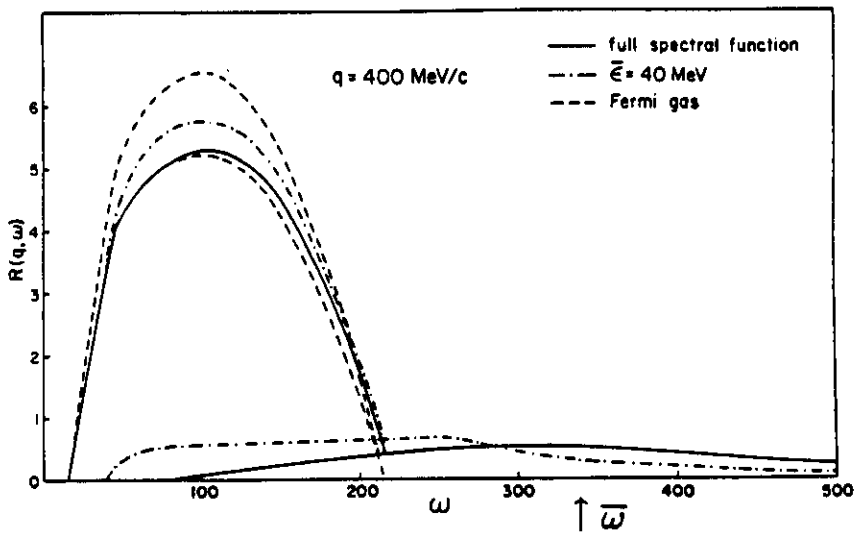

Figure 36. *Impulse approximation response function for nuclear matter at $q = 400$ MeV/c using the spectral function of reference.*[68]

Naus and Koch[71] investigated the modification of the virtual photon- nucleon coupling for off-shell nucleons. The usual assumption in writing down the nuclear current operator is that free space form factors can be used. In fact, bound nucleons are off the mass shell, so the form factors will generally depend on two additional Lorentz scalars. These authors and subsequently Tiemeijer and Tjon[72] attempted to gain insight into the magnitude of associated corrections by considering a simple meson-nucleon model and evaluating one-loop corrections to the photon-nucleon vertex function. Even for the modest momentum transfers considered in this review, they find corrections to electromagnetic cross sections ranging from a few percent to perhaps 10%. Therefore, such corrections may not be negligible, but a much more refined model needs to be developed.

There have been a number of calculations of the nuclear response function in QHD.[73] These calculations are performed at the level of mean field theory or relativistic Hartree approximation and generally lead to a substantial suppression of the longitudinal response function. However, it is difficult to gauge the meaningfulness of these results. First, there are some "technical" difficulties. The residual particle-hole interactions generally have point-like vertices and bear little relationship to a realistic representation of the NN-interaction. There are also deep uncertainties as to the validity of the mean field theory as a sensible starting point for systematic evaluation of observables, despite the phenomenological success of various calculations. The mean field theory should be accurate in the high density limit, but nonrelativistic many-body theory tells us that nuclear matter is a low density system in the sense of a hole-line expansion. Since QHD is based on a renormalizable field theory,[74] one hopes to be able to construct a systematic expansion scheme based upon a finite number of parameters fixed by appropriate data. However, it is still a strong coupling theory, so that the task may not be realizable or practical. The most extensive work in this direction has been carried out by Furnstahl *et al.*[75] They

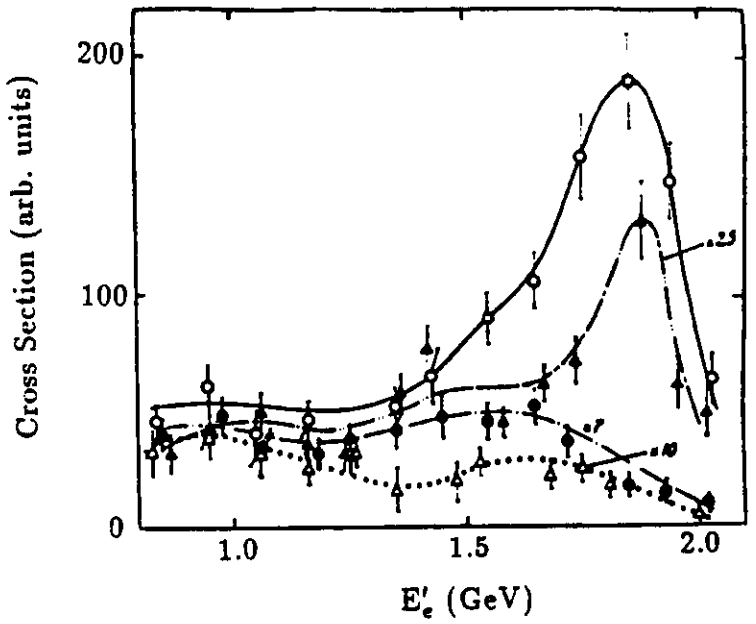

Figure 37. *Spectra of scattered electrons gated on detection of 85–205 MeV protons at 74, 90, 120 and 140° (open circles, solid triangles, solid triangles and open triangles).*[70] *The beam energy was 2 GeV and the electron scattering angle was 15°* .

investigated the loop expansion as a viable scheme and reached the negative conclusion that the expansion is not convergent. Thus, any successes of the mean field or relativistic Hartree approximations remain at the phenomenological level and do not lend confidence in applications to new areas, such as the response function at large momentum and energy transfer.

IV. Summary and Concluding Remarks

Understanding the global features of the electromagnetic response at high momentum and energy transfer is a central problem in nuclear physics. The inclusive response function gives the total cross section for virtual photons and presents several problems. The first generation of coincidence experiments has explored a limited set of reaction channels in a limited kinematic regime but has nevertheless already helped shed considerable light on the issues, in terms of both nuclear structure and reaction mechanism. Theoretical consideration of various dynamical processes holds promise for an overall understanding of those features clearly attributed to one-body processes. However, the lack of a unified treatment precludes our drawing quantitative conclusions. The character of the additional many-body currents, clearly exhibited in the data, has not been accounted for within the scope of current theoretical approaches. In the remainder of this concluding section, we briefly summarize the phenomenology, both experimental and theoretical, and identify needed future activity.

The longitudinal response has been studied experimentally over a very limited range of momentum and energy transfer in the neighborhood of the quasielastic peak. The inclusive and coincidence data, particularly the latter, display one-particle or quasifree characteristics. This was the expectation based on the mean field picture of the nucleus and the fact that pionic processes enter the current operator principally for the transverse response. The momentum transfer dependence, to the extent available, is consistent with the impulse approximation; for example, y-scaling is respected even at very modest

q. The significant problem is that the total strength is substantially less than expected, at least for A$\geq$12. The attempts at explanation fall into two general categories, those that spread the strength into experimentally inaccessible (so far) regimes and those that invoke sub-nucleon degrees of freedom to reduce the total sum rule strength. It is premature to conclude that the latter approach is needed or correct, since there are significant theoretical problems with the framework employed. In addition, two phenomenological problems must be confronted in this approach: the momentum transfer dependence in (e,e'p) for $q \lesssim 1$ GeV/c is consistent with quasifree expectations (recall, however, that the data become predominantly transverse at high q); the sum rule is very well satisfied for A=3, where the average density is already about half that of medium-mass nuclei; the exclusive data for A=3 are quantitatively consistent with the dominance of short-range correlations at large missing momentum. Two mechanisms that spread the longitudinal strength are final state interactions and correlations. The final state interactions play a modest but non-negligible role in the inclusive response, say $\lesssim$10% suppression of the quasielastic peak cross section. The coincidence cross section in parallel kinematics shows little strength for missing energies beyond the hole region, consistent with expectations based on final state interactions. Correlations can also play a significant role. An RPA calculation, including particle and hole spreading, shows about a 10% suppression for the inclusive ^{12}C response at the peak. A schematic calculation of short-range correlation effects shows that the energy dependence of the spectral function is very important and that peak suppressions of $\sim$ 15% are quite possible. Unfortunately, the three calculations just alluded to are not performed in a unified framework and considerable double counting may result. Nevertheless, the general scale of the effects needed appears within reach to describe the inclusive longitudinal response. Further experimental studies of the longitudinal response are essential. One would like precision inclusive data in the large energy transfer quasielastic tail and coincidence data away from the quasifree (parallel) kinematics. Polarization observables should provide additional information on the reaction dynamics. This difficult program likely cannot succeed without the combination of high energy, duty factor and intensity to be available at CEBAF.

The transverse response has been studied over a significantly greater kinematic range. One-body characteristics are seen clearly in both the quasielastic and Δ-excitation regimes over the entire range of coincidence measurements. The (e,e'p) spectrum in the Δ-region qualitatively indicates the same Δ spreading into pion annihilation channels as seen in pion-nucleus scattering. Two problems remain: the transverse/longitudinal ratio is larger than that of the impulse approximation in the quasielastic region, even for the "single particle" part; there is evidence of strong multinucleon processes throughout the quasielastic and Δ regions, as first realized for the "dip" region between these two dominant features of the inclusive response. Within the "traditional" framework, two mechanisms have been identified which enhance the transverse/longitudinal ratio. Spin-orbit final state interactions enhance the (e,e'p) ratio to specific hole states by typically 10% to 20% consistent with the data. The effect on the inclusive response has not been evaluated. The RPA calculation, including residual tensor forces, provides about a 10% enhancement of the inclusive ratio. This comes principally from a coherence effect in which short-range p-h vertex corrections interfere with the optical potential spreading in the transverse response. The second problem, that of additional many-body currents, remains at the purely phenomenological level. The experimental evidence is seen directly in the (e,e'p) missing energy spectra, where significant strength is found well beyond the region of hole states.

It appears that only the transverse response is affected. It is then natural to assume that a pionic process is responsible, but the inadequacy of available calculations within the usual framework may point to different physics, e.g. new currents or reaction processes. The excess transverse strength also grows significantly with q, implying that its origin may be of short-range character. In the dip region, where the tails of one-body processes are relatively small, the coincidence data suggest that up to half the total strength resides in direct multi- nucleon (i.e., at least three-nucleon) ejection. This is reminiscent of the situation in pion-nucleus absorption studies, but no quantitative connection has been established in the absence of a dynamical model for either process. More data are called for. Again, coincidence data away from the quasifree kinematics may be very helpful. In addition, direct multi-nucleon detection with a large acceptance detector should provide crucial information for model- building.

It should be clear that significant theoretical progress is needed as well. Within the conventional framework, a unified treatment of the various mechanisms described above is required for drawing quantitative conclusions. For example, a two-hole calculation for nuclear matter and a full treatment of the A=3 system are technically daunting but possible and important. A greater conceptual challenge is that of developing relativistic many-body theory, including sub-nucleon degrees of freedom, into a framework for systematically addressing observables. Phenomenologies of this type suggest major implications even for the modest momentum transfers probed so far, but the meaningfulness of these effects cannot be judged reliably within current theoretical frameworks. The problem will only become more urgent as the data span a greater kinematic range with the coming generation of accelerator facilities.

References

[1] J. S. O'Connell *et al.*, Phys. Rev. Lett. **53**, 1627 (1984); Phys. Rev. **C35**, 1063 (1987).

[2] K. Dow *et al.*, Phys. Rev. Lett. **61**, 1706 (1988).

[3] E.J. Moniz *et al.*, Phys. Rev. Lett. **26**, 445 (1971).

[4] P.E. Ulmer *et al.*, Phys. Rev. Lett. **59**, 2259 (1987).

[5] T. DeForest Jr., Nucl. Phys. **A414**, 347 (1984).

[6] H. Meier-Hajduk, CH. Hajduk, P.U. Sauer and W. Theis, Nucl. Phys. **A395**, 332 (1983).

[7] R. Schiavilla and V.R. Pandharipande, Phys. Rev. **C36**, 2221 (1987); see also: R. Schiavilla, Phys. Lett. **218B**, 1 (1989).

[8] T.S. Ueng *et al.*, to be published.

[9] C. Marchand *et al.*, Phys. Lett. **153B**, 29 (1985).

[10] R. Schiavilla *et al.*, Nucl. Phys. **A473**, 267 (1987).

[11] D.H. Beck, Phys. Rev. Lett. **64**, 268 (1990).

[12] R. Schiavilla *et al.*, Phys. Rev. **C40**, 1484 (1989).

[13] D. Day *et al.*, Phys. Rev. Lett. **43**, 1143 (1979).

[14] C. Marchand *et al.*, Phys. Rev. Lett. **60**, 1703 (1988).

[15] C. Ciofi degli Atti, E. Pace and G. Salmè, Phys. Lett. **141B**, 14 (1984).

[16] P.H.M. Keizer *et al.*, Phys. Lett. **157B**, 255 (1985).

[17] E. van Meijgaard and J.A. Tjon, Phys. Rev. **C42**, 96 (1990).

[18] E. Jans *et al.*, Phys. Rev. Lett. **49**, 974 (1982); Nucl. Phys. **A475**, 687 (1987).

[19] M. Bernheim *et al.*, Nucl. Phys. **A365**, 349 (1981); S. Turck-Chieze *et al.*, Phys. Lett. **142B**, 145 (1984).

[20] P. Barreau *et al.*, Nucl. Phys. **A402**, 515 (1983).

[21] J. M. Finn, R. W. Lourie and B. H. Cottman, Phys. Rev. **C29**, 2230 (1984).

[22] Z.E. Meziani *et al.*, Phys. Rev. Lett. **52**, 2130 and **54** 1233 (1984); M. Deady *et al.*, Phys. Rev. **C33**, 1897 (1986); R. Altemus *et al.*, Phys. Rev. Lett. **44**, 965 (1980); C.C. Blatchley *et al.*, Phys. Rev. **C34**, 1243 (1986).

[23] D.T. Baran *et al.*, Phys. Rev. Lett. **61**, 400 (1988).

[24] A. Magnon, private communication.

[25] R. Schiavilla, Nucl. Phys. **A499**, 301 (1989).

[26] S.A. Dytman *et al.*, Phys. Rev. **C38**, 800 (1988).

[27] J. Koch and N. Ohtsuka, Nucl. Phys. **A435**, 765 (1985).

[28] J.W. Van Orden and T.W. Donnelly, Ann. Phys. (N.Y.), **131**, 145 (1980).

[29] R.W. Lourie *et al.*, Phys. Rev. Lett. **56**, 2364 (1986).

[30] H. Baghaei *et al.*, Phys. Rev. **C39**, 177 (1989).

[31] J.M. Laget, private communication.

[32] G. van der Steenhoven *et al.*, Nucl. Phys. **A484**, 445 (1988).

[33] J.B.J.M. Lanen *et al.*, Phys. Rev. Lett. **64**, 2250 (1990).

[34] G. van der Steenhoven *et al.*, Phys. Rev. Lett. **57**, 182 (1986); **58**, 1727 (1987).

[35] T. Takaki, Phys. Rev. Lett. **62**, 395 (1989); Phys. Rev. **39**, 359 (1989).

[36] D. Ashery and J.P. Schiffer, Ann. Rev. Nucl. Part. Sci. **36**, 207 (1986).

[37] S. Homma *et al.*, Phys. Rev. **C27**, 31 (1983).

[38] M. Kanazawa *et al.*, Phys. Rev. **C35**, 1828 (1987).

[39] J. Morrison *et al.*, to be published.

[40] L.B. Weinstein *et al.*, Phys. Rev. Lett. **64**, 1646 (1990).

[41] D. Reffay-Pikeroen *et al.*, Phys. Rev. Lett. **60**, 776 (1988).

[42] D.F. Geesaman *et al.*, Phys. Rev. Lett. **63**, 734 (1989).

[43] Y. Horikawa, F. Lenz and N.C. Mukhopadhyay, Phys. Rev. **C22**, 1680 (1980);
P.M. Boucher and J.W. Van Orden, to be published.

[44] E.J. Moniz, in *Electron and Pion Interactions with Nuclei at Intermediate Energies*, Eds. W. Bertozzi, S. Costa and C. Schaerf, Harwood Academic (1979).

[45] H. Bertini *et al.*, Oak Ridge National Laboratory internal report CCC-156.

[46] R. Segal, private communication.

[47] C. Giusti and F. Pacati, Nucl. Phys. **A473**, 717 (1989); **A485**, 461 (1988).

[48] T.D. Cohen, J.W. Van Orden and A. Picklesimer, Phys. Rev. Lett. **59**, 1267 (1987);
T. Suzuki, Phys. Rev. **C37**, 549 (1988);
M. Kohno, Phys. Rev. **C38**, 584 (1988).

[49] H.J. Bulten *et al.*, contributed paper at PANIC XII (1990).

[50] A. Magnon *et al.*, Phys. Lett. **222B**, 352 (1989).

[51] J.M. Laget, Rapport DPh-N/Saclay n°2576 (1989).

[52] R. Schiavilla, Phys. Rev. Lett. **65**, 835 (1990).

[53] J.H. Koch, this volume.

[54] M. Hirata, F. Lenz and K. Yazaki, Ann. Phys. **108**, 116 (1977);
M. Hirata, J.H. Koch, F. Lenz and E.J. Moniz, Ann. Phys. **120**, 205 (1979).

[55] J.V. Noble, Phys. Rev. Lett. **46**, 412 (1981).

[56] M. Baumgartner *et al.*, Nucl. Phys. **A489**, 647 (1988).

[57] M. Steinacher *et al.*, to be published.

[58] R.D. Ransome *et al.*, Phys. Rev. **C42**, 1500 (1990); Phys. Rev. Lett. **64**, 373 (1990).

[59] W.J. Burger *et al.*, Phys. Rev. Lett. **57**, 58 (1986); Phys. Rev. **C41**, 2215 (1990).

[60] V. Bernard and U.-G. Meissner, Nucl. Phys. **A489**, 647 (1988).

[61] G.E. Brown and M. Rho, Phys. Lett. **222B**, 324 (1989).

[62] A.E.L. Dieperink and P.K.A. de Witt Huberts, Ann. Rev. Nucl. Part. Sci. **40**, 239 (1990).

[63] G. van der Steenhoven *et al.*, Nucl. Phys. **A480**, 547 (1988).

[64] P.K.A. de Witt Huberts, J. Phys. G: Nucl. Part. Phys. **16**, 507 (1990).

[65] M. Buballa, S. Drożdż, S. Krewald and J. Speth, to be published;
S. Drożdż *et al.*, Nucl. Phys. **A501**, 487 (1989).

[66] G. Bertsch, P.F. Bortignon and R.A. Broglia, Rev. Mod. Phys. **55**, 287 (1987).

[67] X. Ji and J. Engel, Phys. Rev. **C40**, R497 (1989).

[68] X. Ji and R.D. McKeown, Phys. Lett. **236B**, 130 (1990).

[69] O. Benhar, A. Fabrocini and S. Fantoni, Nucl. Phys. **A497**, 423c (1989);
P. Grange, J. Cugnon and A. Lejeune, Nucl. Phys. **A473**, 365 (1987).

[70] K. Sh. Egiyan, *CEBAF Summer Workshop* (1987).

[71] H.W.L. Naus and J.H. Koch, Phys. Rev. **36**, 2459 (1987);
H.W.L. Naus, S.J. Pollock, J.H. Koch and U. Oelfke, Nucl. Phys. **A509**, 717 (1990).

[72] P.C. Tiemeijer and J.A. Tjon, Phys. Rev. **C42**, 599 (1990).

[73] H. Kurasawa and T. Suzuki, Nucl. Phys. **A454**, 527 (1986);
K. Wehrberger and F. Beck, Nucl. Phys. **A491**, 587 (1989); Phys. Rev. **C35**, 298 (1987); **C37**, 1148 (1988);
R. Brockmann, D. Drechsel, J. Frank and P.-G. Reinhard, Z. Phys. **A332**, 51 (1989);
X. Ji, Phys. Lett. **219B**, 143 (1989); Phys. Rev. **C39**, 1668 (1989);
C.J. Horowitz, Phys. Lett. **208B**, 8 (1988); C.J. Horowitz and J. Piekarewicz, Phys. Rev. Lett. **62**, 391 (1989).

[74] J.D. Walecka, Ann. Phys. (N.Y.) **83**,491 (1974); B.D. Serot and J.D. Walecka, *The Relativistic Nuclear Many-Body Problem*, Adv. Nucl. Phys. **16**, Eds. J.W. Negele and E. Vogt, Plenum Press (1986).

[75] R.J. Furnstahl, R.J. Perry and B.D. Serot, Phys. Rev. **C40**, 321 (1989).